NATIONAL ADVISORY COMMITTEE FOR AERONAUTICS

TECHNICAL NOTE 2404

AN ANALYTICAL INVESTIGATION OF EFFECT OF HIGH-LIFT FLAPS ON TAKE-OFF OF LIGHT AIRPLANES

By Fred E. Weick, L. E. Flanagan, Jr., and H. H. Cherry

Agricultural and Mechanical College of Texas

Washington

September 1951

NATIONAL ADVISORY COMMITTEE FOR AERONAUTICS

TECHNICAL NOTE 2404

AN ANALYTICAL INVESTIGATION OF EFFECT OF HIGH-LIFT FLAPS ON TAKE-OFF OF LIGHT AIRPLANES

By Fred E. Weick, L. E. Flanagan, Jr., and H. H. Cherry

SUMMARY

An analytical study has been made to determine the effects of promising high-lift devices on the take-off characteristics of light (personal-owner-type) airplanes.

Three phases of the problem of improving take-off performance by the use of flaps were considered. The optimum lift coefficient for take-off was determined for airplanes having loadings representative of light aircraft and flying from field surfaces encountered in personal-aircraft operation. Power loading, span loading, aspect ratio, and drag coefficient were varied sufficiently to determine the effect of these variables on take-off performance, and, for each given set of conditions, the lift coefficient and velocity were determined for the minimum distance to take off and climb to 50 feet. Existing high-lift and control-device data were studied and compared to determine which combinations of such devices appeared to offer the most suitable arrangements for light aircraft. Computations were made to verify that suitable stability, control, and performance can be obtained with the optimum devices selected when they are applied to a specific airplane. In addition, a typical mechanism to provide for actuation of the movable surfaces for both high lift and lateral control is presented.

As a result of the study, a single slotted, full-span flap was selected as the high-lift device best suited for a four-place, private-owner-type airplane.

An optimum speed for take-off was determined for each combination of airplane span loading and power loading, this speed varying only slightly with changes in drag and aspect ratio. For each combination of aspect ratio, span loading, and power loading, an optimum lift coefficient for take-off was determined.

It was found that shortest take-off distances are obtained with low span loadings, power loadings, and aspect ratios and that air drag

and ground friction are relatively unimportant at these low loadings. Working charts were prepared for the prediction of take-off distance and for the determination of the take-off speed and the resultant lift coefficient desired.

Calculations indicate that considerable improvement in take-off performance of light airplanes is possible by the use of suitable high-lift flaps. Reductions of approximately 25 percent in the distance required to take off and climb to 50 feet are possible.

INTRODUCTION

The present trend toward the use of light (personal-owner-type) aircraft in farming and ranching activities and the indication that nearness to centers of population is important to the success of airport operation make it increasingly desirable that the personal airplane be able to take off in short distances from poorly prepared airfield surfaces. Since very little reduction in take-off distance is obtained from the flaps now in use on light airplanes, even though very effective high-lift flaps are in use on some military and transport aircraft, it seems likely that much can be done to improve take-off by judicious selection of high-lift-device arrangements.

Take-off distances and the corresponding lift coefficients have been determined for a hypothetical transport airplane employing flaps (reference 1) and for a liaison-type airplane using boundary-layer control (reference 2), but the problem of take-off for light airplanes equipped with high-lift devices has not been dealt with adequately. (Boundary-layer control in its present phase of development is considered impractical for personal aircraft and is not considered in this analysis.)

This report covers three phases of investigation of the problem of improving take-off performance by the use of flaps. The first part is concerned with the determination of the optimum lift coefficient for take-off for airplanes having loadings representative of personal aircraft and flying from field surfaces encountered in personal-aircraft operation. The analysis is made for airplanes carrying four people and enough fuel and oil for 5 hours' flight at 65 percent of full power. Power loading, span loading, aspect ratio, and drag coefficient are varied sufficiently to determine the effect of the variables on take-off performance, and for each given set of conditions the lift coefficient and the velocity are determined for the minimum distance to take off and climb to 50 feet.

In the second part, existing high-lift and control-device data are studied and compared in order to determine which combinations of such

devices appear to offer the most suitable arrangements for aircraft of the private-owner type.

In the third part, computations are made to verify that suitable stability, control, and performance can be obtained with the optimum devices selected when they are mounted on feasible airplane configurations.

This work was conducted at the Personal Aircraft Research Center, Texas A. & M. Research Foundation, under the sponsorship and with the financial assistance of the National Advisory Committee for Aeronautics.

SYMBOLS

ρ	mass density of air, slugs per cubic foot
S	wing area, square feet
D	airplane drag, pounds
W	gross weight of airplane, pounds
C_L	airplane lift coefficient $\left(\frac{W}{\frac{1}{2}\rho V_o^2 S}\right)$
A	aspect ratio $\left(b^2/S\right)$
e	wing efficiency factor based on variation of spanwise loading from an elliptical loading with no ground effect
C_D	airplane drag coefficient $\left(\frac{D}{\frac{1}{2}\rho V_o^2 S}\right)$
b	span, feet
T_o	static thrust, pounds
P	brake horsepower
T	thrust, pounds
$T_{V_{max}}$	thrust at maximum velocity, pounds

V velocity, feet per second

C_n yawing-moment coefficient (N/qSb)

N yawing moment, foot-pounds

q dynamic pressure, pounds per square foot $\left(\rho V^2/2\right)$

t wing root thickness, feet

F fuselage frontal area, square feet

w weight of airplane components, pounds

L lift, pounds

C_{D_i} induced drag coefficient $\left(C_L{}^2/\pi Ae\right)$

C_{D_o} wing profile drag coefficient $\left(\frac{\text{Wing profile drag}}{\frac{1}{2}\rho V_o{}^2 S}\right)$

g acceleration due to gravity, feet per second^2

μ ground friction coefficient

$A_P = T_o/P$

$B = 2\left(T - T_o\right)/P\rho V^2$

$C = T_{V_{max}}/P$

} constants for calculating propeller thrust

s_t total take-off distance, feet

h altitude at which take-off is assumed complete, 50 feet

θ angle of flight path during climb with respect to horizontal, degrees

c_{d_o} section profile drag coefficient

c_{l_i} design section lift coefficient

c_m section pitching-moment coefficient

f	equivalent parasite area $\left(C_D \times S\right)$
V_s	stalling speed, feet per second
C_m	pitching-moment coefficient (M/qcS)
M	pitching moment, foot-pounds
c_l	section lift coefficient
$\frac{pb}{2V}$	helix angle generated by wing tip in roll
p	angular velocity in rolling, radians per second
R	Reynolds number
δ_f	flap deflection, degrees
s_g	ground-run distance, feet
c	chord, feet
α	wing angle of attack, degrees
c_d	section drag coefficient

Subscripts:

eff	effective
max	maximum conditions
min	minimum conditions
o	free-stream conditions
opt	optimum conditions
t	conditions at take-off of airplane
u	useful load
l	conditions during ground run of airplane

ANALYSIS

DETERMINATION OF OPTIMUM LIFT COEFFICIENT

In order that the results of this investigation might be correlated with those of references 1 and 2, similar assumptions were made whenever feasible. The assumptions of reference 2 particularly were followed, except in the case of the weights of the power plant and propeller. Here values applicable to personal aircraft were derived. Drag data of reference 2 were adopted without change.

Assumptions

The airplane was assumed to carry four people and baggage and enough fuel and oil for 5 hours' cruising flight at 65 percent of full power.

Weight breakdown.- The expressions giving the weights of the components are tabulated below.

WEIGHTS OF COMPONENTS

Component	Expression	Reference
Wing	$0.046SA^{0.47}\left(\frac{W}{b}\right)^{0.53}\left(\frac{b}{t}\right)^{0.115}$	3
Fuselage and landing gear	0.28W	Derived from study of five typical airplanes
Empennage	0.25S	3
Propeller	0.24P + 5.0	Derived from study of six typical propellers
Engine	1.533P + 71.5	Derived from a study of 38 engines in 50- to 200-hp class
Passengers and gear	800 lb (200 lb per passenger)	
Fuel and oil	1.62P	3

Airplane configuration.- The assumptions pertaining to the airplane components are as follows:

(1) Wing: Cantilever and rectangular in plan form.

(2) Fuselage: The frontal area F was determined from the following expression of reference 4:

$$F = 0.15 w_u^{2/3}$$

where w_u was taken as 1500 pounds. The fuselage frontal area of 19.63 square feet thus obtained was found to be a representative value for personal airplanes with side-by-side seating.

(3) Landing gear: Extended during the entire take-off and climb to 50 feet.

(4) Empennage: Area assumed to be 25 percent of the wing area.

(5) Propeller: Fully automatic and permits development of full power and speed at all airspeeds.

(6) Fuel and oil: Sufficient for 5 hours of cruising at 65-percent power.

Aerodynamic characteristics.- The aerodynamic characteristics of the assumed airplane are as follows:

(1) Wing: The curve of profile drag coefficient against lift coefficient (fig. 1) was obtained from reference 2. (The curve of fig. 1 is approximately an envelope of the curves for different deflections of a double slotted flap given on p. 221 of reference 5. The maximum value of L/D was obtained with a flap deflection of 35°.) The curve was extrapolated for lift coefficients greater than 2.8. The induced drag coefficient was obtained by the expression:

$$C_{D_i} = \frac{C_L^2}{\pi A e}$$

where e is the wing efficiency factor and was assumed to be 0.9.

(2) Fuselage: The fuselage drag coefficient was assumed to be 0.20 based on fuselage frontal area (reference 3).

(3) Landing gear: The landing-gear drag coefficient was assumed to be 0.05 based on fuselage frontal area (reference 3).

(4) Empennage: The empennage drag coefficient was assumed to be 0.0025 based on wing area (reference 3).

The total drag coefficient based on wing area is determined by the expression:

$$C_D = 0.0025 + \frac{(19.63)(20 + 0.05)}{S} + \frac{C_L^2}{0.9\pi A} + C_{D_o}$$

Take-off maneuver.- The take-off is assumed to consist of three phases:

(1) An accelerated ground run in the attitude of least resistance until take-off speed is reached

(2) A circular transition arc from the end of the ground run to the beginning of the steady climb

(3) Steady climb to an altitude of 50 feet

The entire maneuver is assumed to be made at full power and with no wind, starting from sea level in standard atmosphere.

Calculations

The horizontal distance covered in each of the three phases of the take-off is derived in reference 1. These distances are:

$$\text{Ground-run distance} = \frac{W/S}{\rho g\left(\mu C_{L_1} - C_{D_1}\right) - B\frac{W/S}{W/P}} \log_e \left[1 + \frac{\left(\mu C_{L_1} - C_{D_1}\right) - B\frac{W/S}{W/P}}{\left(\frac{A_P}{W/P} - \mu\right)C_{L_t}}\right]$$

$$\text{Transition distance} = \frac{2W/S}{\rho g}\left(\frac{1}{C_{L_{max}} - C_{L_t}}\right)\left[\frac{A_P}{W/P} - \left(B\frac{W/S}{W/P} + C_{D_t}\right)\frac{1}{C_{L_t}}\right]$$

$$\text{Climb distance} = \frac{h - \frac{2W/S}{\rho g}\left(\frac{1}{C_{L_{max}} - C_{L_t}}\right)\left\{1 - \cos \sin^{-1}\left[\frac{A_P}{W/P} - \left(B\frac{W/S}{W/P} + C_{D_t}\right)\frac{1}{C_{L_t}}\right]\right\}}{\tan\left\{\sin^{-1}\left[\frac{A_P}{W/P} - \left(B\frac{W/S}{W/P} + C_{D_t}\right)\frac{1}{C_{L_t}}\right]\right\}}$$

The total take-off distance s_t is the sum of these three terms and may be simplified into the expression:

$$s_t = \frac{W/S}{\rho g}\left\{\frac{1}{\left(\mu C_{L_1} - C_{D_1}\right) - B\frac{W/S}{W/P}} \log_e \left[1 + \frac{\left(\mu C_{L_1} - C_{D_1}\right) - B\frac{W/S}{W/P}}{\left(\frac{A_P}{W/P} - \mu\right)C_{L_t}}\right] + \frac{\rho g h}{\frac{W}{S}\tan\theta} + \frac{2\tan\frac{\theta}{2}}{C_{L_{max}} - C_{L_t}}\right\}$$

Note that C_{L_t} is assumed to be equal to $0.9C_{L_{max}}$ and $C_{L_1} = \pi\mu Ae/2$, from reference 1.

The procedure involved in making a set of calculations for given values of W/P, W/S, A, and μ is as follows:

(1) Assume a value of $C_{L_{max}}$.

(2) Compute values of C_{L_t}, C_{L_1}, C_{D_t}, and C_{D_1}. Note that to obtain C_{D_t} and C_{D_1} it is necessary to know the wing area S. The weight W, the wing area S, the power P, and the span b can be found from figure 2, 3, or 4. The wing profile drag coefficient C_{D_o} can be found from figure 1.

(3) Determine V_{max} from figure 5, 6, or 7. The equation of these curves is given in reference 2 as

$$T_{V_{max}} = \frac{\rho}{2} V_{max}^2 S C_D$$

where

$$T_{V_{max}} = P \times C$$

and

$$C = 3.09 - 0.005 V_{max}$$

(4) Find A_P and B from figure 8.

(5) Compute s_t.

(6) Repeat for as many values of $C_{L_{max}}$ as necessary.

For each airplane assumed, the take-off distance s_t is plotted against $C_{L_{max}}$ to obtain the minimum s_t and the corresponding $C_{L_{max}}$. Figure 9 shows typical curves.

These calculations were made for various combinations of power loading, span loading, and aspect ratio (see figs. 10 to 13). The minimum take-off distance is plotted against power loading for various span loadings for an aspect ratio of 7.5 in figure 10. Figure 12 is a cross plot of figure 10 and shows the minimum take-off distance obtainable for a given power loading and span loading at an aspect ratio of 7.5. Figures 11 and 13 show the same variation for aspect ratios of 5 and 10, respectively.

Take-off velocities are computed from the expression

$$V_t = \frac{W/S}{(\rho/2) C_{L_t}}$$

The main results of the computations are shown in table I.

Parameters Developed

The distance required to take off and climb to a height of 50 feet is influenced mainly by four basic factors, weight, power, span, and drag. It is convenient to combine the first three of these into two ratios, power loading W/P and span loading W/b^2.

Curves showing the take-off distances obtained for various values of span loading and power loading with the assumed airplane are shown for aspect ratios of 5, 7.5, and 10 in figures 11, 12, and 13, respectively. From these figures the approximate take-off run from a fairly soft field ($\mu = 0.2$) can be obtained for an airplane equipped with a constant-speed propeller, with the assumption that a reasonably low drag, high-lift flap is available to produce a high enough lift coefficient to obtain the optimum take-off speed. It is obvious from the charts that short take-off distances are obtained only with low power loadings and low span loadings ($W/P = 10$, $W/b^2 = 1$), at least within the range of loadings that represent feasible construction. (These three charts can be used as working charts to obtain approximate take-off runs for personal airplanes in general, taking off from fairly soft fields. If a constant-speed controllable propeller is not used, the power should be taken as that available at take-off.)

Effect of Drag

The fourth basic variable, drag, is made up of two portions, ground or rolling friction and air drag. For most of the computations in this report, the ground friction coefficient μ was assumed to have a value of 0.2, corresponding to a fairly soft unpaved field or one with high grass. In order to show the effect of the ground friction on the take-off run, a few additional computations were made for certain loadings assuming values of μ of 0, 0.05, and 0.10. The results of some of these computations are shown in figure 14. For low loadings ($W/P = 10$, $W/b^2 = 1$) the ground friction has a relatively minor influence, whereas with fairly heavy loadings ($W/P = 20$, $W/b^2 = 2$) the take-off run is very greatly influenced by the ground friction, the distance with $\mu = 0.2$ being nearly three times as great as that with $\mu = 0$. It is apparent that airplanes with high power loadings and span loadings will profit greatly from smooth paved runways ($\mu = 0.03$).

For the consideration of the air drag of the airplane represented in figures 11 to 13, the airplane, as stated previously, was assumed to have a relatively low drag, high-lift wing and flap (see fig. 1). In order to find the effect for a somewhat higher drag, computations for certain combinations of loadings were made assuming increases in the total drag coefficient at take-off of 0.1 and 0.2. The latter represents approximately the additional drag that would be obtained from a split

flap deflected sufficiently to obtain a substantial lift increase. The results of the computations are given in figure 15. As in the case of the ground friction, it is apparent that the additional drag has little effect in the case of light loadings (about 20 percent for $W/P = 10$ and $W/b^2 = 1$) but that it has an exceedingly important effect with the higher loadings. In fact, with a power loading of 20 and a span loading of 2, the airplane will not take off at all with $\Delta C_D = 0.2$.

Optimum Speed for Take-Off

The computations of the take-off runs with various combinations of drag, span loading, and power loading brought out the interesting fact that, for any given set of values of span and power loadings, the optimum take-off speed is very nearly the same for the entire range of drags and aspect ratios investigated. In other words, for each combination of weight, power, and span, there is an approximate optimum take-off speed. If the take-off is made at a lower speed, the high induced drag increases the total length of the run (including the climb to 50 ft). If a higher take-off speed is used, the extra ground run required lengthens the total distance. Curves of constant take-off speed are plotted for various span and power loadings in figure 16.

When used in conjunction with the lines of constant take-off distance plotted for various values of span and power loadings (figs. 11 to 13), it is apparent that the loading combinations which give short take-off distances require low take-off speeds.

Aspect Ratio and Lift Coefficient

Since, for any set of values of the weight, span, and power, there is an optimum take-off speed, and since $W = L = qC_LS$, in order to obtain the optimum take-off speed the product C_LS remains a constant. Thus it appears that the optimum take-off speed, and to the first approximation the minimum take-off distance, can be obtained by the use of a narrow-chord, high-aspect-ratio wing with a high lift coefficient or with a low-aspect-ratio wing with a correspondingly low lift coefficient. In figure 17 the take-off distance is plotted against aspect ratio for one combination of span and power loadings, and the maximum lift coefficients that will give the optimum take-off speed in each case are noted on the curves $\left(\text{the take-off being made at } 0.9C_{L_{max}}\right)$. It is apparent from this curve that the shortest take-off distance was obtained with the very lowest aspect ratio for which computations were made, 2.5, and that the optimum lift coefficient for this case was only 1.2. For an aspect ratio of 7.5 the take-off distance to a height of 50 feet would

be only 5 percent longer, however, assuming that a lift coefficient of 3.2 could be obtained at the drag value shown in figure 1.

The explanation of the shortest take-off run's occurring with a very low value of aspect ratio can be obtained from an examination of the curve of C_L against C_{D_o} (fig. 1). The slight variation in take-off run shown in figure 17 is caused only by the difference in airfoil profile drag coefficients obtained with the different lift coefficients and flap settings. From figure 1 it is apparent that the minimum drag for a given lift, or the maximum ratio of L/D, occurs at a lift coefficient of approximately 1.4. This represents the condition under which the shortest take-off distance would occur. With any given set of span and power loadings the lift coefficient of 1.4 would always require a very low aspect ratio in order to obtain the optimum take-off speed and the shortest take-off distance.

If the only design consideration was to obtain a short take-off distance, it appears from these results that, for any given span loading, a very low aspect ratio should be used and that a high lift coefficient would not be required.

Compromise

The designer of an airplane must, of course, consider other performances also, including particularly cruising speed, range, and rate of climb. Application of the same line of reasoning as has been used here for take-off performance would lead to the use of the airfoil and flap at the maximum ratio of L/D, or at a lift coefficient of 1.4 with the flap deflected 35° for the airfoil of the computations, for each of these conditions of flight. This would result in aspect ratios of the order of 20 for best rate of climb and of the order of 100 for optimum cruising performance. Obviously, considering that the aspect ratios of current personal airplanes vary from about 6 to 8, the climbing and cruising performances have already been severely compromised in order to obtain reasonably satisfactory low-speed characteristics.

The problem of obtaining an optimum compromise for the personal airplane will be considered later in this report.

If it is assumed that the presently used aspect ratios are likely to be fairly close to the optimum, and values found in general use often are, then it appears from these computations that the shortest take-off run would generally be obtained with a lift coefficient of approximately 3. The approximate gain by the use of such a lift coefficient is shown for one set of span and power loadings in figure 18 in which the take-off distance is given for various values of the maximum lift coefficient.

In this particular case the shortest take-off distance was obtained with a value of $C_{L_{max}}$ of 3.2. Most present personal airplanes are likely to have maximum lift coefficients available for the take-off condition of approximately 1.4. Even if flaps are used, this condition is approximately true because the particular types of flaps generally used do not shorten the total take-off distance if they are deflected more than a small amount. For the loadings and aspect ratios used in figure 18 it appears that the distance required to take off and climb to 50 feet could be reduced by 680 feet (or by about one-third) and the take-off speed could be reduced from 64 miles per hour to 45 miles per hour, if a lift coefficient of 3.2 could be obtained. Although a lift coefficient of 3.2 appears slightly beyond the range of present high-lift devices (for an entire wing with good stalling characteristics), it appears that a value approximating 2.5 might be available with a practical flap arrangement and that this might give a reduction in take-off distance of 25 percent.

The effect of aspect ratio on V_{max} is shown in figure 17 for an intermediate span loading and power loading. The variation of V_{max} with aspect ratio is slight for power loadings from 10 to 20 and span loadings from 1 to 3. The slope of the curve increases slightly with increases in power loading at each span loading. Values of V_{max} for various configurations are given in table I. Figures 5 to 7 present further information concerning V_{max}.

SELECTION OF HIGH-LIFT DEVICE

From the analysis given in the section "Determination of Optimum Lift Coefficient," it is apparent that, with aspect ratios commonly used in present-day personal airplanes, the optimum high-lift device for take-off over a 50-foot obstacle would produce an airplane lift coefficient of about 3.0 with as low a drag as possible. It was also shown that the take-off distance would be shortest if an aspect ratio of about 3 were used but that the selection of the aspect ratio involves a compromise between the take-off performance and the climb, cruising, and high-speed performance. All of the latter performances would dictate the use of substantially higher aspect ratios than those currently used in personal aircraft. For the present study, it will be assumed that the generally used aspect ratios ranging from about 6 to 8 are reasonably representative of the optimum compromise.

This phase of the report is concerned with the selection of the existing high-lift devices that best fulfill the above-mentioned requirement of a lift coefficient of about 3.0 with low drag and at the same

time meet certain other design requirements. An optimum arrangement must have reasonably low drag for the cruising and high-speed end of the performance range and the entire high-lift and lateral-control arrangement must be simple in form and free from mechanical complications. In order to be useful in connection with personal aircraft, it must be low in cost and easy to maintain in satisfactory operating condition.

The high-lift device must also fit in with a satisfactory lateral-control system which probably must permit the flaps to cover the entire wing span because, even with full-span flaps, no simple high-lift flap is available as yet that will give an airplane lift coefficient as high as 3.0 with reasonably low drag at the low values of the Reynolds number involved.

Recapitulating, the optimum high-lift arrangement for the present purpose will fulfill the following requirements:

(1) Maximum lift coefficient of approximately 3.0

(2) Low drag at high lift

(3) Low minimum drag coefficient

(4) Simplicity of structure

(5) Feasibility of satisfactory lateral control

Available lift and drag data on high-lift devices (references 2 and 5 to 54) have been examined and compared in search for those which might be considered optimum. Only a few were found to be of interest in connection with the present problem. The pertinent data on these are listed in table II, which also shows data on other typical high-lift devices, for the purpose of comparison. In spite of the large quantity of test data available, only one test (item 7 of table II) covers any of the best arrangements at approximately the Reynolds number representing the take-off condition for a personal airplane. It has been necessary, therefore, to correct the other results to the value of the Reynolds number of interest in this problem. The value of Reynolds number of 1,500,000 has been selected as representative of the best take-off performance likely to be obtained and the value of the maximum lift coefficient has been corrected accordingly by the method described in appendix A. Appendix A also describes a method of correcting drag coefficients at high lifts and gives the corrected values for the two most promising arrangements (items 6 and 11 of table II). (Item 7 is omitted because of high drag.)

It is obvious from an examination of table II that there are not sufficient satisfactory test data available for the selection of an

optimum high-lift arrangement with assurance that the field has been well-covered. Only two of the devices listed (items 6 and 11) were tested in a wind tunnel having low turbulence, and the drag data for all of the others show substantially higher values which are of questionable accuracy. Section data on low-drag as well as four-digit and five-digit sections employing promising single and double slotted flaps at Reynolds numbers of approximately 1,000,000 obtained from a low-turbulence wind tunnel would be of considerable value in future work of the nature of this investigation.

Five criteria have been set up as a basis for selection of the existing high-lift-device arrangement best suited for use on typical personal aircraft. Although a considerable number of arrangements were studied (table II), lack of drag data at high lift and the obviously excessive complications of some devices left only a few practical ones from which to choose. However, the complete study may be of some interest in showing the effect of thickness, camber, thickness form, Reynolds number, surface roughness, and type of high-lift device on certain airfoil characteristics.

Curves showing some of these effects are included in figures 19 to 25. The effect of camber on $c_{l_{max}}$ is shown in figure 19, and the effect of thickness is shown in figure 20. Figure 21 shows the effect of thickness form on $c_{l_{max}}$. The effect of thickness on $c_{l_{max}}$ for flapped airfoils with both rough and smooth surface conditions is shown in figure 22. Figure 23 shows the variation of L/D at $0.9c_{l_{max}}$ with design lift coefficient for several thicknesses, and figure 24 shows the effect of Reynolds number on L/D at $0.9c_{l_{max}}$ for several sections. The effect of Reynolds number on c_{d_o} at $0.9c_{l_{max}}$ for various airfoil sections is shown in figure 25.

Maximum lift coefficient.- Fortunately, comparative tests with flapped and unflapped airfoils have shown that, for airfoils of a given thickness ratio, the increment in lift due to the flap is approximately the same regardless of reasonable variation of airfoil camber. Therefore, for any given flap, the highest lift will most likely be obtained with the basic airfoil giving the highest lift. The test results considered were all obtained from low-turbulence wind tunnels. Unfortunately, they do not indicate clearly that any particular airfoil shape is the best for giving either a high lift coefficient or a low drag at high lift, at a Reynolds number of 1,500,000. This finding is not in accordance with what one would expect from the best previous compilation of airfoil data at various Reynolds numbers, which gives a summary of many results obtained in the NACA variable-density wind tunnel (reference 6). From

this summary, it appeared that our present requirements would have been met by a thick, highly cambered airfoil, such as the NACA 8318. The low-turbulence wind-tunnel data, however, indicate that the camber probably should be relatively low $\left(c_{l_i} = 0.2 \text{ to } 0.4\right)$ and that, considering the airfoil alone, the thickness ratio should not be greater than 12 percent. There is ample information available to show, on the other hand, that a flap will give a substantially larger lift increase on a thick airfoil than on a thin one, and the highest lift coefficient with a flap would probably be obtained with a relatively thick airfoil.

It appears that the maximum lift coefficient obtained may be so critically influenced by a number of factors, such as the exact condition of the airfoil surface and the nature of the air flow in the wind tunnel, that the underlying trends sought are masked. If this is the case, the particular form of airfoil selected for an actual airplane may be of less importance with regard to the maximum lift coefficient obtained than these other factors of surface condition, cleanliness, imperfection of contour in actual construction, and so forth.

Considering the indecisive nature of the data available, no definite recommendation can be made from the information on airfoils alone for obtaining the optimum high-lift condition with a flap. The only course open, then, is the selection of a high-lift wing from the meager satisfactory test data available on flapped airfoils at low Reynolds numbers and with low turbulence. Items 6 and 11 from table II thus appear to be the only ones from which suitable data are available.

From the drag data available on these two high-lift arrangements, it appears that the maximum flap deflections that can be used to improve take-off are approximately 30° for the single slotted flap and 35° for the double slotted flap. At these deflections and at the take-off Reynolds number of approximately 1,500,000, either of these high-lift devices gives a value of the maximum lift coefficient of approximately 2.5, neglecting the effect of roughness. Unfortunately, this is not so high as the value desired (approx. 3.0), but it is high enough to give a substantial improvement in take-off performance over that of present-day personal airplanes.

Drag at high lift.- The optimum high-lift device for take-off must give not only high lift but also low drag at the high lift. Drag data at high lift for most of the arrangements considered are very scarce. A comparison of all the arrangements on the basis of drag at maximum lift is not possible, but items 6 and 11 of table II both have lower drag in the range of higher lift coefficients than the other configurations.

Minimum drag coefficient.- It is obvious that, in order for a flapped airfoil to have a low drag in high-speed or cruising flight,

the airfoil must have a smooth form free from slots and ridges when the flap is retracted. Both the single slotted flap of item 11 and the double slotted flap of item 6 in table II are arranged to fit smoothly into a recess at the rear of the main wing when the flaps are retracted. They both appear to be satisfactory in this report.

Simplicity of structure.- The simplest possible flap arrangement is probably that in which the flap is deflected about a single hinge axis. On the other hand, a greater increase in lift is obtained by flaps which extend rearward, such as the Fowler or Zap types. Flaps of this type have made use of tracks or relatively complicated linkages which, up to the present time, have not been used on personal aircraft, in spite of the fact that their advantages were known to the designers. The single and double slotted flaps of items 6 and 11 in table II appear to accomplish a fair compromise in this respect in personal aircraft. If used with a maximum flap deflection of about 30° or 35°, they can be deflected about a single hinge axis which is placed low enough to provide substantial movement to the rear as the flap is deflected. This arrangement would entail the disadvantages of external hinge brackets, but their drag might be considered acceptable on most personal aircraft. In case this were not so, the external hinges could be replaced by a linkage that is housed entirely within the wing when the flap is retracted.

Since either the single slotted flap or the double slotted flap can use a single hinge axis for the maximum deflection desired for take-off, and since at this deflection both of them give substantially the same value of the maximum lift coefficient, it appears that the single slotted flap is preferable for the present purpose because of its simpler construction.

Lateral control.- As previously mentioned, because of the fact that the best maximum-lift flap yields a lift coefficient substantially under the optimum value of about 3.0, it will be desirable for best take-off performance to use flaps over the entire span of the wing. A number of lateral-control devices permitting full-span flaps have been developed (references 52 to 54). The most likely of these for the present purpose are retractable ailerons or their modifications called plug ailerons. It appears that ailerons of this type could be used satisfactorily, but they do represent extra complications in the form of internal wing compartments, hinges, controls, and the surfaces themselves. They are usable because they provide the rolling moment required, together with relatively satisfactory yawing moments.

The yawing moments are likely to be of critical importance in connection with lateral control obtained at very high lift coefficient, and, if some provision could be made to obtain satisfactory yawing moments without extra control surfaces, extreme simplicity might possibly be achieved by deflecting the flaps themselves differentially in order

to obtain the rolling moment required. The rolling moments required for satisfactory lateral control induce a large adverse yawing moment in flight at high lift coefficients. This induced adverse yawing moment is at least partially opposed by the increased drag of the retractable (spoiler-type) ailerons. The induced adverse yawing moment could obviously be opposed with less cost in drag by means of a rudder control. The idea of coupling the rudder with the lateral-control system, at least to a sufficient extent to counteract the adverse yawing moments caused by the lateral-control system, has been examined in connection with the present problem of applying high-lift flaps to personal airplanes. The following arrangement appears promising.

A single slotted flap of the form of item 11 in table II is used over the full span of each side of the airplane. The flaps are deflected downward 30° for the take-off (or landing) condition and the rolling moment for lateral control is obtained by an extreme differential motion which moves one side up approximately 15°. The other side at first moves down about 2° and then the linkage passes over dead center and at the full deflection of the up-moving flap, the downward-moving flap arrives back at zero (from the original 30° flap position). The rudder is elastically connected to the lateral-control system so that it is deflected the correct amount to overcome the adverse yawing moments. Thus an ideal rolling control free from yawing effect is closely approached. Because the rudder is coupled into the system by an elastic means, the pilot can use his rudder pedals to overcontrol the rudder in any way he sees fit. With a rigid linkage the system would also lend itself to two-control operation.

Under conditions of flight with the flap retracted, the differential action of the flaps used as ailerons is reversed, almost all the deflection being on the downward-moving side. This gives a larger adverse yawing moment than the usual aileron arrangement, but the rudder is still linked with the control system in such a manner that the adverse yawing moment is overcome.

It appears that a very simple control linkage can be used to obtain all of these results. This will be taken up in greater detail in the following section of this report, which will cover the application of the high-lift and lateral-control arrangement to a typical personal-type airplane. The arrangement just described is the simplest that has been found to give promise of satisfactory lateral control with full use of the best high-lift device available for the purpose.

APPLICATION OF SELECTED HIGH-LIFT DEVICE TO TYPICAL AIRPLANE

This phase of this report consists of an analysis of a selected airplane modified by the incorporation of a high-lift device and airfoil section chosen from the various arrangements studied in the second part of the investigation. The analysis is made with respect to performance, stability, and control. General data for the airplane as designed and built and for a modified configuration are listed in table III.

It is proposed to use a full-span single slotted flap of 0.25 chord in conjunction with the NACA 63,4-420 airfoil as shown in figure 3 of reference 7 as the high-lift device. Of all the arrangements investigated, this configuration appears to be the most satisfactory based on the five requirements given in the section "Selection of High-Lift Device." It is not implied, however, that the NACA 63,4-420 section is the best section for use on personal aircraft. External brackets present the most simple form of flap support. Assuming that the flaps would be drooped 5° for the cruise condition, it would be possible to operate the surfaces differentially as ailerons with the allowance for a slight upward movement from the normal position. A description of a type of control linkage for such an arrangement is presented in appendix B.

The high negative values of c_m shown in the section data of figure 3, reference 7, for the flaps down condition indicate that excessive diving tendencies might be experienced with forward center-of-gravity locations. The use of the full-span flaps differentially as ailerons introduces the possibility of excessive adverse yawing tendencies. The investigation in this phase of the study, with respect to stability and control, embraces both the high-speed and low-speed conditions with flaps up and the low-speed condition with flaps down. The empennage characteristics used in the analysis are those of the actual empennage of the typical airplane selected.

Performance.- The performance analysis of the modified version of the selected airplane is generally considered in the light of the change in drag and weight with the change in the wing, since no other differences in configuration are involved.

The existing wing of the selected airplane is a modified NACA 43012 section while the modified version of the wing uses an NACA 63,4-420 airfoil. A measure of the effect of changing sections on the performance may be determined from section data of the two airfoils. Taking the difference between the product of C_{D_o} for the 43012 airfoil times qS of the original wing and the product of C_{D_o} for the 63,4-420 airfoil times

qS of the modified wing and dividing by the total drag of the airplane give the percentage change in drag.

No data for direct comparison of the NACA 43012 airfoil with the NACA 63,4-420 airfoil are available, but, from table I of reference 6, a comparison of the NACA 43012 and 23012 sections can be obtained. The values of minimum drag coefficient at comparable Reynolds numbers are found to be 0.0070 for the 23012 section and 0.0079 for the 43012 airfoil section.

A value of minimum drag coefficient for the NACA 23012 section has been obtained in the NACA two-dimensional low-turbulence tunnel and is comparable with the section data of the NACA 63,4-420 section as found in figure 12, reference 5. The value of the drag coefficient of the 43012 section used for comparison is taken as that for the 23012 section from reference 5 increased by the difference of the section data from reference 6. The section drag coefficient for comparison then becomes

$$0.0060 + (0.0079 - 0.0070) = 0.0069$$

From reference 7, the section drag coefficient of the NACA 63,4-420 section is (for flaps at 5°) 0.0062.

The change in drag area then becomes

$$f = 0.0062 \times 192 - 0.0069 \times 165$$

$$= 0.005 \text{ sq ft}$$

and, for a total f for the airplane of approximately 7.0 square feet (based on the method of drag estimation outlined in the first phase of this report), the percentage change in the drag is

$$\frac{0.005}{7.0} \times 100 = 0.07 \text{ percent}$$

The change in weight of the airplane with the change in the wing is estimated from the relationship expressed in the equation for wing weight used in the first part of this report. The equation is

$$w = 0.046SA^{0.47}\left(\frac{W}{b}\right)^{0.53}\left(\frac{b}{t}\right)^{0.115}$$

Since the span and gross weight remain constant, the ratio of the weight of the modified wing to that of the original wing becomes

$$\frac{w_m}{w_o} = \frac{S_m A_m^{0.47}\left(\frac{b_m}{t_m}\right)^{0.115}}{S_o A_o^{0.47}\left(\frac{b_o}{t_o}\right)^{0.115}}$$

$$= \frac{192(7.5)^{0.47}\left(\frac{38}{1}\right)^{0.115}}{165(8.75)^{0.47}\left(\frac{38}{0.54}\right)^{0.115}}$$

$$= 1.01$$

The wing weight involves only some 10 percent of the gross weight of the airplane so that the total change in gross weight is only one-tenth of 1 percent.

With this negligible change in drag and in weight, and since no change in span loading or power loading has been made, no further analysis is included for performance items such as speed, climb, ceilings, range, and so forth, for these will all remain substantially unchanged.

The primary consideration of take-off distance is investigated using the method of analysis described in the first phase of this report.

The wing section and high-lift device chosen for the modified version, from section data taken from reference 7, develop a maximum lift coefficient of about 3.0 at 40° flap deflection. Limiting the flap deflection to 30° for lateral-control considerations reduces the maximum section lift coefficient to about 2.8. From the information in the second part of the study, it has been estimated that the effect of decreased Reynolds number, body interference, and surface roughness reduces the expected value of the maximum lift coefficient to 2.3.

From the data in the first part of this report, the optimum lift coefficient for take-off with the aspect ratio of the original version of the selected airplane (8.75) is found to be about 3.5. Decreasing the aspect ratio decreases the optimum lift coefficient, and, for the modified wing of aspect ratio 7.5, the optimum C_L is somewhat less.

Calculations show that, for the airplane with the original wing area and aspect ratio and an estimated value of $C_{L_{max}}$ of 1.4, an increase of the lift coefficient to 2.3 would result in a reduction of 25 percent in the take-off distance over a 50-foot obstacle. This represents a decrease of some 400 feet. By holding the span constant but increasing the chord to reduce the aspect ratio to 7.5, and realizing the value of 2.3 for $C_{L_{max}}$, the take-off distance is reduced some 31.4 percent from the distance computed for the original wing and $C_{L_{max}}$ of 1.4. Curves of take-off distance against $C_{L_{max}}$ for the aspect ratios under consideration are shown in figure 26.

The greatest percentage improvement results from the increase in maximum lift coefficient, but some improvement is realized from the lower aspect ratio, which decreases the optimum lift coefficient and reduces the difference between the optimum and attainable values.

For a reduced pay-load condition (useful load of 500 lb) the same increase in $C_{L_{max}}$ from 1.4 to 2.3 and in aspect ratio from 8.75 to 7.5 results in a calculated reduction of take-off distance of 26.4 percent.

Take-off speeds $\left(\text{at } 0.9C_{L_{max}}\right)$ are also substantially reduced. The speed for the fully loaded condition decreases 27.6 percent and that for the light load condition decreases 27.7 percent with the increase in lift coefficient and decrease in aspect ratio between the original airplane and modified version.

The landing distance for the modified version of the selected airplane is of some consideration since, for simplicity of construction and for assurance of adequate lateral control at low speed, the flap deflection has been limited to 30°. At this deflection, the flap drag has not greatly increased and, consequently, the landing distance over a 50-foot obstacle can be expected to be somewhat adversely affected because of the relatively high values of L/D and the resulting flap glide path and long transition distance.

The landing distance may be influenced by several factors but, since the primary interest is in designing for a short take-off using high lift, the drag is the important variable for landing considerations. The increased drag needed for a steep glide path and shorter landings may be either profile or induced drag. An increase in profile drag, when not available with increased flap deflection because of certain restrictions, may be obtained with an additional drag flap. This solution, however, adds weight and requires an extra control to provide for

the difference in configuration for landing where the drag is required and for take-off where the extra drag cannot be tolerated. Such drag devices must be of considerable size to be effective in decreasing the landing distance.

The induced drag may be substantially increased with a decrease in aspect ratio, but variations in this fundamental parameter should be made with careful consideration of its effect on other performance items.

Calculations of landing distance over a 50-foot obstacle are based on the method described in reference 55. The equations are listed below:

$$\text{Distance to glide} \quad d_{GL} = \frac{50(C_L)_{GL}}{(C_D)_{GL}}$$

$$\text{Transition distance} \quad d_{TR} = \frac{0.0334\left(V_{GL}^2 - V_L^2\right)(C_L)_{TR}}{(C_D)_{TR}}$$

$$\text{Braked roll} \quad d_L = \frac{0.0334V_L^2}{(D/L) - \mu} \log_e \left(\frac{D/L}{\mu}\right)$$

$$\text{Landing distance} = d_{50} = d_{GL} + d_{TR} + d_L$$

The glide is assumed to be made at $1.2V_S$, the touchdown speed, at $1.0V_S$, and the value of μ is taken as 0.5 for the braked roll. The ground effect on the induced drag is also included.

Since take-off and landing distances are so closely related, in that the larger of the two defines the size of the field from which an airplane can be operated, they should be considered simultaneously. Assuming that the span is held constant, changes in weight with changes in wing area were considered, but variations in $C_{L_{max}}$ with Reynolds number were found to be of the order of 1 percent and were neglected. The results of the study of the effect of aspect ratio on take-off and landing distances are shown in figure 27.

The take-off distance with the assumed high-lift wing arrangement having a maximum lift coefficient of 2.3 is found to decrease with a decrease in aspect ratio to a minimum at an aspect ratio of 6 for this particular combination of power loading and span loading. At lower aspect ratios, the higher induced drag and profile drag, as well as the increasing wing weight, tend to cause the distances to increase. The operating conditions are also moving away from the optimum, since it has been shown that lower lift coefficients are desirable for lower aspect ratios. Stated in another manner, at values of aspect ratio below 6 for this particular configuration, small decreases in take-off distances might be realized if the airplane were held on the ground until it had accelerated to a higher speed (represented by the optimum C_L for that aspect ratio) before beginning the climb. The effect of decreasing aspect ratio is found to decrease landing distances over the range of configurations investigated.

Longitudinal stability and control.- The method by which an analysis of the longitudinal stability and control is made is covered in detail in appendix C.

A study of figures 28 to 32 indicates that the selected airplane with the modified wing will be longitudinally stable throughout the range of lift coefficients available. The value of $-\left(dC_m/dC_L\right)$ for the case of flaps down 5° for cruise operation with the center of gravity located at 35 percent mean aerodynamic chord is 0.127. This value increases for flap deflections of 30° and for forward movement of the center of gravity.

For the take-off consideration, with flaps deflected 30° and a speed of 50 miles per hour, 28° up elevator is required for trim with the center of gravity at 15 percent mean aerodynamic chord. The required amount of up elevator decreases as the center of gravity moves rearward, and, for the 50 miles-per-hour speed, is 19.6° for the center of gravity at 25 percent mean aerodynamic chord and 10.7° for 35-percent mean-aerodynamic-chord location. At 45 miles-per-hour take-off speed, the required elevator deflection for trim rapidly increases. Figure 29 shows that 25° up elevator is required for the 25-percent mean-aerodynamic-chord center-of-gravity location and that 14° is required for the center of gravity at 35 percent mean aerodynamic chord. At this low speed and with the configuration studied, the elevator deflection for the center-of-gravity location at 15 percent mean aerodynamic chord is out of the usable range. As the speed increases the elevator becomes more effective and the airplane will trim at lower values of elevator deflection.

The cruise condition with flaps deflected 5° is found to be less critical than the take-off consideration. This is as expected since

the pitching-moment coefficient for flaps down 5° is only some 30 percent of the value for the 30° flap deflection. Elevator deflections from 15° up to about 5° down cover both the center-of-gravity and speed range of the airplane.

Lateral control.- The problem of maintaining adequate lateral control, especially at low speeds, is one of primary importance. If the airplane is to operate successfully, it must not only be capable of demonstrating the level of performance demanded but also possess satisfactory flying and handling qualities.

With the decision to use a full-span flap to obtain the high lift for good take-off performance, the method of securing adequate lateral control must be carefully considered.

A study of the section data of reference 7 shows that the lift coefficient is increased with flap deflection to a deflection of some 30°. At a deflection of 35°, no further increase in c_l is obtained, and, at higher deflections, the value of c_l is decreased.

The investigation of the take-off performance revealed that the 30° flap deflection was about the optimum setting but, for good landing characteristics, it might be desirable to use higher deflections to decrease the value of L/D and steepen the glide path.

Consideration of the lateral-control problem, since the full-span flaps are to be used differentially as ailerons, limits the amount of deflection to be used. It is desired so to arrange the aileron control that, when it is deflected downward, an increase in lift on the wing is obtained. With the flaps full down, the flap on one wing is raised so that the lift decreases and a rolling maneuver is executed. The other flap, with the control linkage assumed, rotates downward a small amount and returns to the original position. In order to eliminate the possibility of a loss of lift with the downward deflection on this wing, the limit flap deflection was taken as 30°.

An example of the method used for the analysis of the lateral-control problem is presented in appendix B.

Using the rolling criterion of reference 56, which sets up the minimum value of $pb/2V = 0.07$, and using the equation for the prediction of aileron effectiveness from the same source, the deflections of the full-span flaps used differentially as ailerons were determined and evaluated.

The adverse yawing tendencies associated with the rolling maneuvers for the flaps-up condition at both low and high speed and for the

low-speed condition with flaps down were determined in the manner described in the example in appendix C.

Figure 33 shows that, for the flaps-up condition and at a fairly low speed (75 mph), only 7° rudder deflection is required to overcome the adverse yaw. The required rudder deflection decreases as the speed increases. For the flaps-down condition at 50 miles per hour, 10.75° rudder deflection is required, and the deflection decreases to 4.5° at 75 miles per hour.

The present vertical-tail arrangement of the selected airplane allows 15° deflection to either side. All calculated values of the amount of rudder deflection required to overcome the adverse yaw due to rolling throughout the entire speed range and within the deflection limits of the full-span flaps are well within the limits of the existing tail configuration.

CONCLUSIONS

The results of an analytical investigation of the effects of high-lift flaps on the take-off characteristics of light airplanes indicate the following conclusions:

1. The shortest distances to take off and climb to a height of 50 feet are obtained only when both the span loading and the power loading are low.

2. Both the ground friction and the air drag are of critical importance with heavy span and power loadings, but they are relatively unimportant at the lightest loadings considered.

3. For each combination of span and power loadings there is an optimum take-off speed which varies but slightly with changes in drag or aspect ratio.

4. The shortest distances to take off and climb to a height of 50 feet are obtained with aspect ratios of less than 3 and a maximum lift coefficient of approximately 1.4, although distances only slightly greater can be obtained with aspect ratios of 6 to 8 if proportionately higher lift coefficients are available so that the same take-off speed is used.

5. The optimum value of maximum lift coefficient for the take-off over a 50-foot obstacle with airplanes having aspect ratios of 6 to 8 is in the neighborhood of 3.0.

6. Although flapped wings with maximum values of section lift coefficient of 3.0 are available, the best of those which are simple enough to be suitable for personal airplanes have values of approximately 2.5.

7. The experimental data available are not adequate to determine the optimum airfoil camber, thickness, or thickness distribution to obtain high lift with low drag. It appears that the maximum lift coefficient is so critically influenced by secondary factors, such as surface condition and the nature of the air flow in the wind tunnel, that the underlying trends due to section variations are masked.

8. For the purpose of the present study, one of the most likely high-lift arrangements for use on personal airplanes is the single slotted flap covering the entire span of the wing. Lateral control can be obtained simply by deflecting the right and left wing flaps differentially as ailerons, with the rudder tied in elastically to overcome the adverse yawing moment.

9. The high-lift and lateral-control arrangement selected, when applied to a typical four-place personal airplane, could improve the take-off distance required to clear a 50-foot obstacle by 25 percent, apparently with no detrimental effect on the speed and climb performances or on the weight or simplicity of construction.

Agricultural and Mechanical College of Texas
College Station, Texas, June 1, 1949

APPENDIX A

METHOD FOR MAKING CORRECTIONS FOR REYNOLDS NUMBER AND ROUGHNESS

DISCUSSION OF METHOD

Table II summarizes data taken from references on high-lift-device arrangements. Most of these data are based on wind-tunnel tests of smooth airfoils of infinite aspect ratio at Reynolds numbers of 3×10^6 and above. The practical application of these data to the problem of personal-airplane take-off requires that they be corrected to a take-off Reynolds number of about 1.5×10^6 and to the airfoil surface roughness likely to occur under operating conditions. A method for making these corrections has been developed.

Correction of $c_{l_{max}}$ for Reynolds number.- The variation of $c_{l_{max}}$ with Reynolds number for various NACA basic airfoils is published in reference 1; curves giving the variation for certain of these airfoils are shown in figure 34. However, there is little information available that shows this variation for the 6-series sections in the low Reynolds number range. The values of $c_{l_{max}}$ for these low-drag basic airfoils at Reynolds numbers of approximately 3, 6, and 9×10^6 were studied, and, for certain of the sections, plots of $\Delta c_{l_{max}}$ against Reynolds number were made and are shown in figure 35. These sections were classified as to the type of curve, as outlined in reference 1, that they most nearly fit. The same types of curves were made for certain 6-series sections with flaps, and it was found that these curves could be similarly classified. This is shown in figure 36.

Correction of c_{d_o} at $0.9c_{l_{max}}$ for Reynolds number.- Because of the difficulties involved in measuring drag at high lift by the usual wind-tunnel techniques, it is felt that published values of c_{d_o} at $0.9c_{l_{max}}$ for basic airfoil sections may be subject to doubt, and the same values for airfoils equipped with high-lift devices are even more doubtful. Since these basic data are questionable, any corrections applied to them will be open to question, also. Reference 7 contains drag data for the NACA 65_3-418 section with a double slotted flap at a Reynolds number of 1.9×10^6 and lift data at a Reynolds number of 6×10^6. An attempt was made to utilize these data in developing the method of correcting c_{d_o} for Reynolds number, but, since the

drag data were not given for the higher lift coefficients for any of the flap deflections and since no data were available for that particular airfoil and flap combination at Reynolds numbers higher than 1.9×10^6, no satisfactory correlation could be obtained. However, a method is outlined for making Reynolds number corrections. This method gave reasonable results when used in the analysis of the particular airfoil and flap configuration selected but is not proposed as being applicable to all other configurations. The method is as follows:

(1) Correct $(c_{d_o})_{min}$ to $R = 1.5 \times 10^6$. This is done by extrapolation from higher Reynolds numbers. Reference 1 suggests a method of extrapolating, but this method should be used with caution when applied to low-drag airfoils. Graphical extrapolation is possible, providing the typical reflex of the curve does not fall in the range of Reynolds numbers involved.

(2) Draw an approximate curve of c_{d_o} against c_l at $R = 1.5 \times 10^6$ through the corrected value of $(c_{d_o})_{min}$ and duplicate the shape of the curve for the next highest Reynolds number for which a curve is known. This approximate curve is drawn only to high enough values of c_l to establish the trend of the increase in c_{d_o} beyond $(c_{d_o})_{min}$ with c_l. Fair out the "bucket" of the drag curve to approximate the typical curve of a conventional airfoil. Locate the value of $c_{l_{opt}}$ at the minimum c_{d_o} of the faired curve. (See fig. 42 of reference 6).

(3) Determine the value of $\frac{0.9c_{l_{max}} - c_{l_{opt}}}{c_{l_{max}} - c_{l_{opt}}}$. From figure 37, taken from reference 6, find Δc_{d_o}. Add this Δc_{d_o} to $(c_{d_o})_{min}$ of the faired curve to obtain c_{d_o} at $0.9c_{l_{max}}$.

Correction of $c_{l_{max}}$ for roughness.- A study of the effect of surface roughness on $c_{l_{max}}$ indicates that this effect varies with Reynolds number and airfoil thickness, the greatest loss in $c_{l_{max}}$ occurring for thin airfoils at high Reynolds numbers. Figure 38, taken from reference 8, shows the effect of roughness on $c_{l_{max}}$ at various Reynolds numbers for several low-drag airfoils with flaps.

Correction of c_{d_o} at $0.9c_{l_{max}}$ for roughness.- In order to correct c_{d_o} at $0.9c_{l_{max}}$ for surface roughness, it is assumed that the effect of roughness is to cause the laminar boundary layer (assumed to exist from the leading edge to the minimum pressure point) to change completely to a turbulent boundary layer. It is further assumed that the change in c_{d_o} with roughness at a given Reynolds number is proportional to the change in the skin-friction drag coefficient that occurs when the boundary layer of a flat plate having a chord equal to the distance from the leading edge of the airfoil to the minimum pressure point changes from completely laminar to completely turbulent. This may be expressed as,

$$\frac{\left[\left(\Delta c_{d_o}\right)_{min}\right]_{R_1}}{\left(c_{f_T} - c_{f_L}\right)_{R_1}} = \frac{\left[\left(\Delta c_{d_o}\right)_{min}\right]_{R_2}}{\left(c_{f_T} - c_{f_L}\right)_{R_2}}$$

It is assumed that Δc_{d_o} at $0.9c_{l_{max}}$ due to roughness will have the same value as $\left(\Delta c_{d_o}\right)_{min}$ due to roughness.

EXAMPLE OF CALCULATION OF CORRECTED COEFFICIENTS

Corrections as outlined in the above method are made for item 11 of table II.

Correction of $c_{l_{max}}$ for Reynolds number.- The curve of Reynolds number against $\Delta c_{l_{max}}$ for the basic NACA 63,4-420 section is shown in figure 35. This variation corresponds to curve D-0 of figure 34. The correction is determined as follows:

At $R = 1.5 \times 10^6$,

$$\Delta c_{l_{max}} = -0.42$$

At $R = 6 \times 10^6$,

$$\Delta c_{l_{max}} = -0.05$$

The change in $c_{l_{max}}$ from the value at $R = 6 \times 10^6$ due to the decrease in R is -0.37 for the basic section. Since no data showing the value of the reduction in $c_{l_{max}}$ for single slotted flaps are available, it is assumed the reduction is the same as that for the basic airfoil.

At $R = 6 \times 10^6$ and $\delta_f = 30^\circ$,

$$c_{l_{max}} = 2.82 \text{ (fig. 39)}$$

At $R = 1.5 \times 10^6$ and $\delta_f = 30^\circ$,

$$c_{l_{max}} = 2.82 - 0.37$$

$$= 2.45$$

$$0.9c_{l_{max}} \text{ (uncorrected for roughness)} = 2.06$$

Correction of c_{d_o} at $0.9c_{l_{max}}$ for Reynolds number.- The correction of c_{d_o} at $0.9c_{l_{max}}$ for Reynolds number is determined as follows:

(1) At $R = 1.5 \times 10^6$,

$$(c_{d_o})_{min} = 0.0059$$

for the basic NACA 63,4-420 section (fig. 40).

$$\left[(c_{d_o})_{min} \text{ at } R = 1.5 \times 10^6\right] - \left[(c_{d_o})_{min} \text{ at } R = 6 \times 10^6\right] = 0.0059 - 0.0058$$

$$= 0.0001 \text{ (fig. 41)}$$

Assuming that the $\left(c_{d_o}\right)_{min}$ increment holds good for a flap deflection of 30°,

$$\left[\left(c_{d_o}\right)_{min} \text{ at } R = 1.5 \times 10^6\right] = \left[\left(c_{d_o}\right)_{min} \text{ at } R = 6 \times 10^6\right] + 0.0001$$

$$= 0.0097 + 0.0001$$

$$= 0.0098 \text{ (fig. 42)}$$

(2) Using $\left(c_{d_o}\right)_{min} = 0.0098$, an approximate curve of c_{d_o} against c_l at $R = 1.5 \times 10^6$ and $\delta_f = 30°$ is drawn (fig. 42). The low-drag "bucket" of this curve is faired out, and $c_{l_{opt}} = 0.5$ is located at $c_{d_o} = 0.0102$.

$$(3) \quad \frac{0.9c_{l_{max}} - c_{l_{opt}}}{c_{l_{max}} - c_{l_{opt}}} = \frac{2.06 - 0.8}{2.45 - 0.8} = 0.764$$

$$\Delta c_{d_o} = 0.014 \text{ (fig. 37)}$$

$$c_{d_o} \text{ at } 0.9c_{l_{max}} \text{ (uncorrected for roughness)} = 0.0102 + 0.0123$$

$$= 0.0225$$

Correction of $c_{l_{max}}$ for roughness.- A study of roughness effect indicates that a reduction in $c_{l_{max}}$ of 0.10 at a Reynolds number of 1.5×10^6 is reasonable. At $R = 1.5 \times 10^6$ and $\delta_f = 30°$, $c_{l_{max}} = 2.45 - 0.10 = 2.35$ and $0.9c_{l_{max}} = 2.11$.

Correction of c_{d_o} at $0.9c_{l_{max}}$ for roughness.- For the basic airfoil at $R = 6 \times 10^6$, the increase in $(c_{d_o})_{min}$ due to roughness is 0.0045 (fig. 41).

$$c_{f_L} = 2.65(R)^{-1/2}, \text{ from reference 1}$$

$$c_{f_T} = 0.910(\log R)^{-2.58}, \text{ from reference 1}$$

For the first 30 percent of the chord:

At $R = 6 \times 10^6$,

$$c_{f_L} = 2.65\left(0.3 \times 6 \times 10^6\right)^{-1/2} = 0.00198$$

$$c_{f_T} = 0.910 \log \left(0.3 \times 6 \times 10^6\right)^{-2.58} = 0.00798$$

At $R = 1.5 \times 10^6$,

$$c_{f_L} = 2.65\left(0.3 \times 1.5 \times 10^6\right)^{-1/2} = 0.00395$$

$$c_{f_T} = 0.910 \log \left(0.3 \times 1.5 \times 10^6\right)^{-2.58} = 0.01045$$

Thus,

$$\frac{\left[\left(\Delta c_{d_o}\right)_{min}\right]_6}{\left(c_{f_T} - c_{f_L}\right)_6} = \frac{\left[\left(\Delta c_{d_o}\right)_{min}\right]_{1.5}}{\left(c_{f_T} - c_{f_L}\right)_{1.5}}$$

$$\frac{0.0045}{0.00798 - 0.00198} = \frac{\left[\left(c_{d_o}\right)_{min}\right]1.5}{0.01045 - 0.00395}$$

$$\left[\left(\Delta c_{d_o}\right)_{min}\right]1.5 = 0.00650$$

Therefore,

$$c_{d_o} \text{ at } 0.9c_{l_{max}} = 0.0225 + 0.0065 = 0.0290$$

A similar analysis was made of the NACA 65,3-118 airfoil and flap (item 6 of table II); a flap deflection of 20° was used because data at higher deflection angles were insufficient to use with this method. The following values were obtained:

$c_{l_{max}}$ ($R = 6 \times 10^6$, $\delta_f = 20°$) = 2.45

$c_{l_{max}}$ ($R = 1.5 \times 10^6$, $\delta_f = 20°$) = 2.20

$c_{l_{max}}$ ($R = 1.5 \times 10^6$, $\delta_f = 20°$, corrected for roughness) = 2.10

c_{d_o} at $0.9c_{l_{max}}$ ($R = 6 \times 10^6$, $\delta_f = 20°$) = 0.021

c_{d_o} at $0.9c_{l_{max}}$ ($R = 1.5 \times 10^6$, $\delta_f = 20°$) = 0.0306

c_{d_o} at $0.9c_{l_{max}}$ ($R = 1.5 \times 10^6$, $\delta_f = 20°$, corrected for roughness) = 0.0370

Note that the value of c_{d_o} at the low Reynolds number appears very conservative.

APPENDIX B

FLAP AND AILERON CONTROL MECHANISM

The consideration of improving the take-off performance of personal-type airplanes led to the selection of a full-span, single slotted flap as the high-lift device best suited to this purpose (from section "Selection of High-Lift Device"). Since it is desired to present a practical solution to the problem and since satisfactory lateral control is of primary importance, it is felt that the presentation of a simple form of control mechanism that will actuate the movable surfaces both as flaps and as ailerons should be included.

In the following explanation, the movable wing surfaces are referred to as flaps when they are being actuated as flaps and as ailerons when they are actuated for lateral control.

For the externally hinged surface, the normal "up" position of the flaps for the cruise condition is 5° down. No appreciable increase in drag over 0° flap deflection is indicated by section data (reference 4) for the range of lift coefficients involved. This allows some small upward movement of the surfaces for aileron action. Section data show that, as the flaps are deflected above 30°, no further increase in C_L is obtained, and above 35° the maximum value of C_L begins to decrease. Since a decrease in lift with a downward deflection of ailerons is undesirable, the maximum down position of the flap is limited to 30°. This is adequate for both the take-off and landing consideration.

The control mechanism operates push rods connected to bell cranks. Dual cables may be routed from these bell cranks to a bell crank in each wing. The bell crank in the wing, through a push rod, can raise or lower the surfaces for both flap and aileron action. Some types of installations may lend themselves more readily to a complete push-rod system. The type of system is of no consequence, since the total action is governed by the central control mechanism.

The control mechanism is made up of a "T" arrangement consisting of a crossbar mounted on a vertical shaft which is capable of rotation in two planes. This is provided by incorporating a universal joint in the shaft at the base of the T. The shaft is free to rotate in a tube which is rigidly connected at the base of the T to an axis perpendicular to the center shaft. The universal joint permits rotation of the crossbar of the T by a rigidly mounted power source driving the center shaft, even though the tube housing the shaft may be rotated away from the vertical.

Push rods connect the bell cranks to the crossbar. Rotating the crossbar operates the surfaces together as flaps. Rotation about the axis at the base of the T operates the surfaces as ailerons. This action is, of course, provided by connections to the control wheel. Since flap action and aileron action are separately provided, simultaneous operation of both mechanisms is possible. Schematic diagrams will serve to illustrate the action of the system.

Figure 43(a) shows the flaps in the cruise or "up" position with ailerons neutral. It should be noted that, in the front view (fig. 43(b)), a line joining the pin connections between the crossbar and push rods to the base of the T is at an angle of 60° to a vertical plane passing through the axis of rotation.

Control movement for a left bank with the flaps in the cruise position is shown in figure 43(c). It was determined that a 15° displacement between the ailerons is required to provide a satisfactory rate of roll. The T section is rotated about its base, or x-axis, and that rotation is taken as 0° to 360° in a clockwise direction. The left side of the crossbar is rotated from 300° through 270° (dead center) to a stop position at 240°. This 60° displacement actuates the bell-crank system so that the left aileron is moved upward approximately 2° and returned to the original 5° down position. The right side of the crossbar is rotated from its original position at 60° to 0°, and this movement actuates the bell cranks to lower the right aileron to 20°. This action provides the required aileron displacement and a rolling moment resulting in a bank to the left. Rotation of the control wheel to the right produces the same effect in the opposite direction.

Rotation of the crossbar about the vertical or z-axis actuates the bell cranks together to result in deflecting the flaps. A schematic diagram of the action is shown in figure 43(d). Note in the front view of the diagram (fig. 43(e)) that the positions of the ends of the crossbar are now reversed, with the pin connecting the push rod to the left aileron at 60° and the pin connecting the push rod to the right aileron at 300°.

Figure 43(f) shows a diagram of the system for a left bank. For control-wheel rotation to the left, the pin connection at 60° moves to 0° actuating the bell crank to raise the left aileron to 15°. The pin connection at 300° moves down through 270° to 240°, but, with the crossbar in the position for flaps down, this lowers the right aileron approximately 2° and returns it to its original position of 30° down. This provides an aileron displacement to produce a rolling motion to the left. Opposite movement of the control wheel produces the opposite aileron deflection and a bank to the right.

When the crossbar is rotated so that both pin connections in the front view are at 0°, the flaps are deflected to the midposition. Movement of the control wheel in either direction produces equal up-and-down deflection of the ailerons. The stop limit of 60° to either side is still satisfactory since the radius (in the front view) about the x-axis is greatly reduced, which reduces the lateral displacement of the pin connections. Full movement of the control wheel produces only a 15° displacement between ailerons.

The same aileron differential has been maintained throughout the range of flap deflection. The slope of the lift curve decreases somewhat with flap deflection, resulting in increased aileron effectiveness at the high deflections. This, in turn, results in slightly increased values of $pb/2V$ for the take-off and landing configuration. This was considered desirable for the low-speed condition. Variations in aileron differential action with flap deflection could be realized by simply varying the length and angular displacement of the crossbar. This would change the radius of the push rod connecting pins with respect to the x-axis of rotation, thus changing the lateral displacement of the pin connections and the angular movement of the bell cranks.

The high-lift device selected with the hinge location shown in figure 3, reference 7, indicates the use of either external hinges or tracks. For simplicity, external brackets were assumed for this analysis. Another type of flap support which may be housed within the wing contour is shown in figure 44. The linkage shown will not provide exactly the same movement throughout the range of flap deflections as that with the external hinge or track. Two positions (probably the cruise and take-off positions) may be selected and the mechanism may be designed to provide correct positioning at these deflections. Intermediate deflections will slightly alter the width of the slot.

There are a number of variations of the mechanism that would actuate the system. There are, no doubt, differences in weight and complexity for each design but no attempt is made to analyze various arrangements. The control mechanism presented is simply one method by which the desired operation may be obtained.

APPENDIX C

STABILITY AND CONTROL

Longitudinal stability and control.- The airfoil data for the modified configuration of the typical airplane described in this report were taken from reference 7, figure 3. The procedure followed in this analysis is from reference 57, chapter 4.

The equation for the pitching-moment coefficient for the complete airplane is given as

$$C_m = \left[\left(\frac{\delta}{c} - \frac{h}{c}\right) - \eta_t \frac{lS_t}{cS} \frac{1 - \left(a_o/\pi A\right)}{1 + \left(a_o/\pi A_t\right)}\right] C_L + C_{m_o} + \eta_t \frac{lS_t}{cS} \frac{a_o}{1 + \left(a_o/\pi A_t\right)} \alpha_d$$

where

δ	distance of center of gravity from wing leading edge
h	distance of aerodynamic center from leading edge
η_t	tail efficiency factor
l	tail length
c	mean aerodynamic chord
S_t	tail area
S	wing area
a_o	slope of section lift curve (assumed the same for both wing and tail)
A	wing aspect ratio
A_t	tail aspect ratio
C_{m_o}	moment coefficient about aerodynamic center
α_d	decalage angle $\left(\alpha_{wing} - \alpha_{tail}\right)$

A schematic diagram of the skeleton airplane shows the forces and notations:

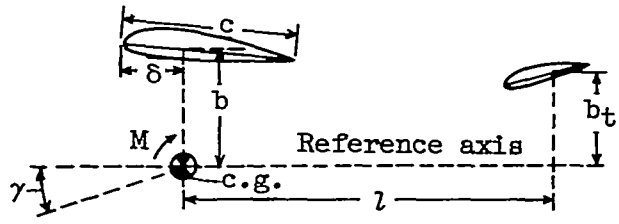

The effect of vertical center-of-gravity displacement is taken into account by the empirical correction stating that

$$\frac{\delta_{eff}}{c} = \frac{\delta_{true}}{c} - \frac{l}{10}\frac{b}{c}$$

where b is the vertical displacement of the wing chord line from the reference axis and the effect of the destabilizing influence of the fuselage is taken as

$$\Delta\left(\frac{dC_m}{dC_L}\right)_{fuselage} = 0.03$$

A full explanation of these factors is contained in reference 57.

The equation for the trim condition of the airplane with the corrections included becomes

$$C_m = \left\{\left[\frac{\delta_{true}}{c} - \frac{l}{10}\frac{b}{c} + \Delta\left(\frac{dC_m}{dC_L}\right)_{fuselage} - \frac{h}{c}\right] - \eta_t \frac{lS_t}{cS}\frac{1 - \left(a_o/\pi A\right)}{1 + \left(a_o/\pi A_t\right)}\right\}C_L +$$

$$C_{m_o} + \left[\eta_t \frac{lS_t}{cS}\frac{a_o}{1 + \left(a_o/A_t\right)}\right]\alpha_d$$

It is assumed that the modified wing is of rectangular plan form and that the incidence is the same as that for the original airplane. Using section data from figure 3 of reference 7 and the methods described in chapter 1 of reference 57, the characteristics of the modified wing were determined. All other dimensions and areas were taken directly from drawings and data on the selected airplane.

Since it is assumed in the basic theory that the moment coefficient remains constant with aspect ratio, and since the angle of zero lift is constant, it is not necessary to determine the characteristics of the finite wing. All terms of the above equation can be taken from the section data, dimensions, or assumed values from reference 57.

The first condition investigated is for flaps deflected 30°. The equation for the moment coefficient in terms of the lift coefficient C_L for the center of gravity at 25 percent mean aerodynamic chord becomes,

$$C_m = \left[\left(0.25 - \frac{1}{10}\frac{30.52}{60.9} + 0.03 - 0.25\right) - 0.80\,\frac{(161.21)(38.4)}{(60.9)(192)}\,\frac{1 - (6.02/7.5\pi)}{1 + (6.02/3.64\pi)}\right]C_L +$$

$$C_{m_o} + 0.80\,\frac{(161.21)(38.4)}{(60.9)(192)}\,\frac{6.02}{1 + (6.02/3.64\pi)}\,(0.301)$$

$$= \left[(-0.02) - (0.206)\right]C_L + C_{m_o} + 0.503$$

$$= -0.226C_L + C_{m_o} + 0.503$$

With a longitudinal shift in the center of gravity, the value of δ/c will change and, for the conditions selected, the values of the first term in the above equation become $-0.334C_L$ for the center of gravity at 15 percent mean aerodynamic chord, $-0.226C_L$ for the center of gravity at 25 percent mean aerodynamic chord, and $-0.118C_L$ for the center of gravity at 35 percent mean aerodynamic chord.

For conditions of a deflected elevator, the value of the decalage will change. From reference 57, page 150,

$$\Delta\alpha_d = -Ke$$

where

K function of ratio of elevator to total tail chord (from fig. 4.9, reference 57)

e elevator deflection, positive for down elevator

The value of K for the horizontal surface is, for

$$\frac{\text{Elevator chord}}{\text{Mean tail chord}} = \frac{13.5"}{37.0"} = 0.365$$

$$K = 0.67$$

For the values of elevator deflection selected, for a center-of-gravity position at 25 percent mean aerodynamic chord, the values of C_m due to decalage are as follows:

10° down elevator $\left(C_m\right)_{\alpha_d} = 0.308$

0° elevator $\left(C_m\right)_{\alpha_d} = 0.503$

10° up elevator $\left(C_m\right)_{\alpha_d} = 0.699$

20° up elevator $\left(C_m\right)_{\alpha_d} = 0.894$

Values of C_m for various values of C_L were computed for different center-of-gravity locations and elevator deflections. Curves for the results are shown in figure 28.

For the condition of flaps down 5° for the cruise operation, the last two terms of the moment-coefficient equation will change. The

values of C_{m_o} for various values of C_L are obtained from the section data of reference 7. The last terms of the equation vary with the decalage angle. Since

$$\alpha_d = \alpha_{wing} - \alpha_{tail}$$

Then, for the modified airplane, with the elevator at 0° deflection,

$$\alpha_d = (5 + 2.25) - (-1)$$

$$= 8.25^\circ$$

$$= 0.144 \text{ radian}$$

For values of elevator deflections selected for the 25-percent center-of-gravity position, the values of C_m due to decalage are

$$10^\circ \text{ down elevator } \left(C_m\right)_{\alpha_d} = 0.045$$

$$0^\circ \text{ elevator } \left(C_m\right)_{\alpha_d} = 0.241$$

$$10^\circ \text{ up elevator } \left(C_m\right)_{\alpha_d} = 0.436$$

$$20^\circ \text{ up elevator } \left(C_m\right)_{\alpha_d} = 0.631$$

Values of C_m for various values of C_L were computed for different center-of-gravity locations and elevator deflections. Results are plotted in figure 30.

Lateral control.- The method by which the amount of rudder deflection required to overcome the adverse yaw during a roll was obtained is covered in the following example. The basic conditions are:

Gross weight $W = 2280$ pounds

Velocity $V = 100$ miles per hour

Lift coefficient $C_L = 0.465$

From reference 56 a satisfactory measure of the rate of roll based on aileron effectiveness is given by the expression:

$$\frac{pb}{2V} = \left(\frac{C_{l_\delta}}{k}\right) \frac{(k)(\Delta\delta_a)}{(114.6)C_{l_p}} = 0.07$$

where

C_{l_δ} rate of change of rolling-moment coefficient with aileron angle δ

k aileron effectiveness factor; effective change in angle of attack of wing-aileron section per unit aileron deflection $(\Delta\alpha/\Delta\delta)$

$\Delta\delta_a$ angular difference between up and down ailerons, degrees

C_{l_p} rate of change of rolling-moment coefficient with helix angle

Using the curves in figure 2, reference 56, for the taper ratio and aspect ratio selected, and assuming that there is no loss in lift across the fuselage:

$$C_{l_p} = 0.54$$

From a cross plot of the data in figure 16, reference 58, and figure 1, reference 56, for values of C_{l_δ}/k against A,

$$C_{l_\delta}/k = 0.87$$

For the cruise condition, with flaps deflected 5°, the change in angle of attack with flap deflection at the value of lift coefficient involved is:

$$\frac{\Delta\alpha}{\Delta\delta} = k = 0.33$$

This approximate value, taken from the section data of figure 3, reference 7, holds for aileron deflections up to about 20°.

Substituting these values in the equation for aileron effectiveness

$$(0.87)\frac{(0.33)(\Delta\delta_a)}{(114.6)(0.54)} = 0.07$$

$$\Delta\delta_a = 0.07\frac{(114.6)(0.54)}{(0.87)(0.33)}$$

$$= 15.1^\circ$$

The condition under investigation is for a coordinated maneuver in which there is no sideslip and the rudder forces are determined for that condition.

Assuming a differential aileron movement for which a tentative linkage has been studied, the angular displacement of 15.1°, starting from a position of 5° down, will be obtained with a 5° deflection on one wing and 20.1° on the other.

From a cross plot of the curves in figure 13, reference 52, for the aspect ratio and taper ratio involved,

$$C_l/\Delta\alpha = 0.0078$$

where C_l is the rolling-moment coefficient, and, since

$$\Delta\alpha = k\,\Delta\delta_a$$

$$= 0.33 \times 15.1^\circ$$

$$= 4.98^\circ$$

then,

$$C_l = 0.0078 \times 4.98^\circ$$

$$= 0.0388$$

The induced yawing moment for ailerons with differential deflection is calculated from the theory developed in reference 52. The increment C_n/C_l for the aileron differential of 15.1° is based on a mean deflection of -7.55° and determined from the equation,

$$\Delta(C_n/C_l) = k\,\Delta\alpha_m$$

where

C_n yawing-moment coefficient

$\Delta\alpha_m$ incremental effective angle-of-attack change resulting from aileron deflection

The value of k, taken from figure 15, reference 52, and corrected for aspect ratio is

$$k = \frac{6}{7.5}(0.0145)$$

$$= 0.0116$$

and, based on the previously determined value of change in angle of attack with aileron deflection,

$$\Delta\alpha_m = 0.33 \times -7.55^\circ$$

$$= -2.49^\circ$$

Then

$$\Delta(C_n/C_l) = k\,\Delta\alpha_m$$

$$= (0.0116)(-2.49^\circ)$$

$$= -0.0289$$

For the effect of equal up and down deflection for the total angular difference of 15.1°, from the theory of reference 52,

$$C_n/C_l = kC_L$$

From a cross plot of the data in figure 13, reference 52, for the given aspect ratio and taper ratio,

$$k = \frac{C_n/C_l}{C_L} = 0.15$$

For $C_L = 0.465$,

$$C_n/C_l = -(0.15)(0.465) = -0.0697$$

$$\Delta(C_n/C_l) = -0.0289$$

$$\text{Total } C_n/C_l = -0.0986$$

For $C_l = 0.0388$,

$$C_n = (-0.0986)(0.0388)$$

$$= -0.003825$$

and the total induced yawing moment is

$$N = C_n qSb$$

$$= (-0.003825)(25.56)(192)(38)$$

$$= -714 \text{ foot-pounds (adverse yaw)}$$

The yawing moment due to the profile drag of the differentially deflected ailerons (5° and 20.1°) taken from section data of figure 3, reference 7, would be

$$N_{C_{D_o}} = \left[\left(-C_{D_o}\right)_{20.1^\circ}\right](S/2)(b/4)q + \left[\left(C_{D_o}\right)_{5^\circ}\right](S/2)(b/4)q$$

$$= \left\{\left[\left(-C_{D_o}\right)_{20.1^\circ}\right] + \left[\left(C_{D_o}\right)_{5^\circ}\right]\right\}(S/2)(b/4)q$$

$$= (-0.0077 + 0.0062)(192/2)(38/4)(25.56)$$

$$= (-0.0015)(96)(19/2)(25.56)$$

$$= -35.2 \text{ foot-pounds}$$

The total adverse yawing moment is

$$N_{total} = N_{induced} + N_{C_{D_o}}$$

$$= -714 - 35.2$$

$$= 749.2 \text{ foot-pounds}$$

The side force on the vertical surface, then, would be

$$F_v = \frac{N}{l}$$

$$= \frac{749.2}{13.43}$$

$$= 55.6 \text{ pounds}$$

The lift coefficient required from the vertical tail is

$$C_{L_v} = \frac{F_v}{qS}$$

$$= \frac{55.6}{(25.56)(17.43)}$$

$$= 0.1245$$

Using the dimensions of the vertical tail surface of the original airplane, the slope of the lift curve of an NACA 0012 airfoil (reference 5) and a rudder effectiveness factor taken from an extrapolation of figure 11, reference 52 ($\Delta\alpha/\Delta\delta_a$ for unsealed flaps), the rudder angle required to develop the lift coefficient calculated above can be determined.

From data furnished on the airplane, the vertical surface area is 17.48 square feet.

The slope of the lift curve for the aspect ratio of 1.52 and an NACA 0012 airfoil is

$$a = \frac{a_o}{1 + \frac{57.3a_o}{\pi A}}$$

$$= \frac{0.1088}{1 + \frac{(57.3)(0.1088)}{\pi(1.52)}}$$

$$= 0.0473 \text{ per degree}$$

Figure 11 of reference 52 (extrapolated) gives a rudder effectiveness factor of 0.57.

The rudder deflection required to develop the calculated C_L of 0.1245 is

$$\delta_{rudder} = \frac{C_{L_v}}{ak}$$

$$= \frac{0.1245}{(0.0473)(0.57)}$$

$$= 4.62^\circ$$

REFERENCES

1. Wetmore, J. W.: Calculated Effect of Various Types of Flap on Take-Off over Obstacles. NACA TN 568, 1936.

2. Horton, Elmer A., and Quinn, John H., Jr.: Analysis of the Effects of Boundary-Layer Control on the Take-Off Performance Characteristics of a Liaison-Type Airplane. NACA TN 1597, 1948.

3. Wood, Karl D.: Airplane Design. Fourth ed., Cornell Co-Op Soc. (Ithaca, N. Y.), 1939.

4. Ivey, H. Reese, Fitch, G. M., and Schultz, Wayne F.: Performance Selection Charts for Gliders and Twin-Engine Tow Planes. NACA MR L5E04, 1945.

5. Abbott, Ira H., Von Doenhoff, Albert E., and Stivers, Louis S., Jr.: Summary of Airfoil Data. NACA Rep. 824, 1945.

6. Jacobs, Eastman N., and Sherman, Albert: Airfoil Section Characteristics as Affected by Variations of the Reynolds Number. NACA Rep. 586, 1937.

7. Abbott, Ira H., and Fullmer, Felicien F., Jr.: Wind-Tunnel Investigation of NACA 63,4-420 Airfoil with 25-Percent-Chord Slotted Flap. NACA ACR 3I21, 1943.

8. Cahill, Jones F.: Summary of Section Data on Trailing-Edge High-Lift Devices. NACA Rep. 938, 1949.

9. Harris, Thomas A.: Wind-Tunnel Investigation of an N.A.C.A. 23012 Airfoil with Two Arrangements of a Wide-Chord Slotted Flap. NACA TN 715, 1939.

10. Harris, Thomas A., and Recant, Isidore G.: Wind-Tunnel Investigation of NACA 23012, 23021, and 23030 Airfoils Equipped with 40-Percent-Chord Double Slotted Flaps. NACA Rep. 723, 1941.

11. Duschik, Frank: Wind-Tunnel Investigation of an N.A.C.A. 23021 Airfoil with Two Arrangements of a 40-Percent-Chord Slotted Flap. NACA TN 728, 1939.

12. Quinn, John H., Jr.: Wind-Tunnel Investigation of Boundary-Layer Control by Suction on the NACA 65_3-418, $a = 1.0$ Airfoil Section with a 0.29-Airfoil-Chord Double Slotted Flap. NACA TN 1071, 1946.

13. Platt, Robert C.: Aerodynamic Characteristics of a Wing with Fowler Flaps including Flap Loads, Downwash, and Calculated Effect on Take-Off. NACA Rep. 534, 1935.

14. Wenzinger, Carl J., and Harris, Thomas A.: Preliminary Wind-Tunnel Investigation of an N.A.C.A. 23012 Airfoil with Various Arrangements of Venetian-Blind Flaps. NACA Rep. 689, 1940.

15. Wenzinger, Carl J., and Gauvain, William E.: Wind-Tunnel Investigation of an N.A.C.A. 23012 Airfoil with a Slotted Flap and Three Types of Auxiliary Flap. NACA Rep. 679, 1939.

16. Wenzinger, Carl J., and Harris, Thomas A.: Wind-Tunnel Investigation of an N.A.C.A. 23012 Airfoil with Various Arrangements of Slotted Flaps. NACA Rep. 664, 1939.

17. Purser, Paul E., Fischel, Jack, and Riebe, John M.: Wind-Tunnel Investigation of an NACA 23012 Airfoil with a 0.30-Airfoil-Chord Double Slotted Flap. NACA ARR 3L10, 1943.

18. House, R. O.: Tests of an N.A.C.A. 23012 Airfoil with a Slotted Deflector Flap. NACA TN 699, 1939.

19. Fischel, Jack, and Riebe, John M.: Wind-Tunnel Investigation of an NACA 23021 Airfoil with a 0.32-Airfoil-Chord Double Slotted Flap. NACA ARR L4J05, 1944.

20. Bogdonoff, Seymour M.: Wind-Tunnel Investigation of a Low-Drag Airfoil Section with a Double Slotted Flap. NACA ACR 3I20, 1943.

21. Recant, I. G.: Wind-Tunnel Investigation of an NACA 23030 Airfoil with Various Arrangements of Slotted Flaps. NACA TN 755, 1940.

22. Wenzinger, Carl J., and Harris, Thomas A.: Wind-Tunnel Investigation of an N.A.C.A. 23021 Airfoil with Various Arrangements of Slotted Flaps. NACA Rep. 677, 1939.

23. Rogallo, F. M., and Spano, Bartholomew S.: Wind-Tunnel Investigation of an NACA 23012 Airfoil with 30-Percent-Chord Venetian-Blind Flaps. NACA Rep. 742, 1942.

24. Platt, Robert C., and Abbott, Ira H.: Aerodynamic Characteristics of N.A.C.A. 23012 and 23021 Airfoils with 20-Percent-Chord External-Airfoil Flaps of N.A.C.A. 23012 Section. NACA Rep. 573, 1936.

25. Holtzclaw, Ralph W., and Dods, Jules B., Jr.: Wind-Tunnel Investigation of Drooped Ailerons on a 16-Percent-Thick Low-Drag Airfoil. NACA TN 1386, 1947.

26. Lowry, John G.: Wind-Tunnel Investigation of an NACA 23012 Airfoil with Several Arrangements of Slotted Flaps with Extended Lips. NACA TN 808, 1941.

27. Braslow, Albert L., and Loftin, Laurence K., Jr.: Two-Dimensional Wind-Tunnel Investigation of an Approximately 14-Percent-Thick NACA 66-Series-Type Airfoil Section with a Double Slotted Flap. NACA TN 1110, 1946.

28. Cahill, Jones F.: Two-Dimensional Wind-Tunnel Investigation of Four Types of High-Lift Flap on an NACA 65-210 Airfoil Section. NACA TN 1191, 1947.

29. Wenzinger, Carl J., and Shortal, Joseph A.: The Aerodynamic Characteristics of a Slotted Clark Y Wing as Affected by the Auxiliary Airfoil Position. NACA Rep. 400, 1931.

30. Jacobs, Eastman N., Abbott, Ira H., and Davidson, Milton: Investigation of Extreme Leading-Edge Roughness on Thick Low-Drag Airfoils to Indicate Those Critical to Separation. NACA CB, June 1942.

31. Loftin, Laurence K., Jr., and Rice, Fred J., Jr.: Two-Dimensional Wind-Tunnel Investigation of Two NACA Low-Drag Airfoil Sections Equipped with Slotted Flaps and a Plain NACA Low-Drag Airfoil Section for XF6U-1 Airplane. NACA MR L5L11, 1946.

32. Bamber, M. J.: Wind-Tunnel Tests of Several Forms of Fixed Wing Slot in Combination with a Slotted Flap on an N.A.C.A. 23012 Airfoil. NACA TN 702, 1939.

33. Fullmer, Felicien F., Jr.: Wind-Tunnel Investigation of NACA 66(215)-216, 66,1-212, and 65_1-212 Airfoils with 0.20-Airfoil-Chord Split Flaps. NACA CB L4G10, 1944.

34. Davidson, Milton, and Turner, Harold R., Jr.: Tests of an NACA 66,2-216, $a = 0.6$ Airfoil Section with a Slotted and Plain Flap. NACA ACR 3J05, 1943.

35. Abbott, Ira H., and Miller, Ralph B.: Tests of a Highly Cambered Low-Drag-Airfoil Section with a Lift-Control Flap. NACA ACR, Dec. 1942. (See also Supplement, NACA ACR 3D30, 1943.)

48. Fowler, Harlan D.: The Practical Application of Fowler Flaps. Preprint, SAE, 1937.

49. Muse, Thomas C., and Neely, Robert H.: Wind-Tunnel Investigation of an NACA 66,2-216 Low-Drag Wing with Split Flaps of Various Sizes. NACA ACR, Sept. 1941.

50. Molloy, Richard C., and Griswold, Roger W., II: Characteristics of a Deflector-Plate Flap. Preprint, SAE, 1939.

51. Wenzinger, Carl J.: Summary of NACA Investigations of High-Lift Devices. SAE Jour., vol. 44, no. 4, April 1939, pp. 161-172.

52. Weick, Fred E., and Jones, Robert T.: Résumé and Analysis of N.A.C.A. Lateral Control Research. NACA Rep. 605, 1937.

53. Langley Research Staff (Thomas A. Toll, Compiler): Summary of Lateral-Control Research. NACA Rep. 868, 1947.

54. Fischel, Jack, and Ivey, Margaret F.: Collection of Test Data for Lateral Control with Full-Span Flaps. NACA TN 1404, 1948.

55. Jones, Bradley: Elements of Practical Aerodynamics. Third ed., John Wiley & Sons, Inc., May 1946.

56. Gilruth, R. R., and Turner, W. N.: Lateral Control Required for Satisfactory Flying Qualities Based on Flight Tests of Numerous Airplanes. NACA Rep. 715, 1941.

57. Millikan, Clark B.: Aerodynamics of the Airplane. John Wiley & Sons, Inc., 1941.

58. Pearson, Henry A., and Jones, Robert T.: Theoretical Stability and Control Characteristics of Wings with Various Amounts of Taper and Twist. NACA Rep. 635, 1938.

48. Fowler, Harlan D.: The Practical Application of Fowler Flaps. Preprint, SAE, 1937.

49. Muse, Thomas C., and Neely, Robert H.: Wind-Tunnel Investigation of an NACA 66,2-216 Low-Drag Wing with Split Flaps of Various Sizes. NACA ACR, Sept. 1941.

50. Molloy, Richard C., and Griswold, Roger W., II: Characteristics of a Deflector-Plate Flap. Preprint, SAE, 1939.

51. Wenzinger, Carl J.: Summary of NACA Investigations of High-Lift Devices. SAE Jour., vol. 44, no. 4, April 1939, pp. 161-172.

52. Weick, Fred E., and Jones, Robert T.: Résumé and Analysis of N.A.C.A. Lateral Control Research. NACA Rep. 605, 1937.

53. Langley Research Staff (Thomas A. Toll, Compiler): Summary of Lateral-Control Research. NACA Rep. 868, 1947.

54. Fischel, Jack, and Ivey, Margaret F.: Collection of Test Data for Lateral Control with Full-Span Flaps. NACA TN 1404, 1948.

55. Jones, Bradley: Elements of Practical Aerodynamics. Third ed., John Wiley & Sons, Inc., May 1946.

56. Gilruth, R. R., and Turner, W. N.: Lateral Control Required for Satisfactory Flying Qualities Based on Flight Tests of Numerous Airplanes. NACA Rep. 715, 1941.

57. Millikan, Clark B.: Aerodynamics of the Airplane. John Wiley & Sons, Inc., 1941.

58. Pearson, Henry A., and Jones, Robert T.: Theoretical Stability and Control Characteristics of Wings with Various Amounts of Taper and Twist. NACA Rep. 635, 1938.

TABLE I.- SUMMARY OF COMPUTED DATA

Span loading, W/b^2 (lb/sq ft)	Wing loading, W/S (lb/sq ft)	Aspect ratio, A	Power loading, W/P (lb/bhp)	Gross weight, W (lb)	Wing span, b (ft)	Wing area, S (sq ft)	Engine power, P (bhp)	Additional drag coefficient at take-off $\Delta C_{D_t} = 0$					Additional drag coefficient at take-off $\Delta C_{D_t} = 0.1$			Additional drag coefficient at take-off $\Delta C_{D_t} = 0.2$		
								$C_{L_{max}}$	V_{max} (ft/sec)	s_g (ft)	V_{max} (mph)	s_t (ft)	$C_{L_{max}}$	s_g (ft)	s_t (ft)	$C_{L_{max}}$	s_g (ft)	s_t (ft)
Ground friction coefficient $\mu = 0.20$																		
0.75	5.62	7.5	20	3550	68.8	632	178	2.20	---	937	---	1513	----	----	------	--------	--------	--------
1.0	5.0	5.0	10	Above 5000	----	---	---	----------	---	----	---	----	----	----	------	--------	--------	--------
			15	7000	84.6	1400	466	1.80	223	435	152	870	----	----	------	--------	--------	--------
			20	3750	61.2	750	188	1.65	178	1000	121	1640	----	----	------	--------	--------	--------
	7.5	7.5	12.5	4500	67.1	600	360	3.00	252	276	172	680	2.97	335	830	2.98	408	1128
			15	3450	58.6	460	230	2.76	221	437	151	898	----	----	------	--------	--------	--------
			17.5	2980	54.6	398	170	2.62	196	648	134	1204	2.55	914	1,840	2.55	2530	6250
	10	10	12.5	3375	60.0	338	266	4.00	254	300	173	707	----	----	------	--------	--------	--------
			15	2940	53.4	284	190	3.58	224	452	153	923	----	----	------	--------	--------	--------
			20	2425	49.1	243	121	2.95	186	1355	127	2014	----	----	------	--------	--------	--------
1.1	8.25	7.5	10	7300	81.5	885	730	3.30	297	253	202	615	----	----	------	--------	--------	--------
1.5	11.25	7.5	10	4500	54.8	400	450	3.66	282	291	199	686	3.48	333	778	3.44	383	962
			12.5	3180	46.0	283	254	3.30	254	407	173	860	----	----	------	--------	--------	--------
			15	2650	42.1	236	177	3.05	214	635	146	1168	2.96	734	1,580	2.90	1120	2950
			17.5	2430	40.3	216	139	2.75	192	1010	131	1693	----	----	------	--------	--------	--------
	15	10	20	2100	37.4	140	105	3.30	180	2060	123	2958	----	----	------	--------	--------	--------
2.0	5	2.5	15	4200	49.0	840	280	1.23	204	685	139	1364	----	----	------	--------	--------	--------
	10	5	10	4000	44.7	400	400	2.75	279	324	190	754	----	----	------	--------	--------	--------
			15	2675	36.6	268	178	2.25	206	736	140	1390	----	----	------	--------	--------	--------
			20	2250	33.6	225	113	1.82	160	2230	109	3260	----	----	------	--------	--------	--------
	15	7.5	10	3650	43.0	243	365	3.80	289	391	197	838	3.73	444	971	3.70	503	1200
			12.5	2775	37.3	185	222	3.50	242	522	165	1030	3.40	624	1,850	3.28	773	1790
			15	2410	34.8	161	161	3.20	210	790	143	1438	3.00	1075	2,070	2.94	1628	4290
			17.5	2200	33.2	147	126	2.84	187	1382	127	2200	----	----	------	--------	--------	--------
			20	2040	32.0	136	102	2.69	168	2420	114	3540	2.50	6510	13,300	No take-off	No take-off	No take-off
	20	10	10	3330	40.8	168	333	Above 4.4	289	----	197	----	----	----	------	--------	--------	--------
			15	2250	33.6	113	150	4.20	214	841	146	1529	----	----	------	--------	--------	--------
			20	1975	31.5	99	99	3.36	178	3040	121	4268	----	----	------	--------	--------	--------
2.5	18.75	7.5	17.5	2075	28.9	111	119	2.96	182	1687	124	2680	2.65	3380	6,200	--------	--------	--------
2.67	20	7.5	20	1960	26.6	98	98	2.70	165	4250	112	6016	----	----	------	--------	--------	--------
3.0	7.5	2.5	10	5400	42.4	721	540	1.55	272	436	185	922	----	----	------	--------	--------	--------
	15	5	10	3500	34.2	233	350	2.82	284	514	193	1014	----	----	------	--------	--------	--------
			15	2325	28.0	157	157	2.35	200	1100	136	1945	----	----	------	--------	--------	--------
			20	1990	25.8	133	96	1.75	154	4800	105	6760	----	----	------	--------	--------	--------
	20	6.67	10	3220	32.8	161	322	3.70	284	525	193	1025	----	----	------	--------	--------	--------
			15	2225	27.3	111	148	3.02	203	1250	138	2090	----	----	------	--------	--------	--------
			20	1950	25.5	98	98	2.40	160	5580	109	8140	----	----	------	--------	--------	--------
	22.5	7.5	10	3120	32.2	139	312	4.20	283	507	193	1028	----	----	------	--------	--------	--------
			12.5	2480	28.7	110	199	3.82	256	754	161	1414	----	----	------	--------	--------	--------
			15	2240	27.3	100	150	3.30	208	1307	142	2183	----	----	------	--------	--------	--------

TABLE I.- SUMMARY OF COMPUTED DATA - Concluded

Span loading, W/b^2 (lb/sq ft)	Wing loading, W/S (lb/sq ft)	Aspect ratio, A	Power loading, W/P (lb/bhp)	Gross weight, W (lb)	Wing span, b (ft)	Wing area, S (sq ft)	Engine power, P (bhp)	Additional drag coefficient at take-off $\Delta C_{D_t} = 0$					Additional drag coefficient at take-off $\Delta C_{D_t} = 0.1$			Additional drag coefficient at take-off $\Delta C_{D_t} = 0.2$		
								$C_{L_{max}}$	V_{max} (ft/sec)	s_g (ft)	V_{max} (mph)	s_t (ft)	$C_{L_{max}}$	s_g (ft)	s_t (ft)	$C_{L_{max}}$	s_g (ft)	s_t (ft)
Ground friction coefficient $\mu = 0.10$																		
1.0	7.5	7.5	12.5	4500	67.1	600	360	2.70	---	180	---	552	----	---	----	----	---	----
			15	3450	58.8	460	230	2.65	---	260	---	702	----	---	----	----	---	----
			17.5	2980	54.6	398	170	2.40	---	330	---	855	2.41	405	1304	----	---	----
1.5	11.25	7.5	10	4500	54.8	400	450	3.58	---	196	---	585	----	---	----	----	---	----
			12.5	3180	46.0	283	254	3.17	---	252	---	722	----	---	----	----	---	----
			15	2650	42.1	236	177	2.85	---	366	---	884	----	---	----	----	---	----
			17.5	2430	40.3	216	139	2.60	---	479	---	1121	----	---	----	----	---	----
2	15	7.5	10	3650	43.0	243	365	3.70	---	260	---	699	----	---	----	----	---	----
			12.5	2775	37.3	185	222	3.35	---	332	---	830	3.25	377	1014	3.05	463	1418
			15	2412	34.8	161	161	3.03	---	462	---	1065	----	---	----	----	---	----
			17.5	2200	33.2	147	126	2.76	---	657	---	1408	----	---	----	----	---	----
3	22.5	7.5	10	3120	32.2	139	312	4.10	---	348	---	850	----	---	----	----	---	----
			12.5	2480	28.7	110	199	3.60	---	478	---	1100	----	---	----	----	---	----
			15	2240	27.3	100	150	3.10	---	710	---	1520	----	---	----	----	---	----
Ground friction coefficient $\mu = 0.05$																		
1.0	7.5	7.5	12.5	4500	67.1	600	360	2.90	---	156	---	536	----	---	----	----	---	----
			15	3450	58.8	460	230	2.75	---	205	---	647	----	---	----	----	---	----
			17.5	2980	54.6	398	170	2.85	---	273	---	778	----	---	----	----	---	----
1.5	11.25	7.5	10	4500	54.8	400	450	3.60	---	164	---	553	----	---	----	----	---	----
			12.5	3180	46.0	283	254	3.02	---	234	---	672	----	---	----	----	---	----
			15	2650	42.1	236	177	2.80	---	286	---	804	----	---	----	----	---	----
			17.5	2430	40.3	216	139	2.52	---	364	---	1012	----	---	----	----	---	----
2.0	15	7.5	10	3650	43.0	243	369	3.60	---	225	---	656	----	---	----	----	---	----
			12.5	2775	37.3	185	222	3.20	---	281	---	764	3.10	320	936	2.95	380	1312
			15	2412	34.8	161	161	2.90	---	372	---	963	----	---	----	2.75	519	3140
			17.5	2200	33.2	147	126	2.55	---	395	---	1130	----	---	----	----	---	----
3.0	22.5	7.5	10	3120	32.2	139	312	4.00	---	297	---	792	----	---	----	----	---	----
			12.5	2480	28.7	110	199	3.40	---	410	---	1005	----	---	----	----	---	----
			15	2240	27.3	100	150	3.00	---	607	---	1335	----	---	----	----	---	----
Ground friction coefficient $\mu = 0.02$																		
2	15	7.5	12.5	2775	37.3	185	222	3.20	---	252	---	735	----	---	----	----	---	----
Ground friction coefficient $\mu = 0$																		
1	7.5	7.5	12.5	4500	67.1	600	360	2.80	---	133	---	509	----	---	----	----	---	----
			17.5	2980	54.6	398	170	2.20	---	216	---	723	----	---	----	----	---	----
2	11.25	7.5	12.5	2775	37.3	185	222	3.18	---	238	---	721	----	---	----	----	---	----

NACA

TABLE II.- SUMMARY OF HIGH-LIFT-DEVICE DATA

Item	High-lift device	NACA airfoil section	Flap chord	R_{eff}	$c_{l_{max}}$ with take-off flap setting	δ_f for take-off (deg)	$c_{l_{max}}$ corrected for R = 1,500,000	c_{d_0} at take-off $c_{l_{max}}$	c_{d_0} for take-off δ_f at c_l = 1.5	2.0	2.5	Maximum $c_{l_{max}}$	δ_f for maximum $c_{l_{max}}$ (deg)	c_{d_0} for $\delta_f = 0°$	Reference	Configuration
1	Double slotted flap	23012	0.1467 .2566	3.5×10^6	3.08	25, 65	2.94	0.20	——	0.072	0.096	3.35	35, 70	0.0056	17	
2	Double slotted flap	23012	.0270 .2566	3.5	3.15	30, 60	3.01	.17	------	.055	.076	3.45	30, 70	.0083	10	
3	Double slotted flap	23021	.1467 .2566	3.5	3.06	30, 60	2.69	.28	——	.118	.175	3.32	30, 70	.0122	19	
4	Double slotted flap	23021	.0267 .2566	3.5	3.00	30, 50	2.63	.18	0.048	.056	.075	3.56	30, 60	.0122	10	
5	Double slotted flap	23030	.0600 .2566	3.5	3.30	30, 50	——	.22	.102	.110	.192	3.70	40, 80	.0175	10	
6	Double slotted flap	65,3-118	.309	6.0	2.68	35	2.63	.025	.009	.017	.022	3.40	65	.0047	20	
7	Double slotted flap	65_3-118	.69	1.9	2.92	40	2.88	----	.0248	——	------	3.51	65	.0061	12	
8	Single slotted flap	23018	.40	3.5	2.80	40	2.65	.16	.035	.043	.092	2.91	50	.0100	9	
9	Single slotted flap	23021	.40	3.5	2.62	20	2.85	.13	.043	.054	.073	2.87	50	.0140	11	
10	Single slotted flap	23030	.40	3.5	2.48	20	----	.14	.052	.087	-----	2.88	50	.0230	21	
11	Single slotted flap	65_3-418	.85	6.0	2.83	30	2.45	.0397	.0118	.0173	.0232	3.00	40	.0058	7	
12	Slotted deflector flap	23012	.25	3.5	2.70	50	2.56	.13	.076	.097	.110	2.70	50	.0150	18	
13	Slotted flap with auxiliary 0.05c split flap	23012	.2566	3.5	2.74	30, 60	2.60	.12	.036	.050	.074	2.83	40, 70	.0050	15	
14	Slotted flap with auxiliary 0.10c slotted flap	23012	.2566	3.5	2.96	40, 60	2.82	.155	——	.062	.114	2.99	40, 70	.0120	15	
15	Plain flap	23012	.20	3.5	2.38	60	2.24	.19	.152	.154	——	2.40	75	.0090	16	
16	External-airfoil flap	23012	.0667	3.5	2.08	30.2	2.14	.095	.028	.046	——	2.37	40.5	.0100	16	
17	Split flap	23012	.20	3.5	2.29	30	2.15	.115	.080	.083	——	2.54	75	.0090	16	
18	Fowler flap	23012	.30	3.5	3.30	40	3.16	.17	.080	.095	.113	3.30	40	.0090	26	
19	Venetian-blind flap 4 vanes, 0.10c	23012	.40	3.5	3.28	30	3.14	.14	.068	.031	.050	3.60	40, 50 50, 70	.0090	14	
20	Venetian-blind flap 4 vanes, 0.075c	23012	.30	3.5	3.40	30, 30 40, 50	3.26	.17	------	.055	.070	3.40	20, 30 40, 50	.0090	23	

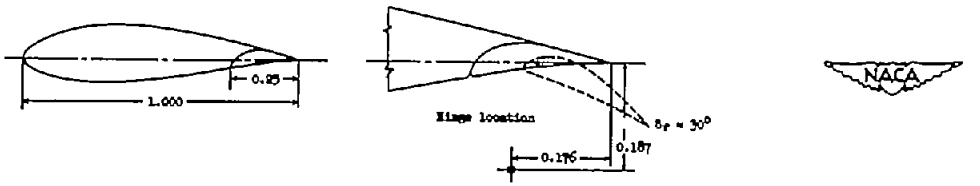

Detail of item 11

Flap-deflection angles δ_f are given for the fore and aft flap, both measured from the basic section chord line, except for item 19. For details of this arrangement, see reference 14.

TABLE III.- GENERAL AIRPLANE DATA[1]

Item	Original	Modified
Gross weight, pounds	2280	2280
Wing area, square feet	165	192
Span, feet	38	38
Aspect ratio	8.75	7.5
Mean aerodynamic chord, inches	52.32	60.9
NACA airfoil section	[2]Modified 43012	63,4-420
Flap type	Partial-span plain	Full-span single slotted
Flap chord, percent chord	19.2	25.0
Horizontal tail area, square feet	38.40	38.40
Vertical tail area, square feet	17.48	17.48

[1]The airplane selected for this analysis is a single-engine, four-place, high-wing monoplane equipped with conventional landing gear and embodying features found in most airplanes of a similar type. It is powered by a 165-horsepower, air-cooled, horizontally opposed, 4-cylinder engine, and this study assumes the use of a constant-speed propeller.

[2]The modification is a fairing out of the characteristic dip in the forward part of the lower surface of the airfoil.

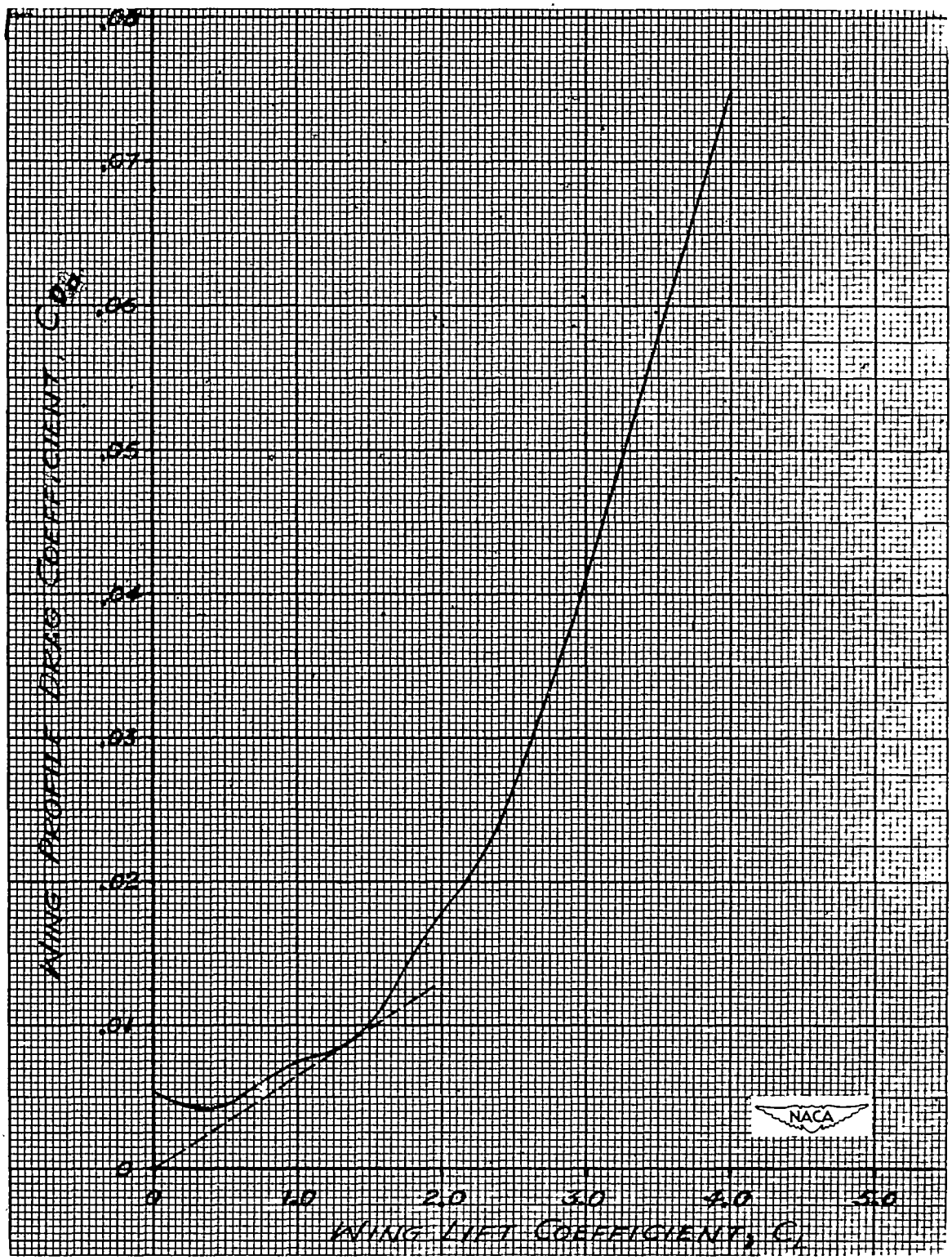

Figure 1.- Assumed profile drag coefficient of wing.

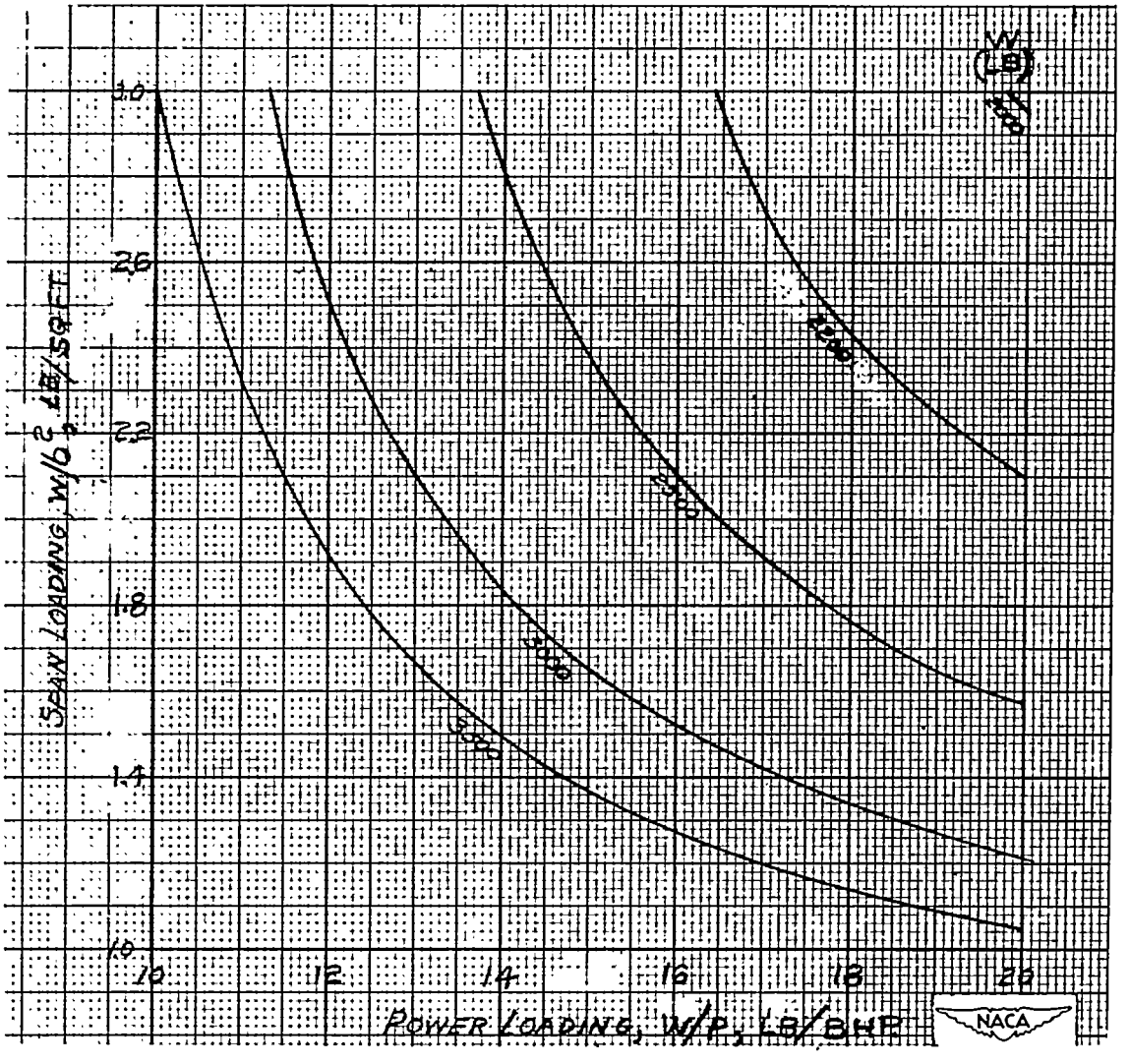

Figure 2.- Weight of assumed airplane. A = 5.

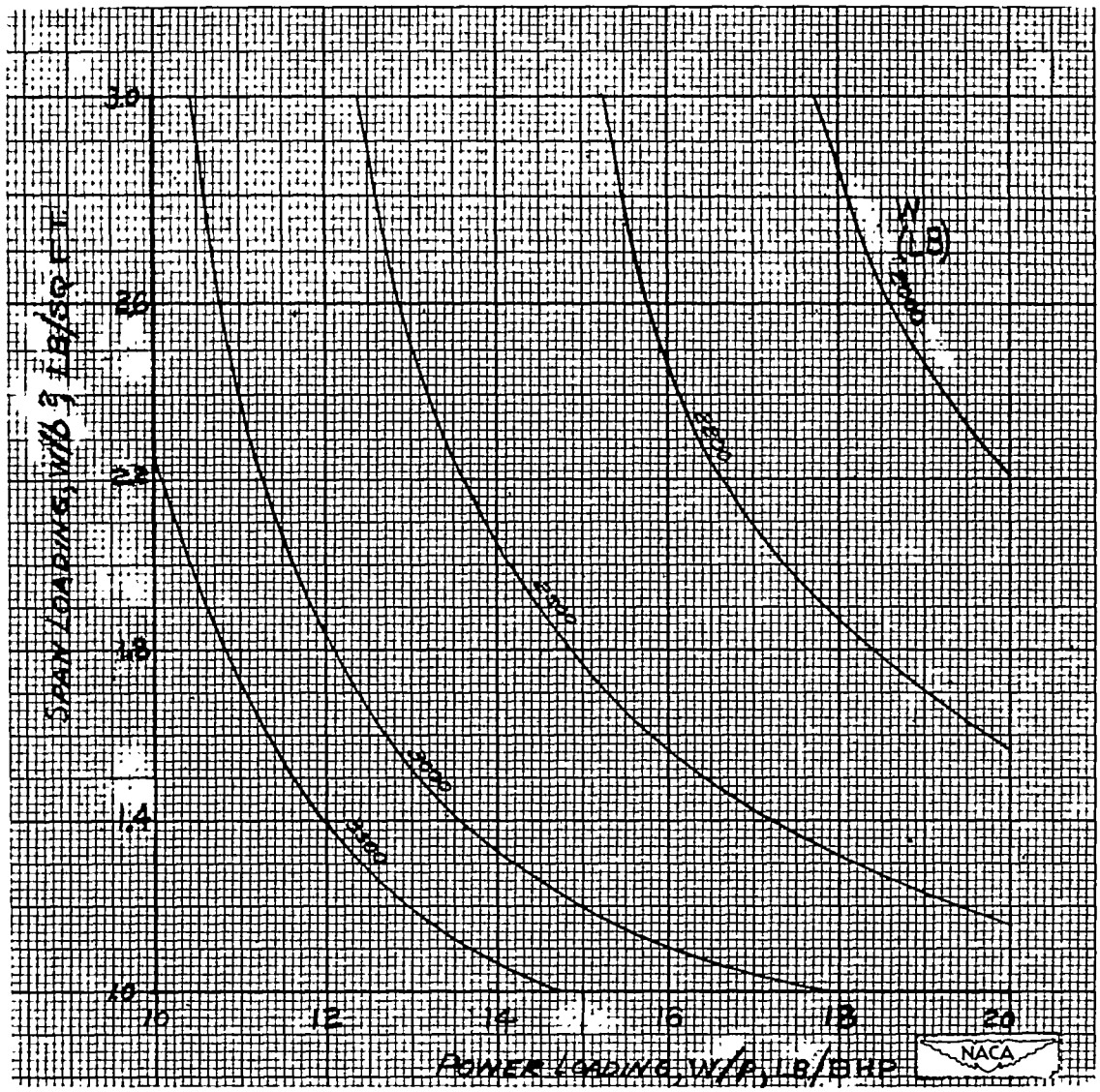

Figure 3.- Weight of assumed airplane. A = 7.5.

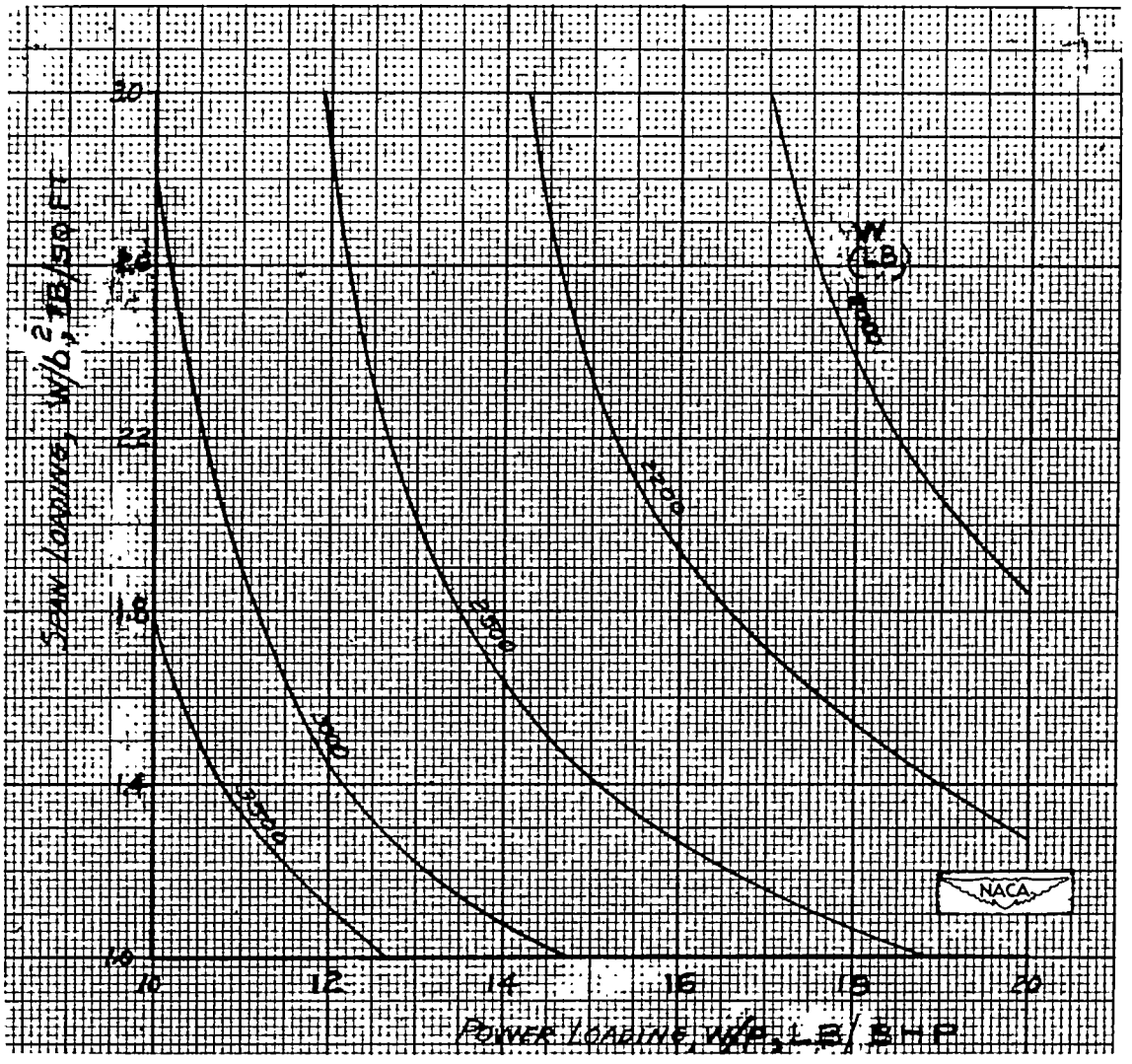

Figure 4.- Weight of assumed airplane. A = 10.

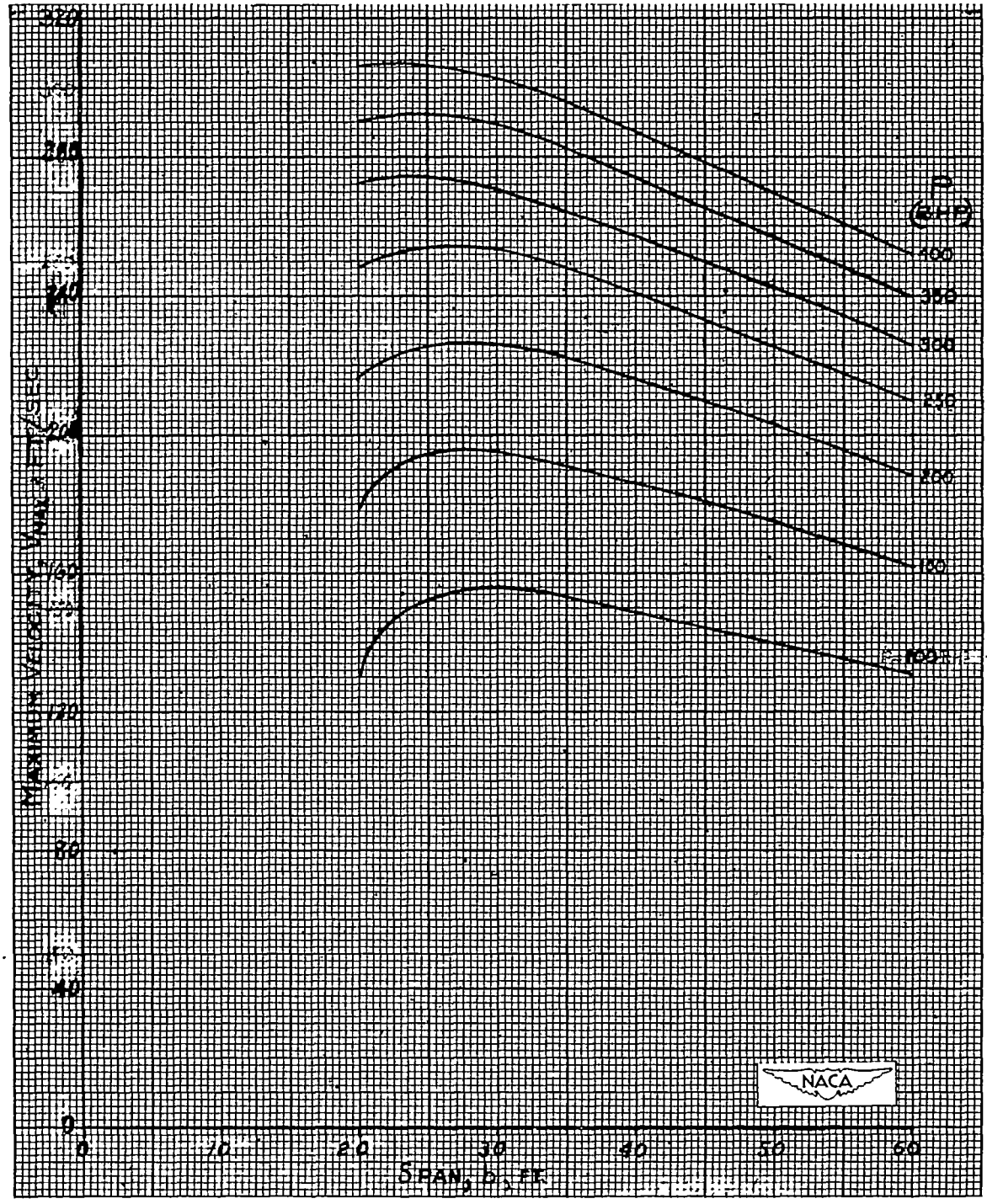

Figure 5.- Maximum speed of assumed airplane. A = 5.

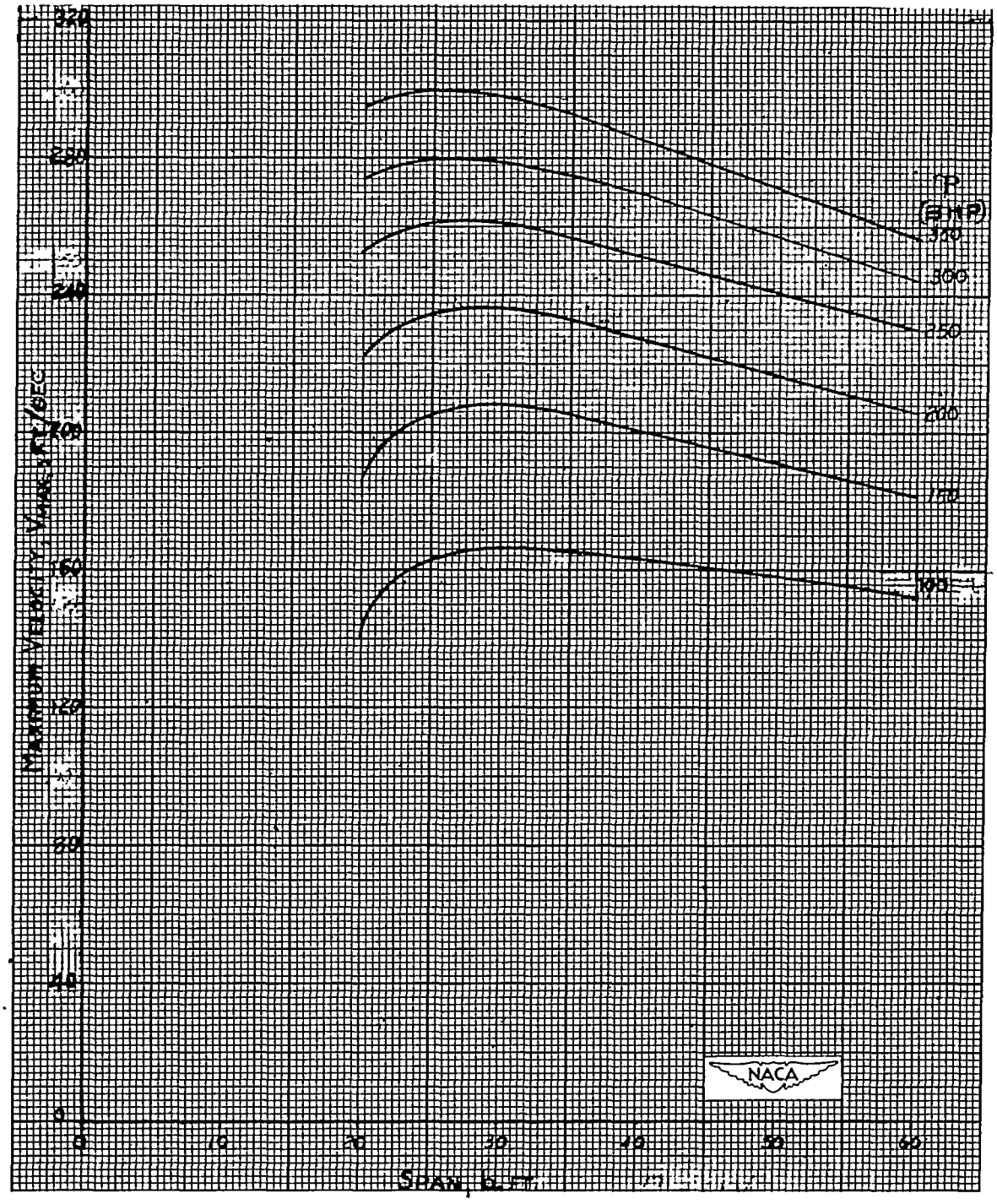

Figure 6.- Maximum speed of assumed airplane. A = 7.5.

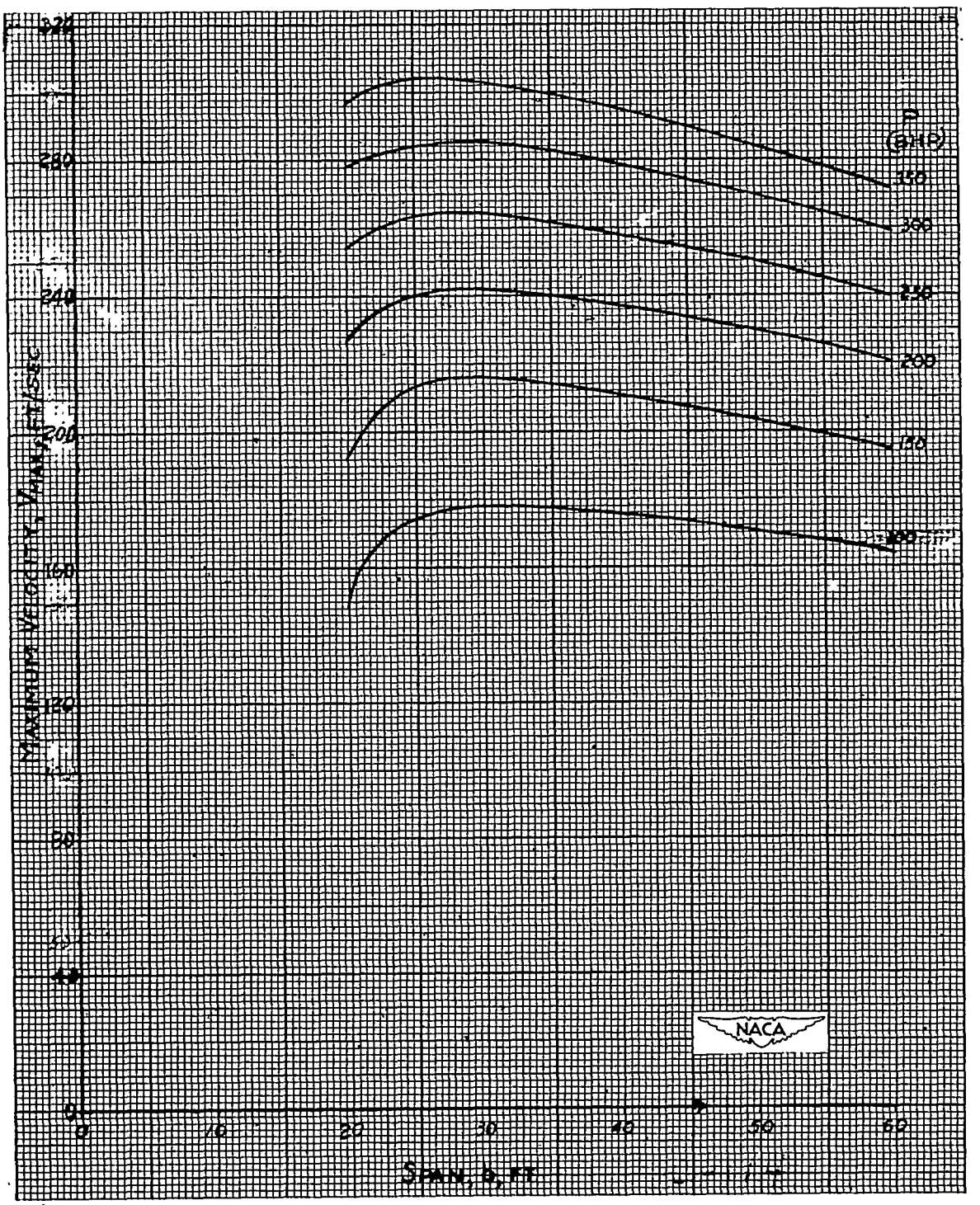

Figure 7.- Maximum speed of assumed airplane. A = 10.

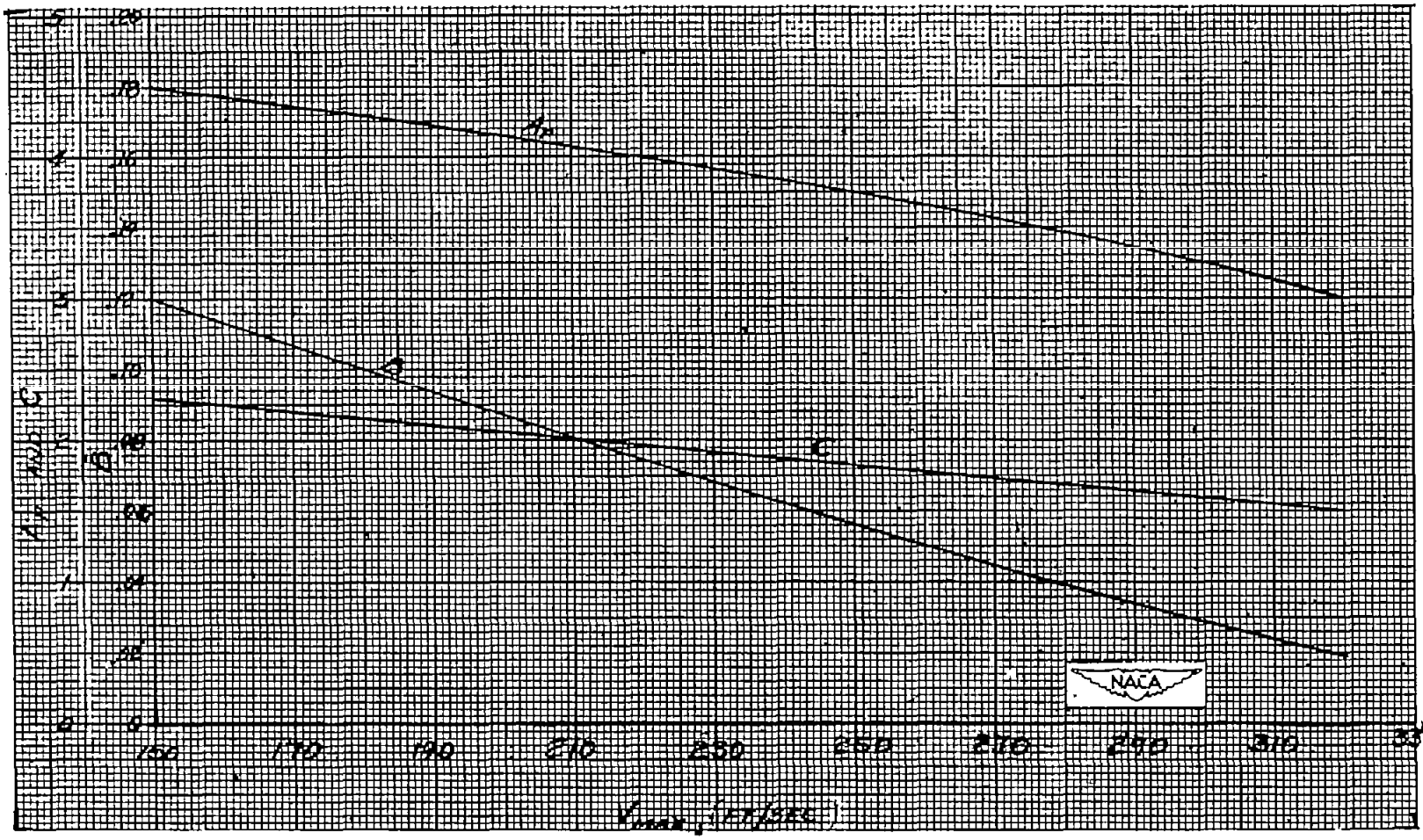

Figure 8.- Thrust factors for automatic propellers.

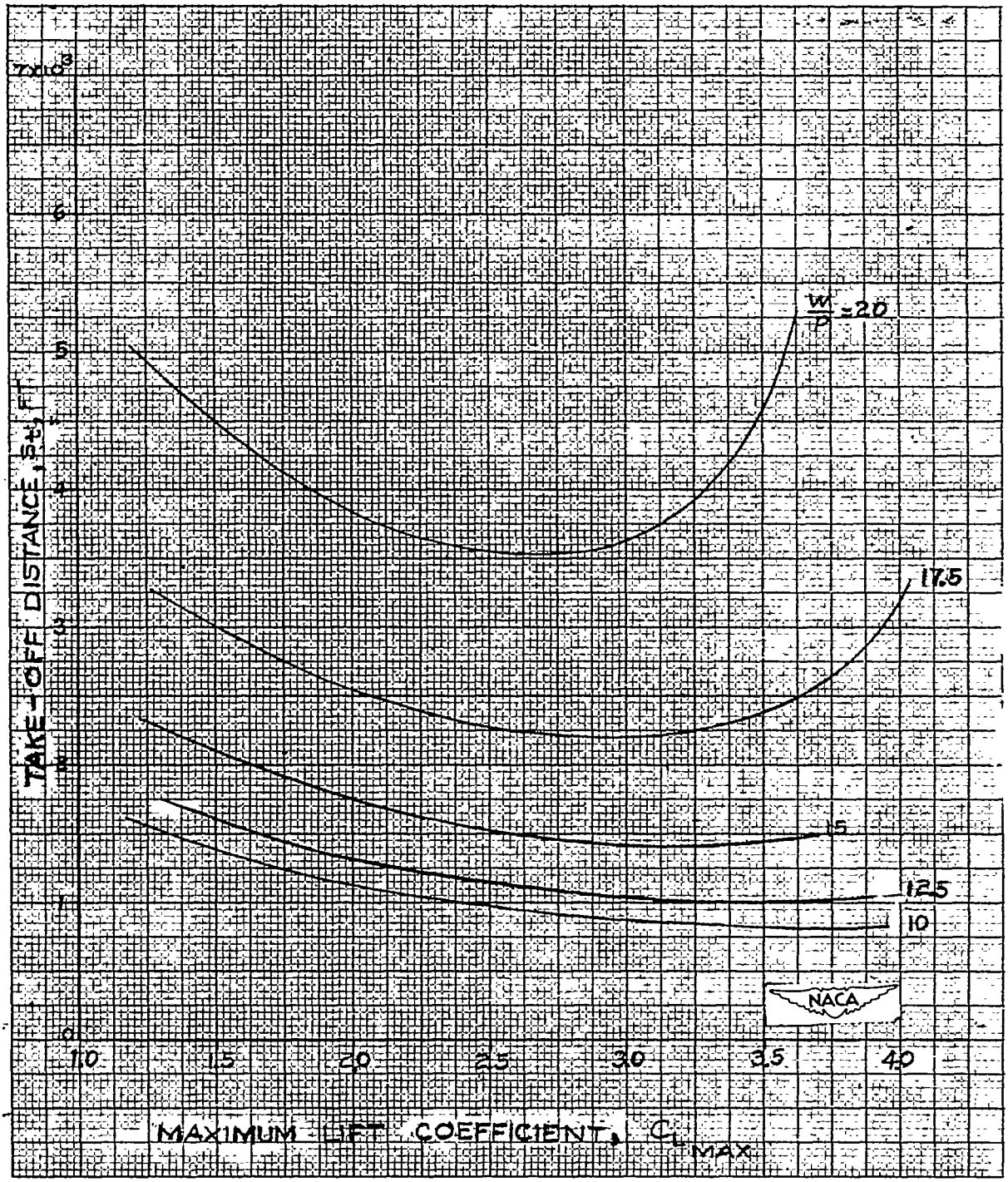

Figure 9.- Total take-off distance as function of maximum lift coefficient. $A = 7.5$; $W/b^2 = 2.0$.

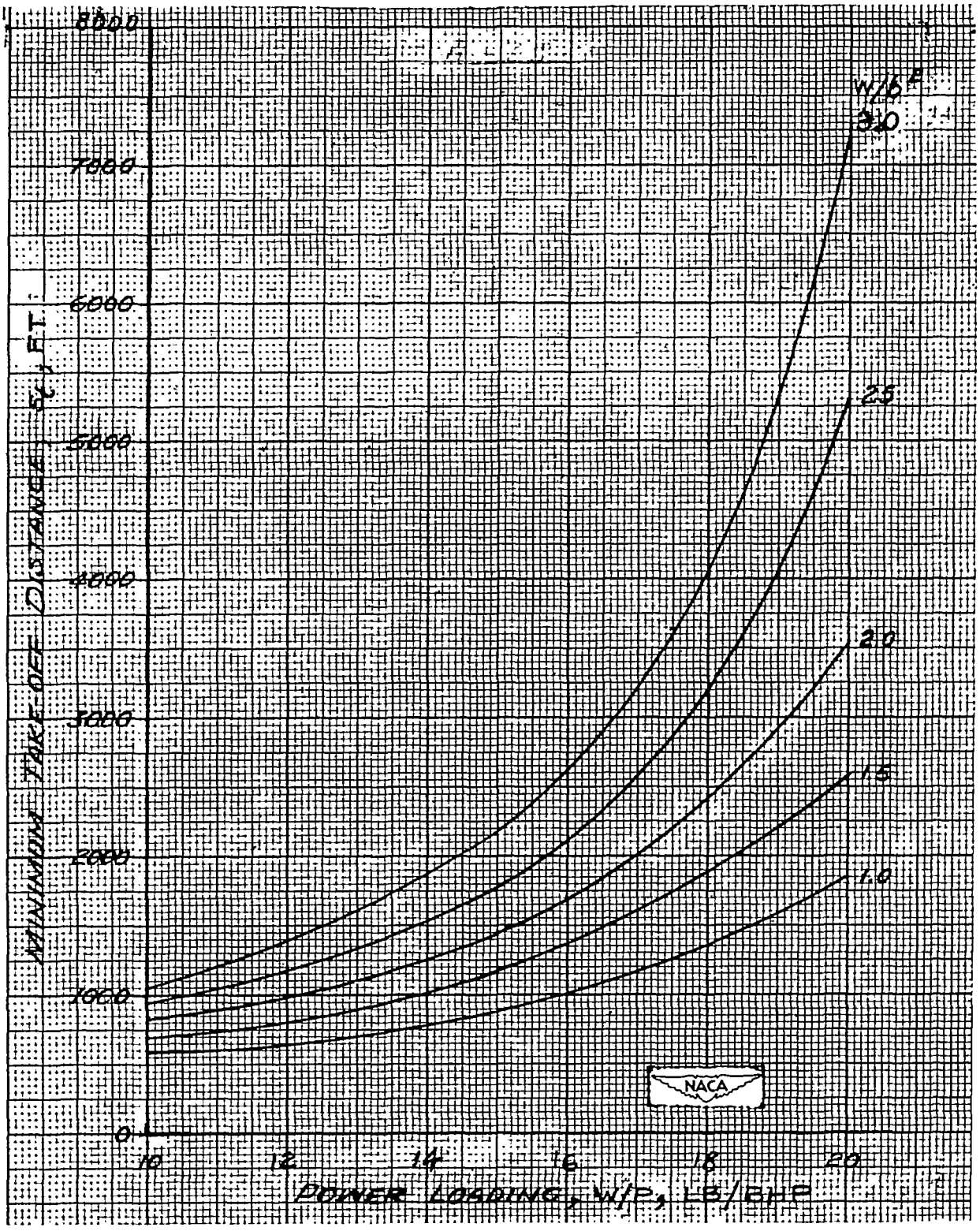

Figure 10.- Minimum take-off distance as function of power loading for various span loadings. A = 7.5.

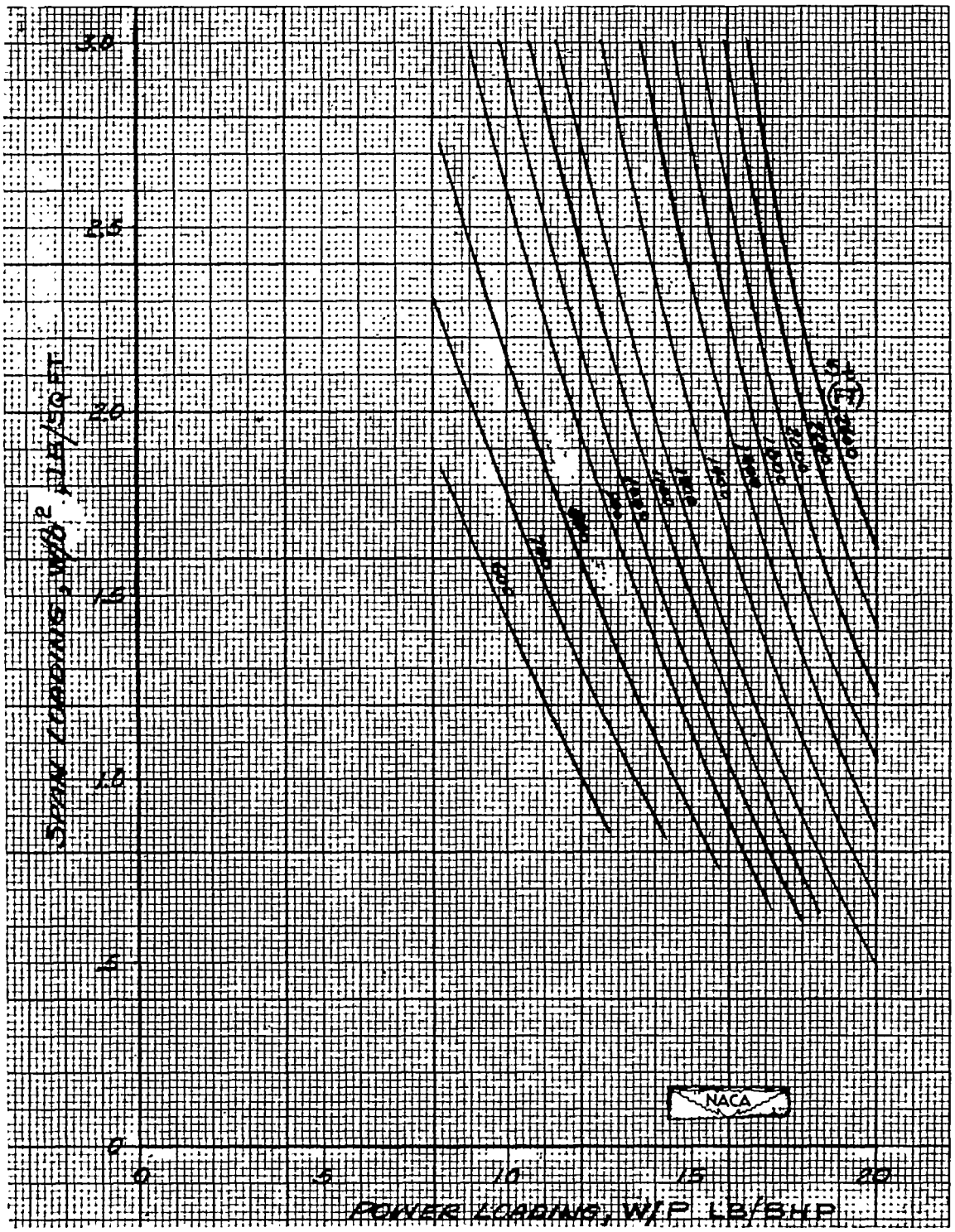

Figure 11.- Minimum take-off distance as function of span loading and power loading. A = 5.

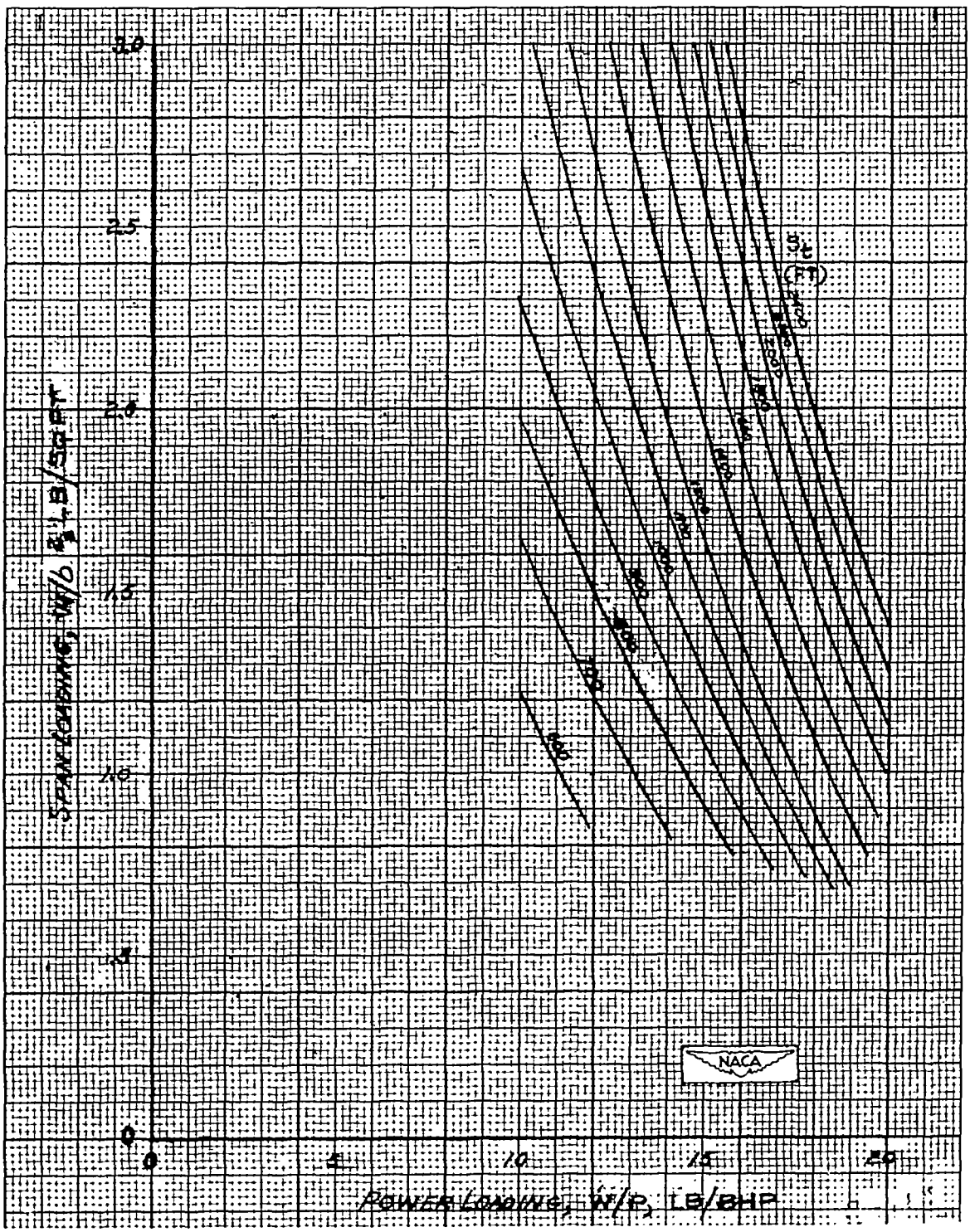

Figure 12.- Minimum take-off distance as function of span loading and power loading. A = 7.5.

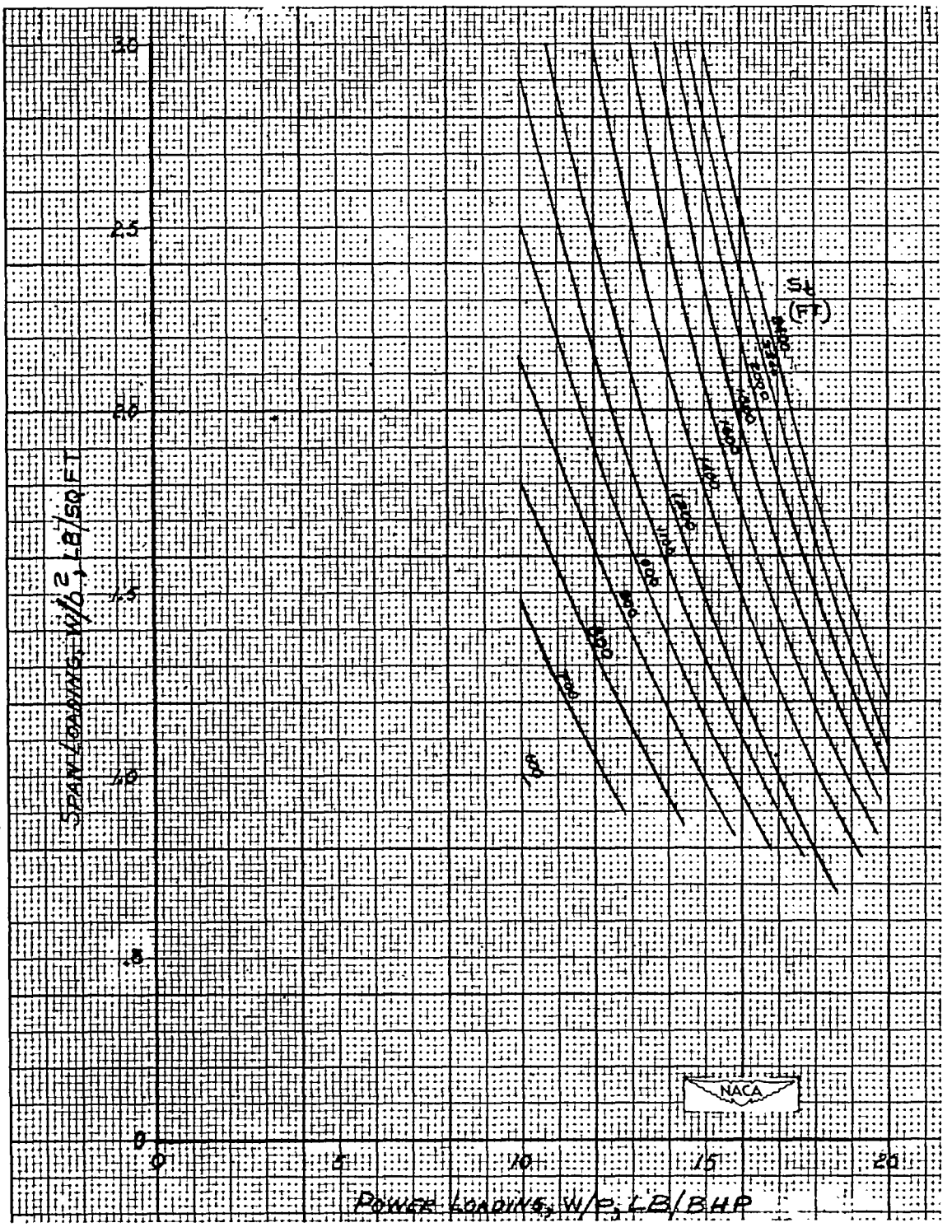

Figure 13.- Minimum take-off distance as function of span loading and power loading. A = 10.

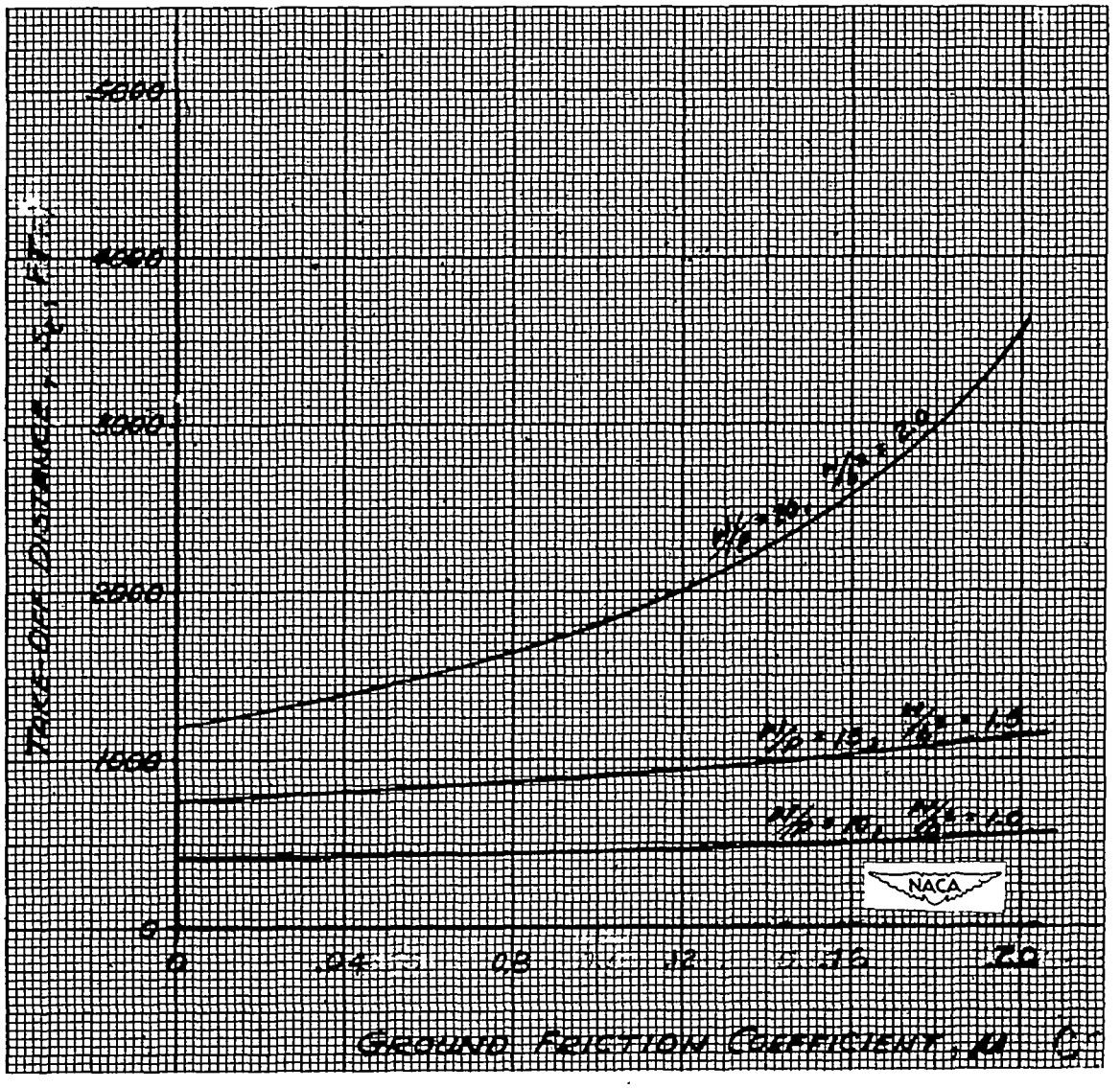

Figure 14.- Effect of ground friction on take-off distance to 50-foot height. $A = 7.5$; $\Delta C_D = 0$.

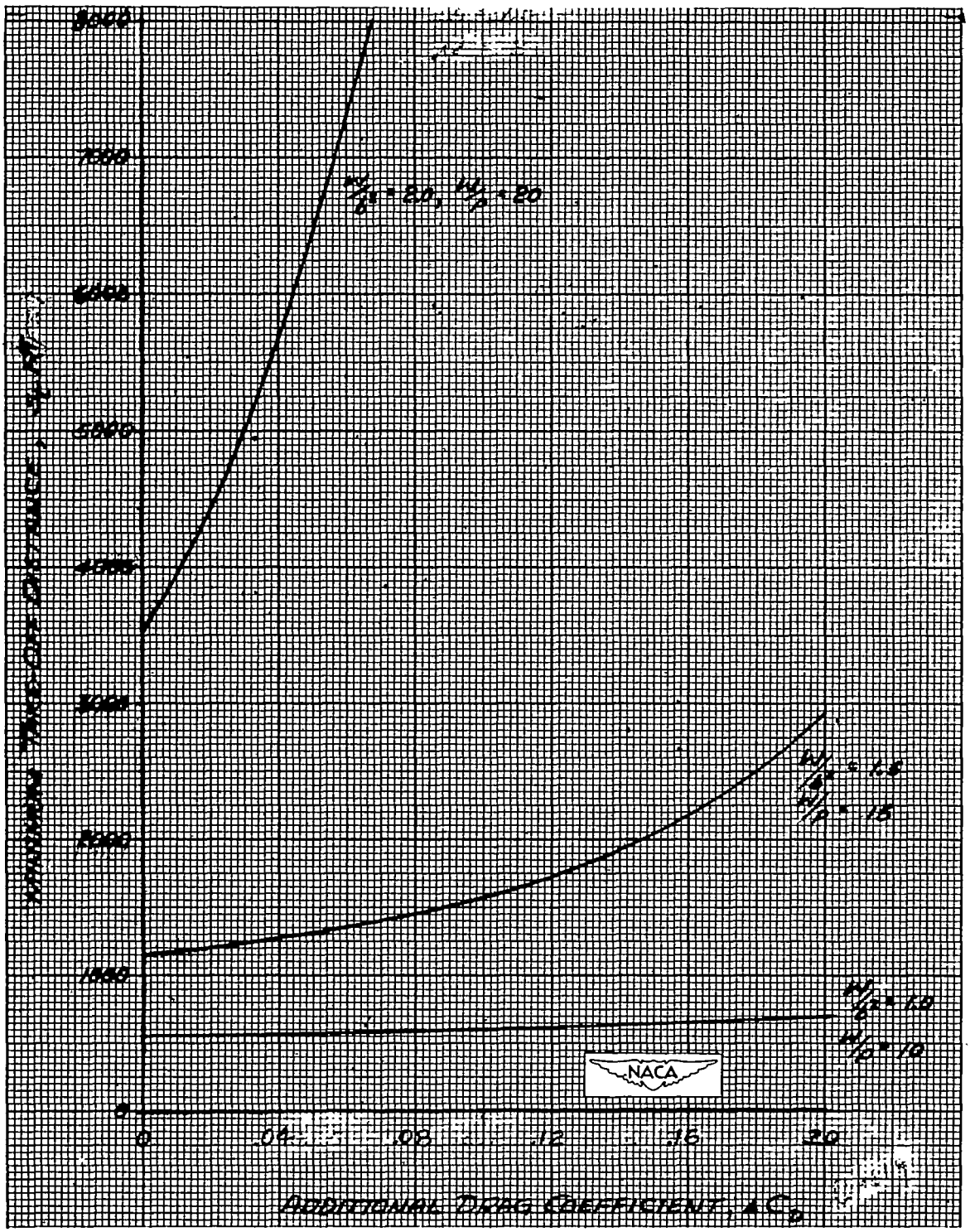

Figure 15.- Effect of additional air drag on take-off distance to 50-foot height. A = 7.5; μ = 0.2.

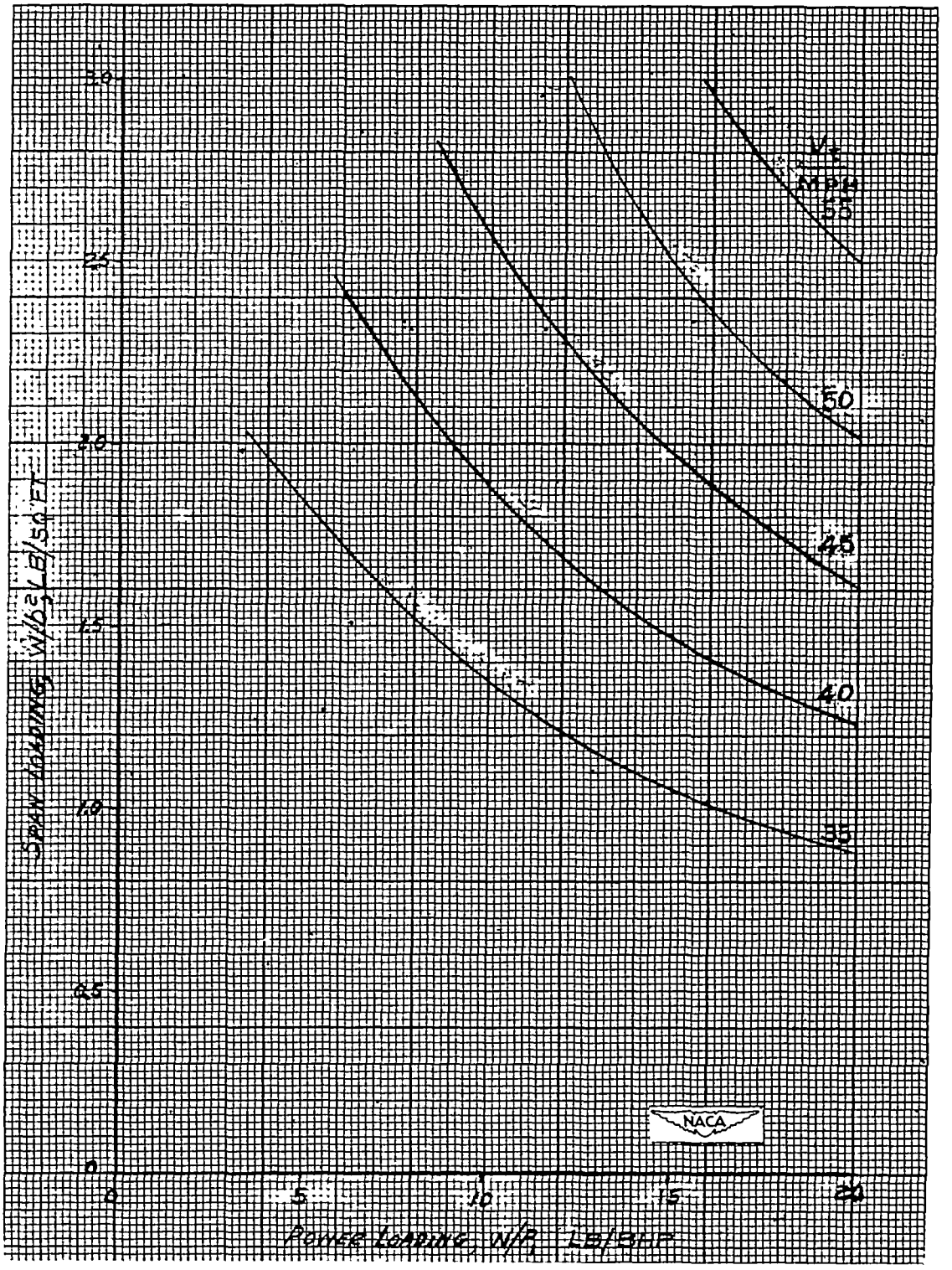

Figure 16.- Optimum take-off velocity.

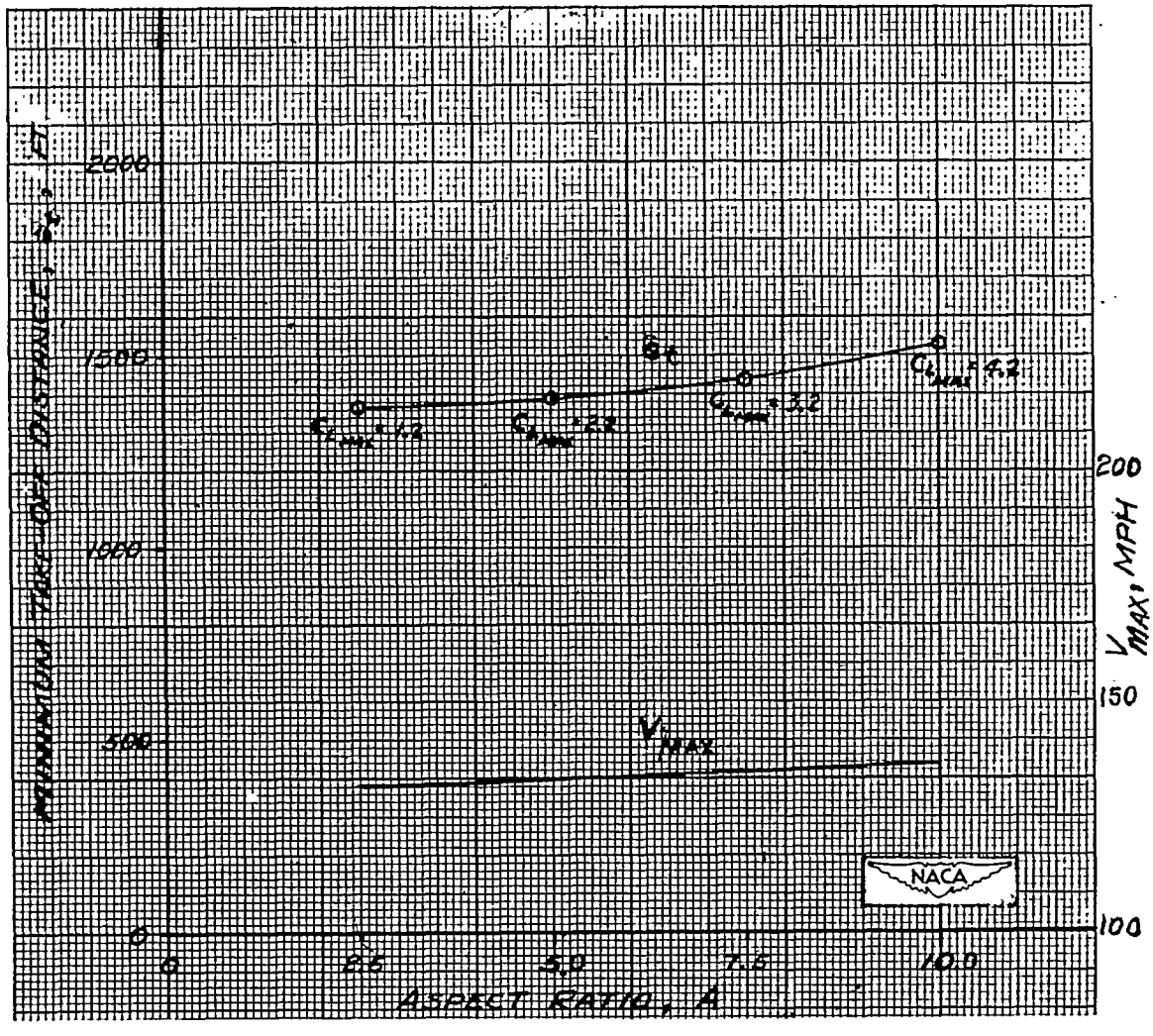

Figure 17.- Variation of minimum take-off distance and maximum velocity with aspect ratio. $W/P = 15$; $W/b^2 = 2.0$.

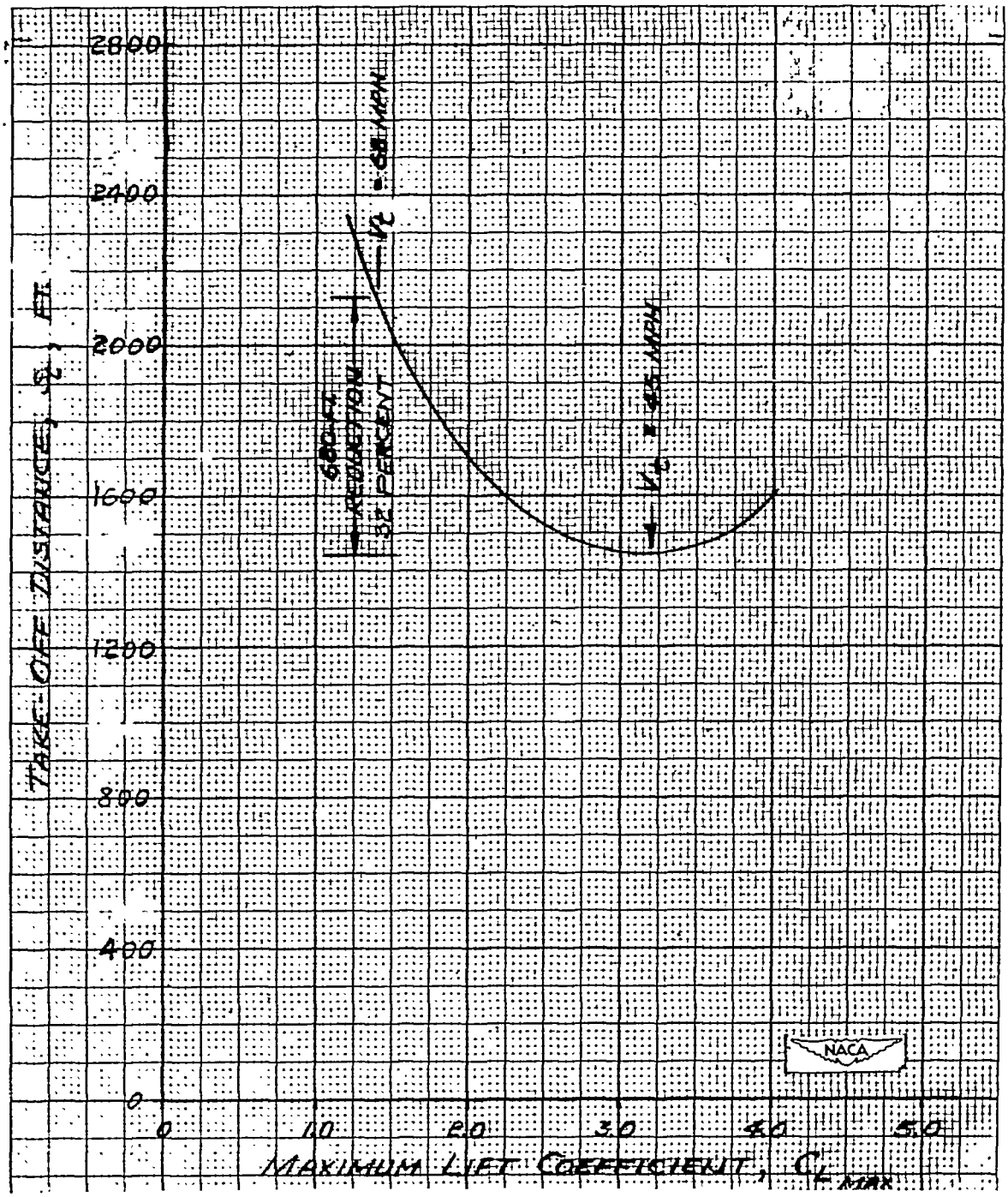

Figure 18.- Reduction of take-off distance of typical personal airplane by using optimum maximum lift. A = 7.5; W/b^2 = 2; W/P = 15; W/S = 15.

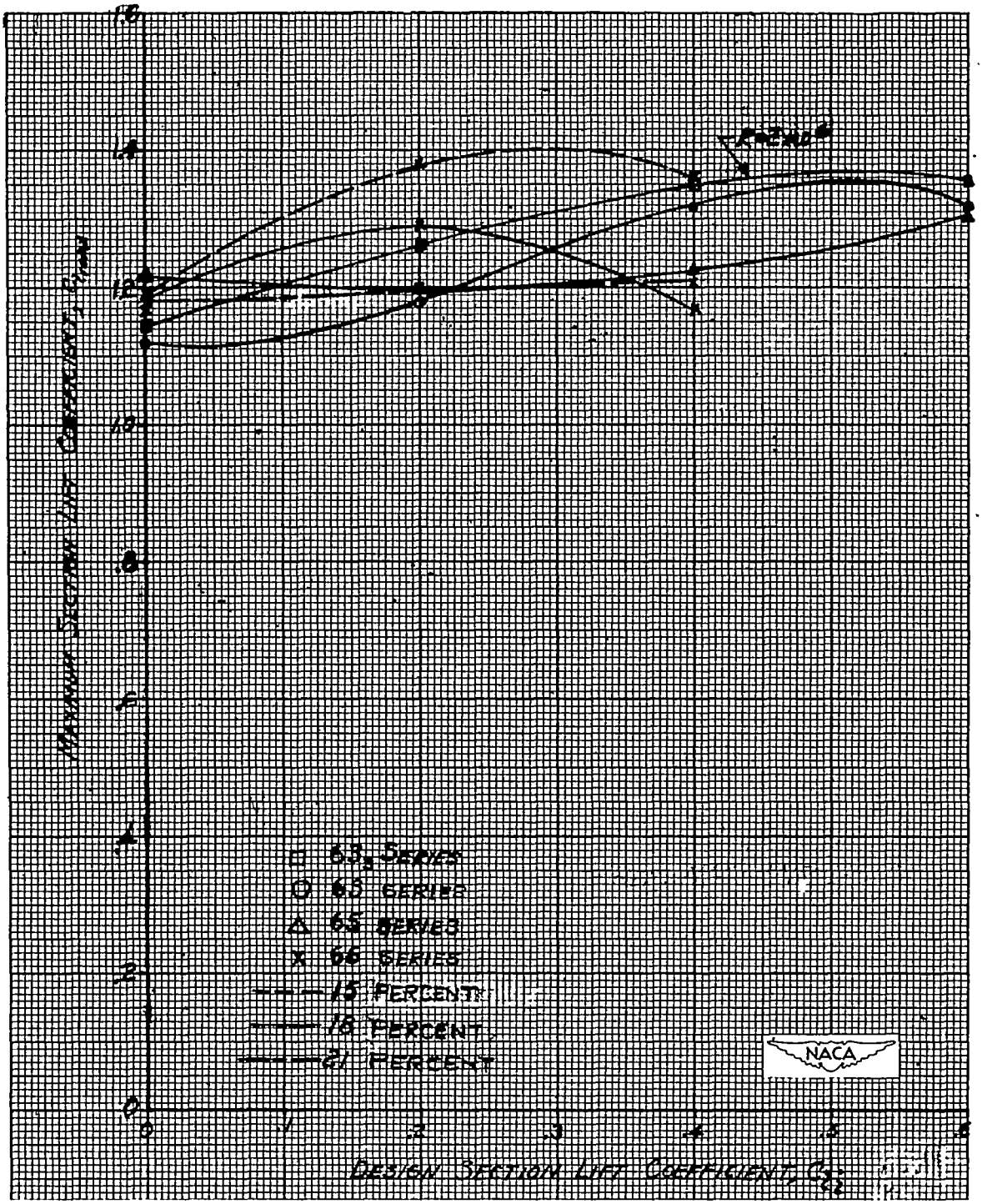

Figure 19.- Variation of maximum section lift coefficient with design section lift coefficient for various airfoils. $R = 1.5 \times 10^6$. Data from reference 5.

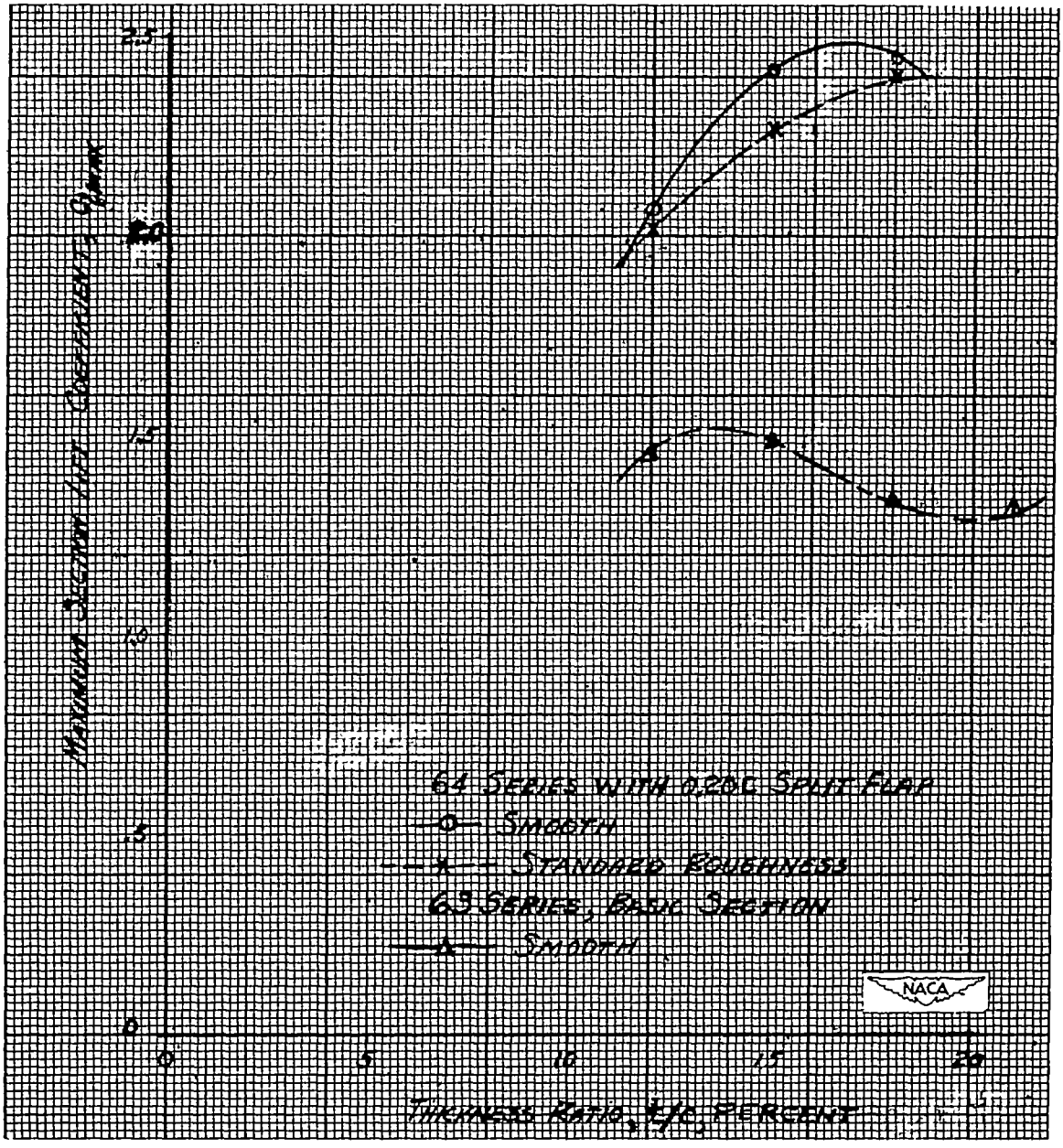

Figure 20.- Variation of maximum lift coefficient with thickness ratio for various smooth and rough airfoils with and without flaps. $R = 2 \times 10^6$. Data from reference 5.

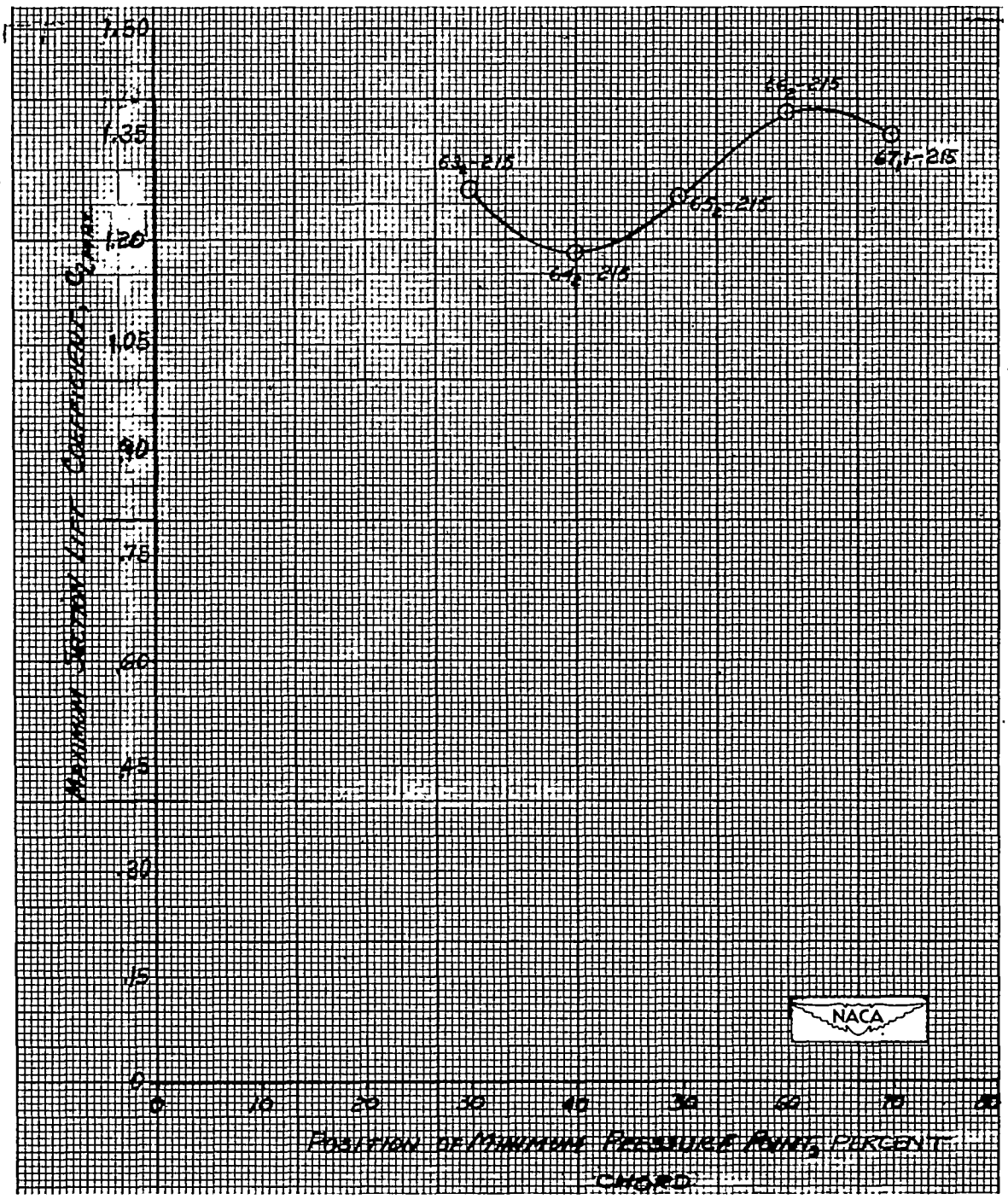

Figure 21.- Variation of maximum section lift coefficient with position of basic section minimum pressure for airfoils having a design lift coefficient of 0.2 and a percent thickness of 15. $R = 1.5 \times 10^6$. Data from reference 5.

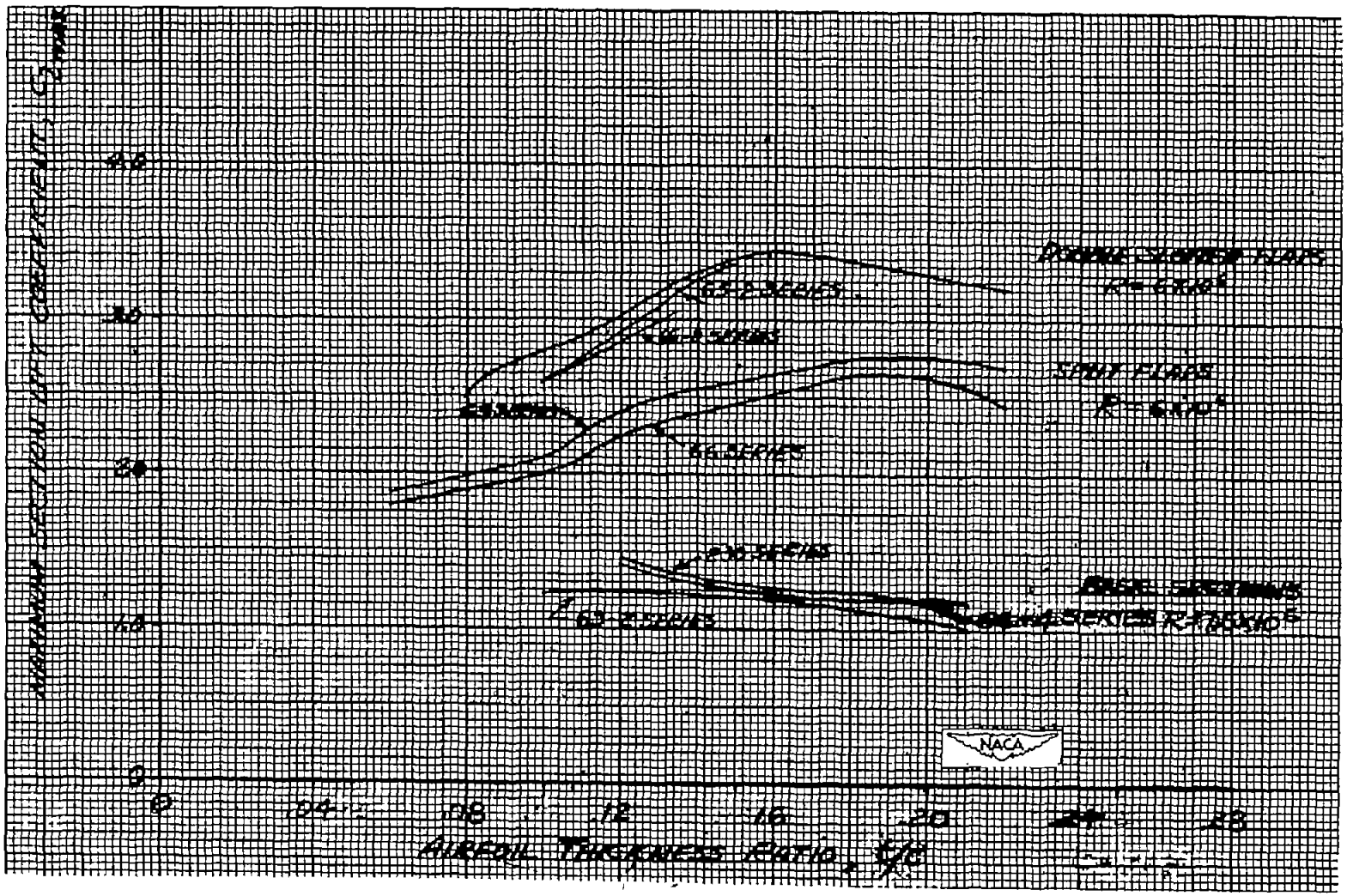

Figure 22.- Maximum section lift coefficient for several NACA airfoil sections with and without flaps. Data from references 5 and 8.

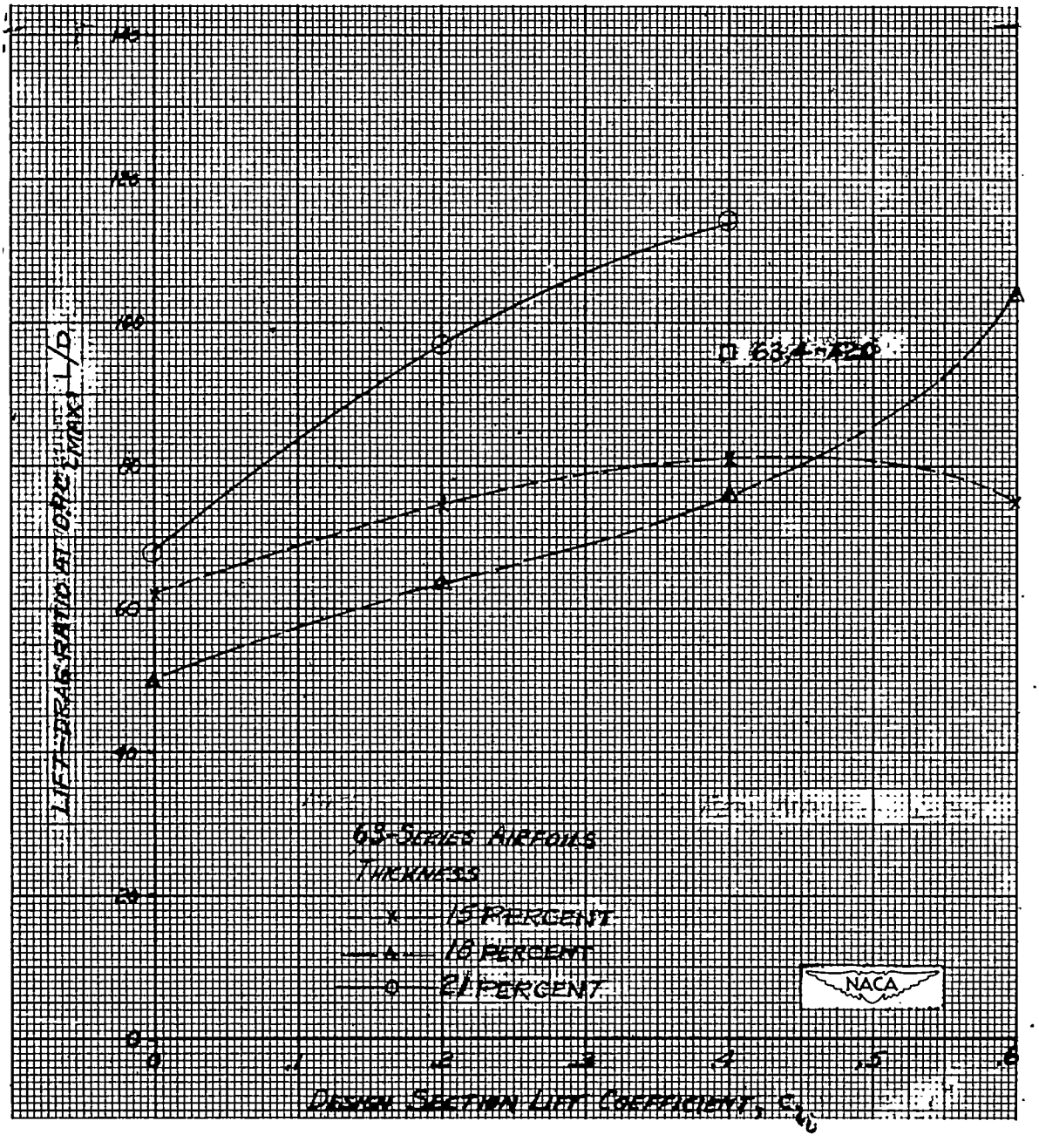

Figure 23.- Variation of L/D with design section lift coefficient for NACA 63-series airfoils. $R = 2 \times 10^6$. Data from reference 5.

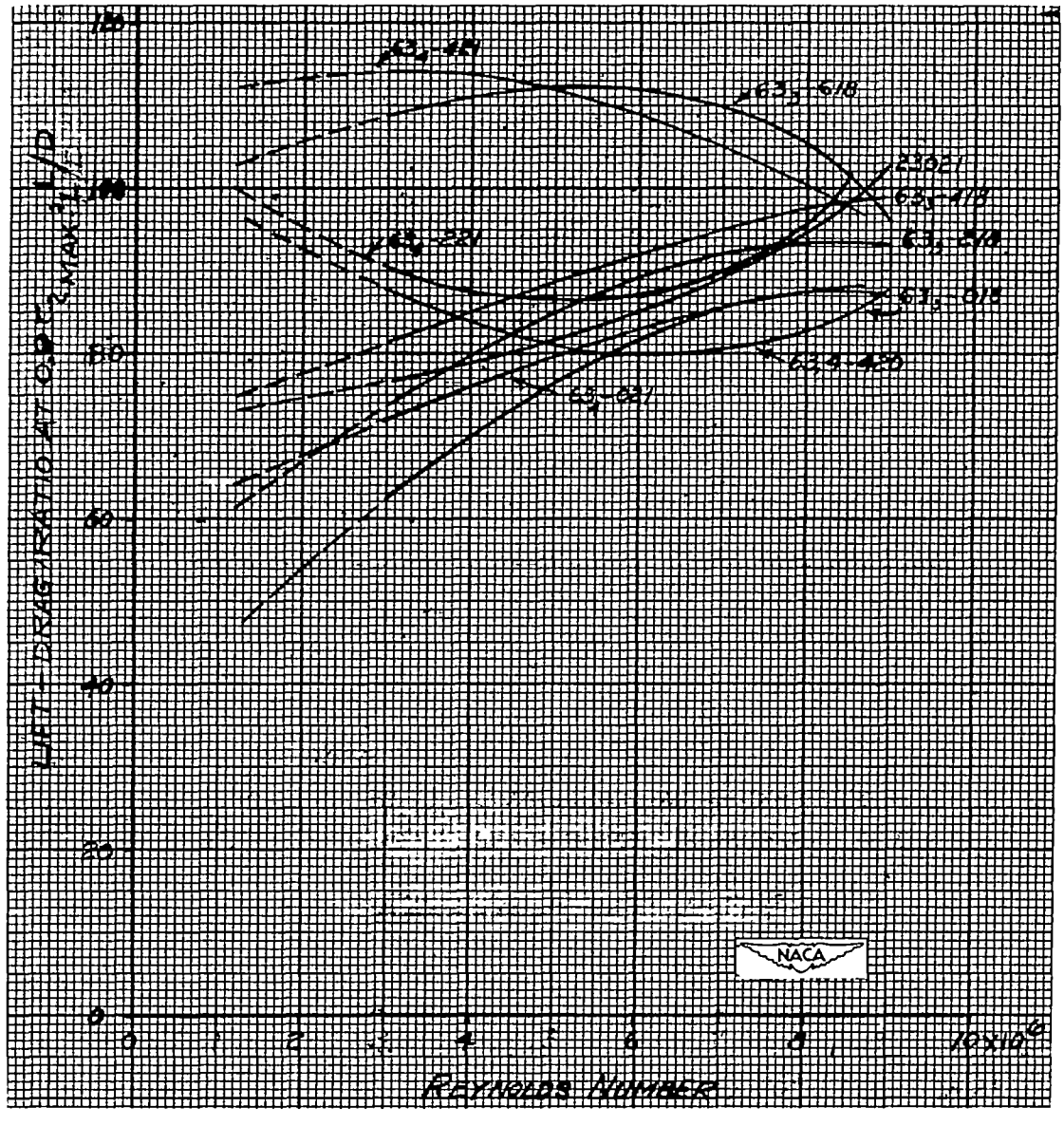

Figure 24.- Variation of L/D at 0.9 maximum section lift coefficient for various airfoils. Data from reference 5; $c_{l_{max}}$ is taken at the particular Reynolds number involved.

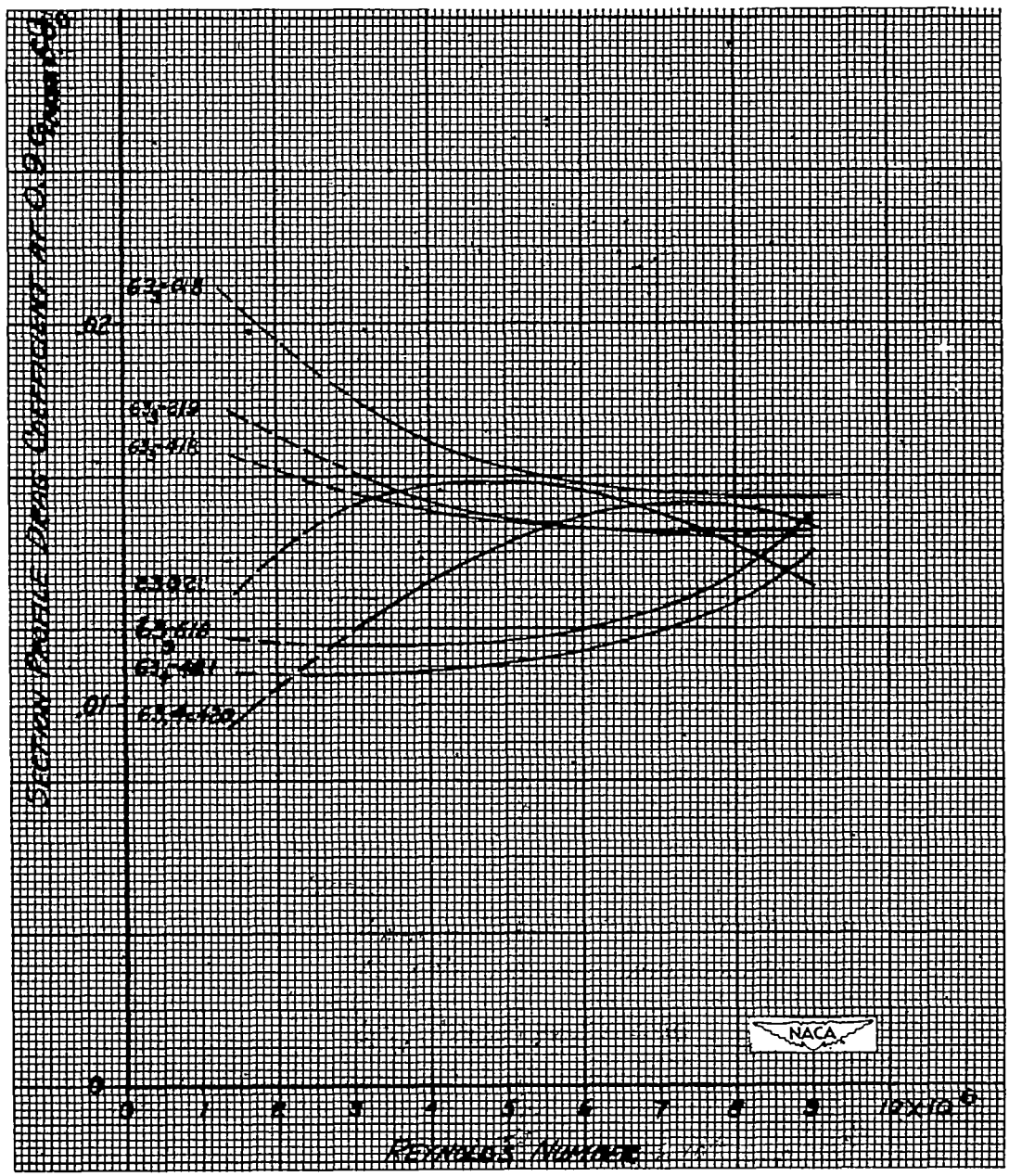

Figure 25.- Variation of section profile drag coefficient at 0.9 maximum section lift coefficient with Reynolds number for various airfoils. Data from reference 5; $c_{l_{max}}$ is taken at the particular Reynolds number involved.

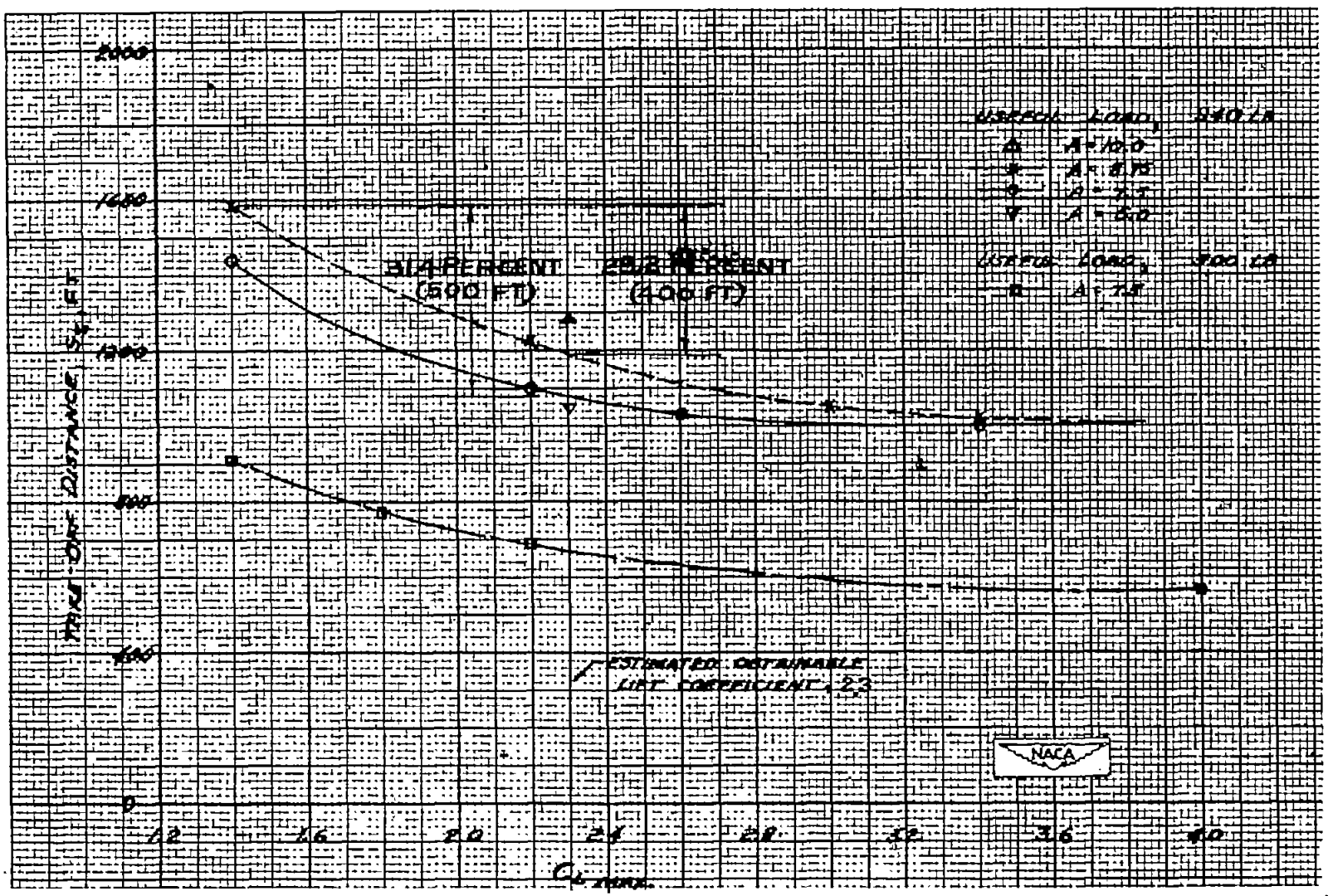

Figure 26.- Effect of $C_{L_{max}}$ on take-off for example airplane.

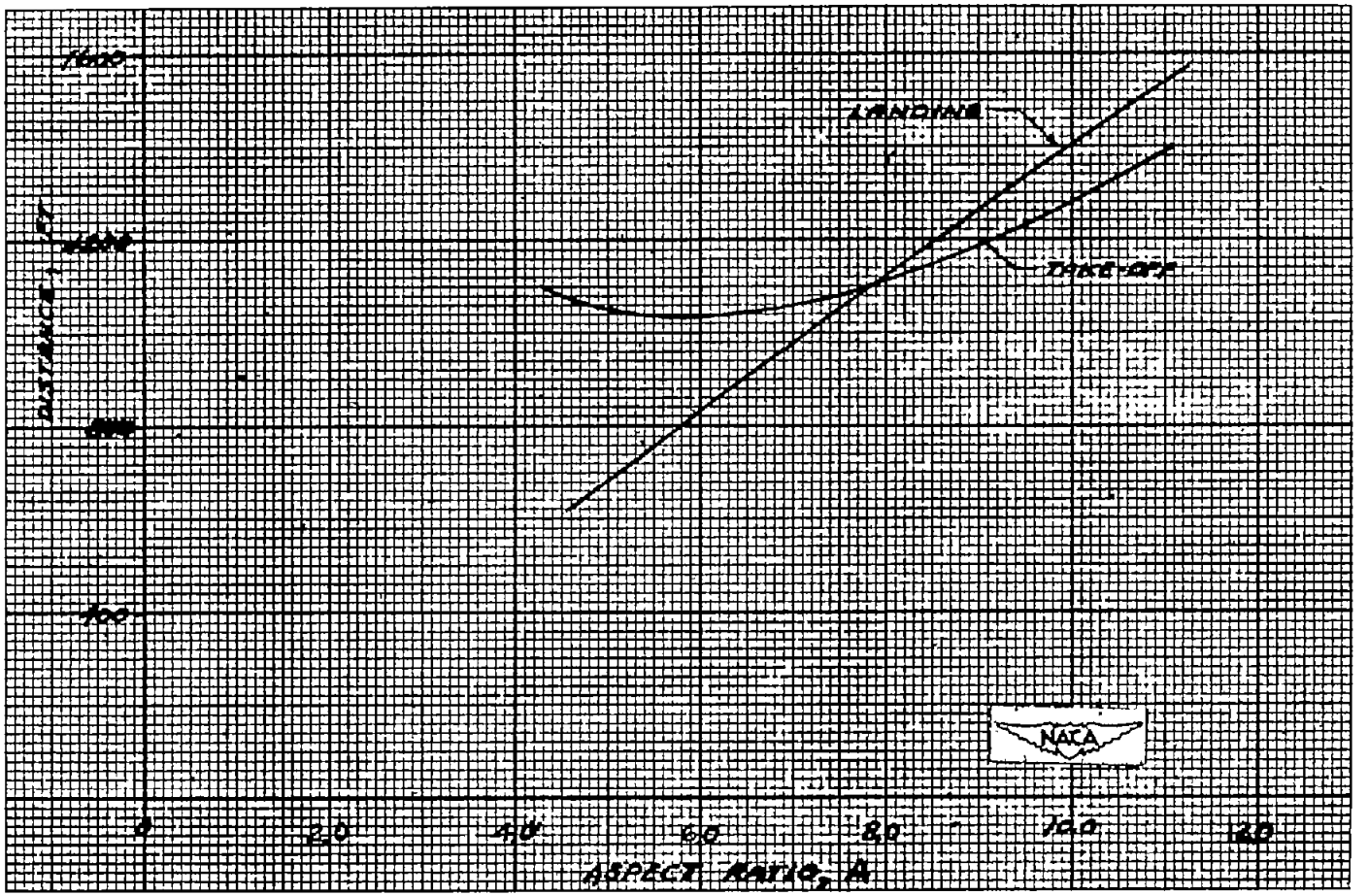

Figure 27.- Effect of aspect ratio on take-off and landing distances.
$C_{L_{max}} = 2.3$.

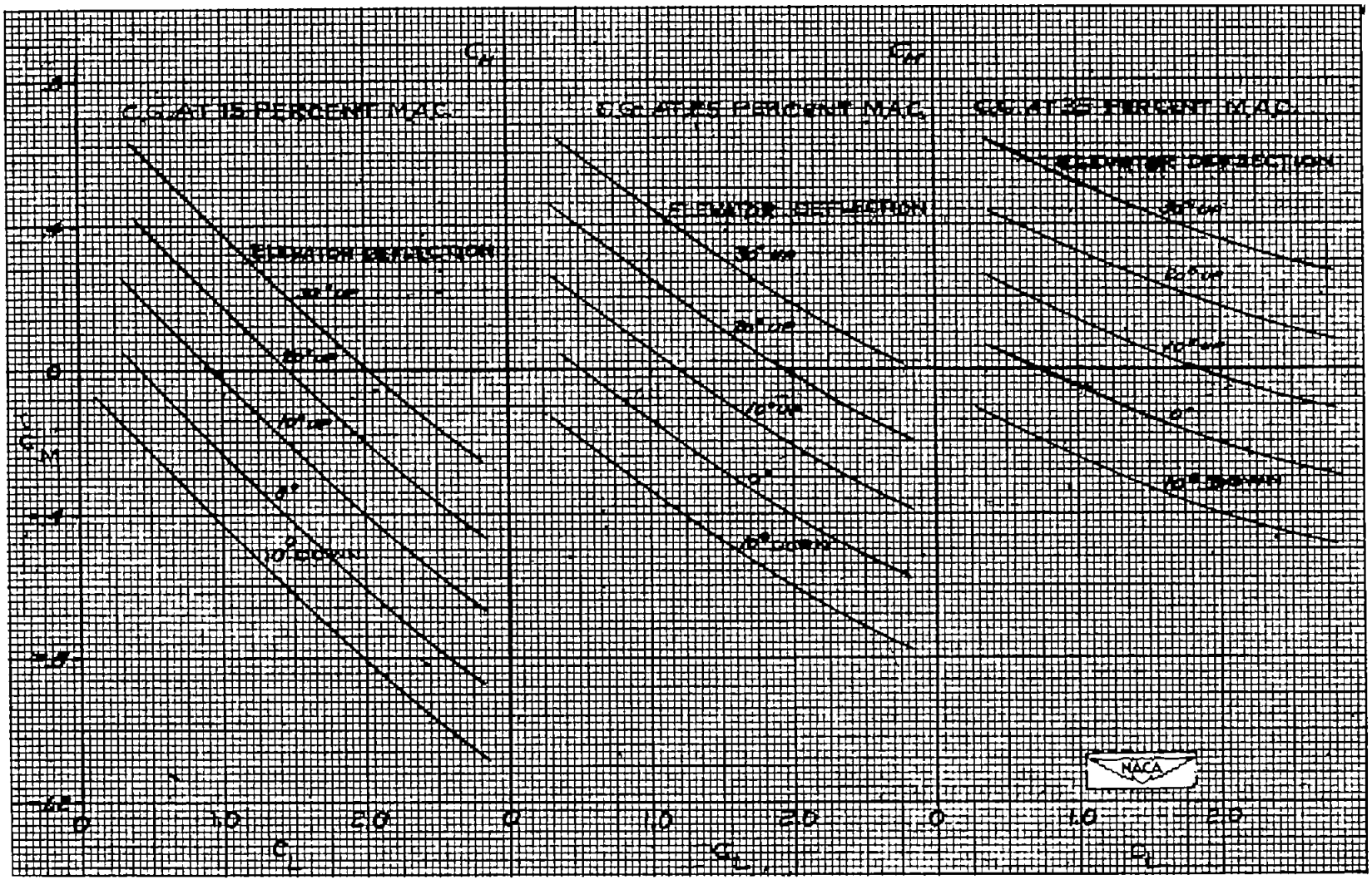

Figure 28.- Longitudinal stability and trim. Airplane with modified wing; flaps down 30°; data from table II.

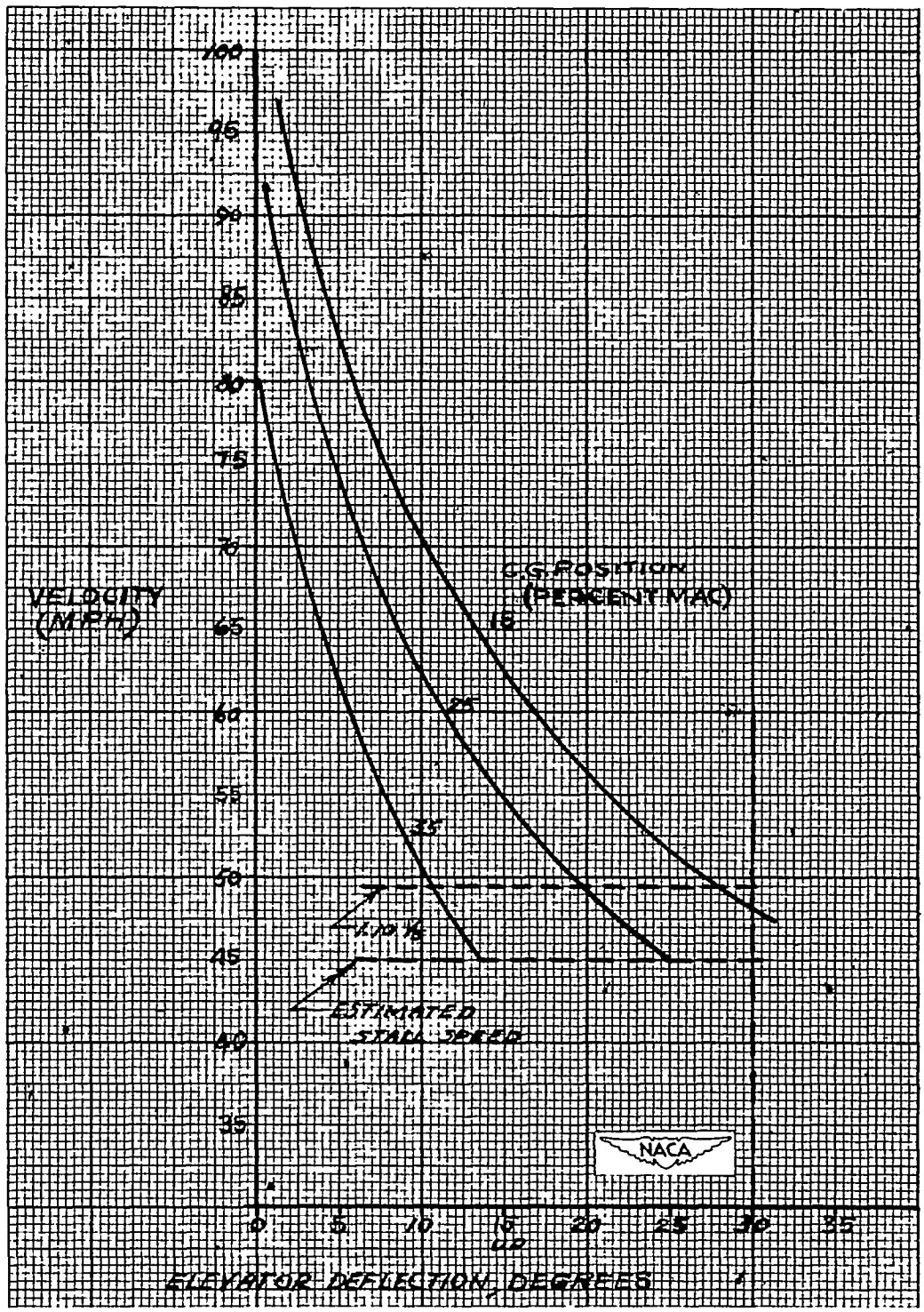

Figure 29.- Longitudinal trim. Airplane with modified wing; flaps down 30°.

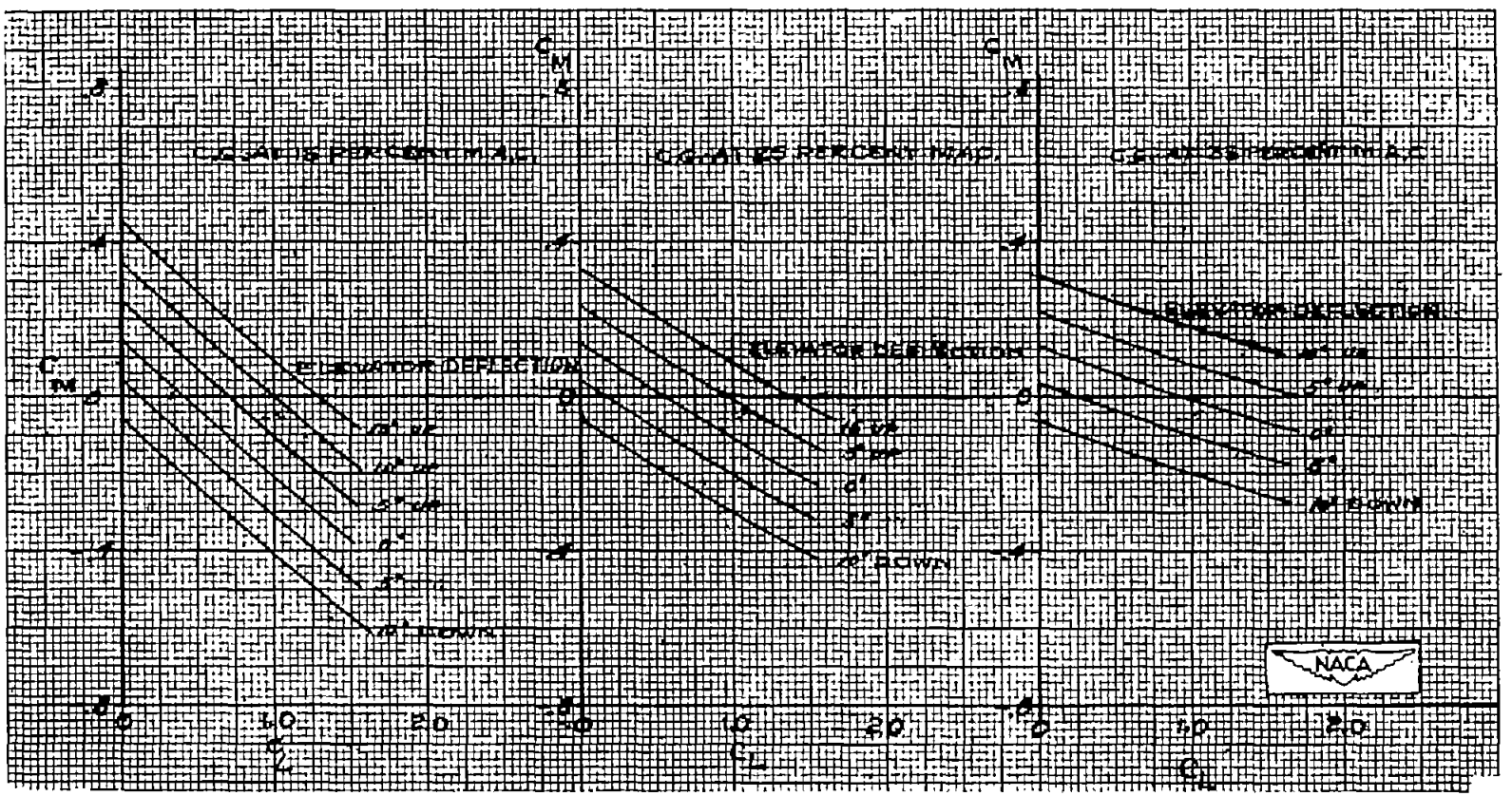

Figure 30.- Longitudinal stability and trim. Airplane with modified wing; flaps down 5°; data from table III.

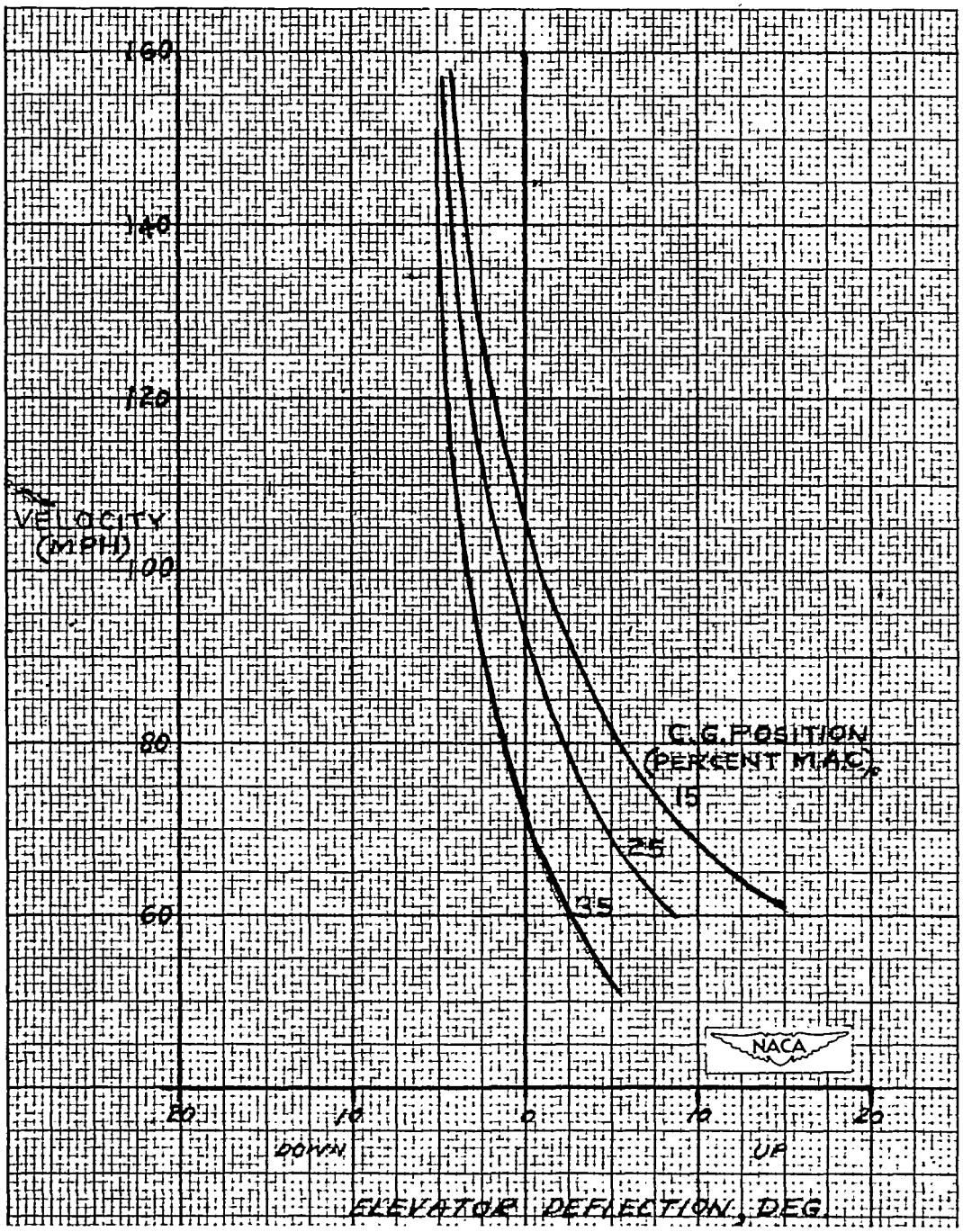

Figure 31.- Longitudinal trim. Airplane with modified wing; flaps down 5°.

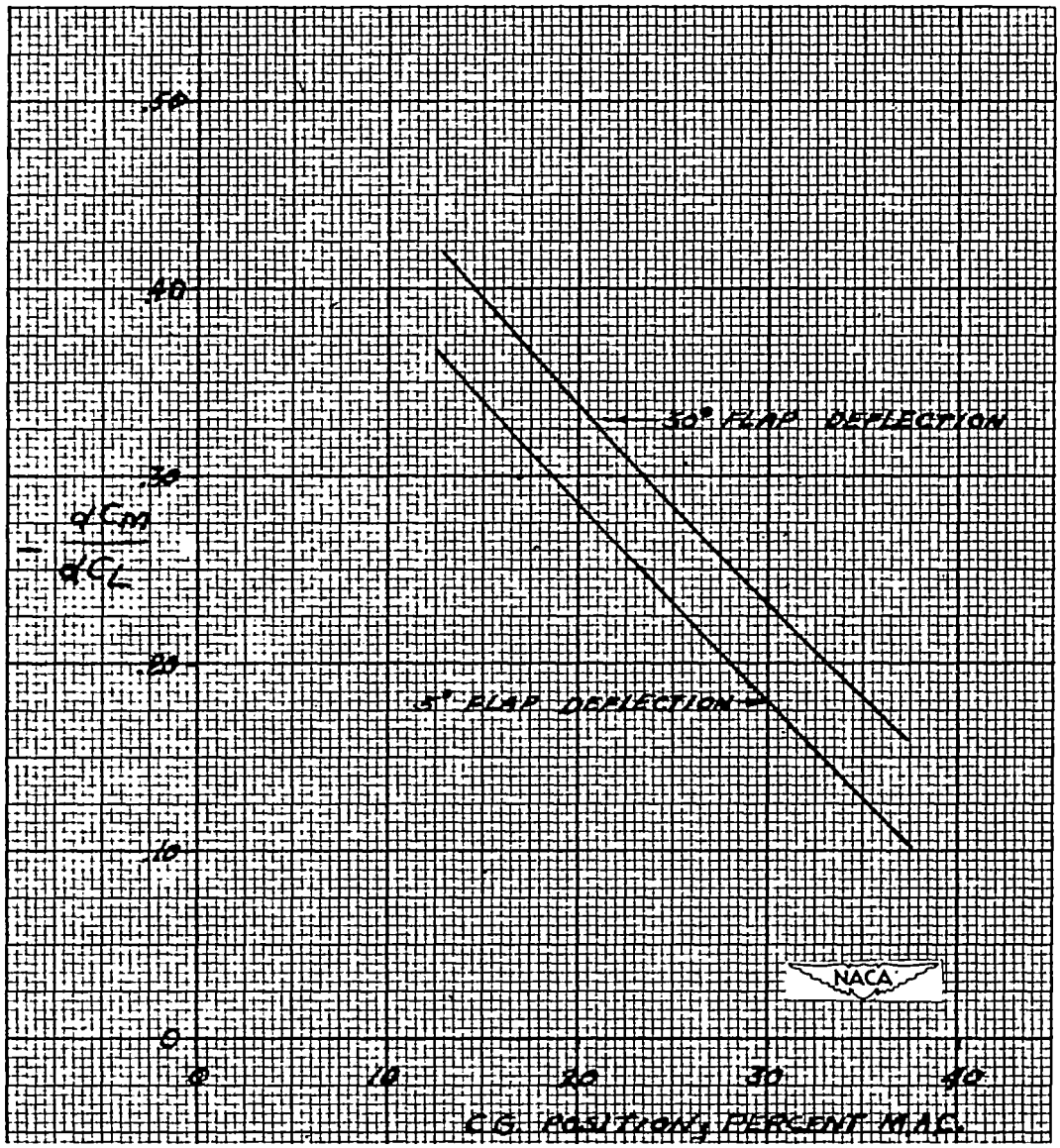

Figure 32.- Longitudinal stability. Airplane with modified wing; power-off condition.

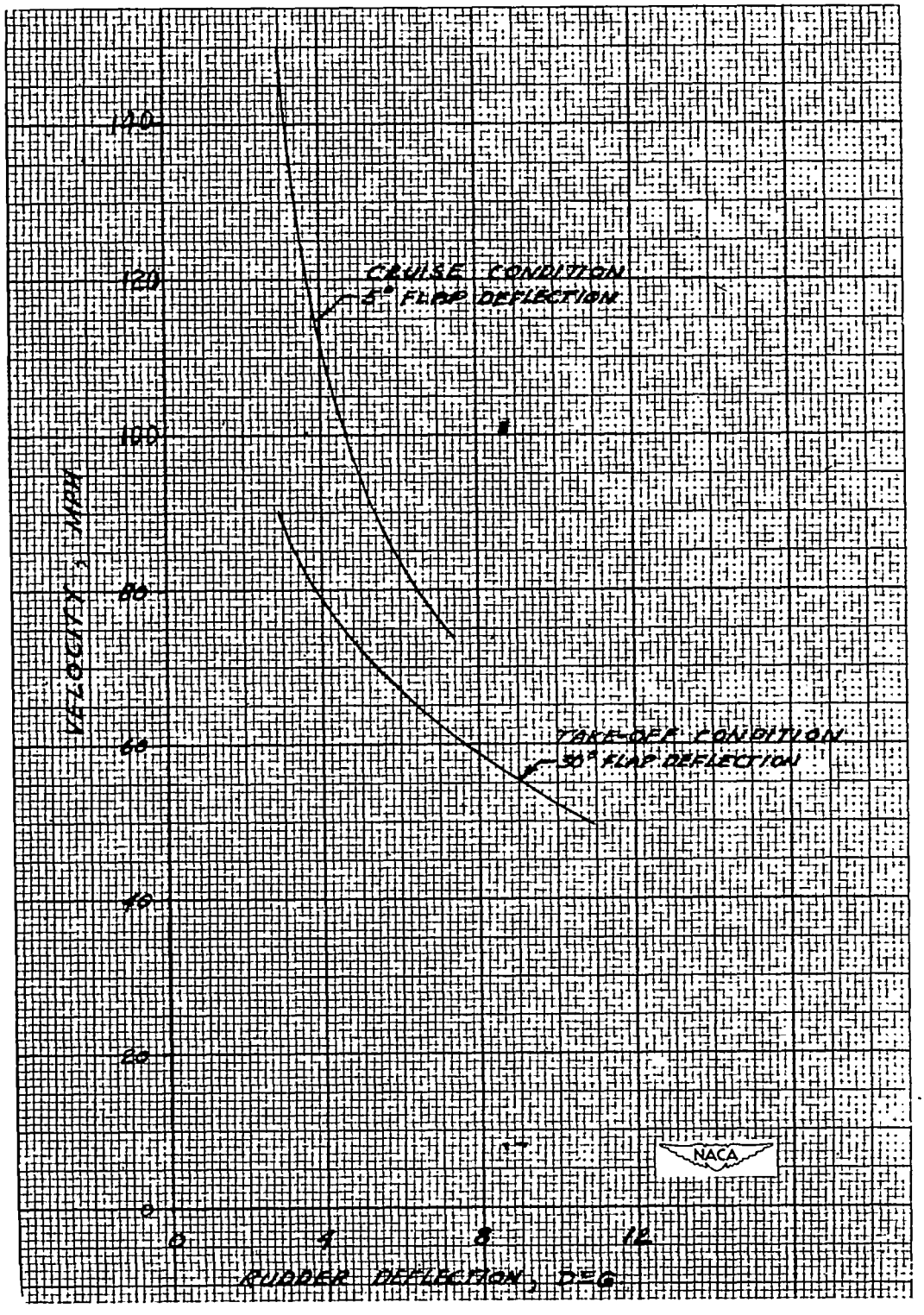

Figure 33.- Lateral control. Airplane with modified wing; rudder deflection required for reverse yaw due to roll pb/2V, 0.07.

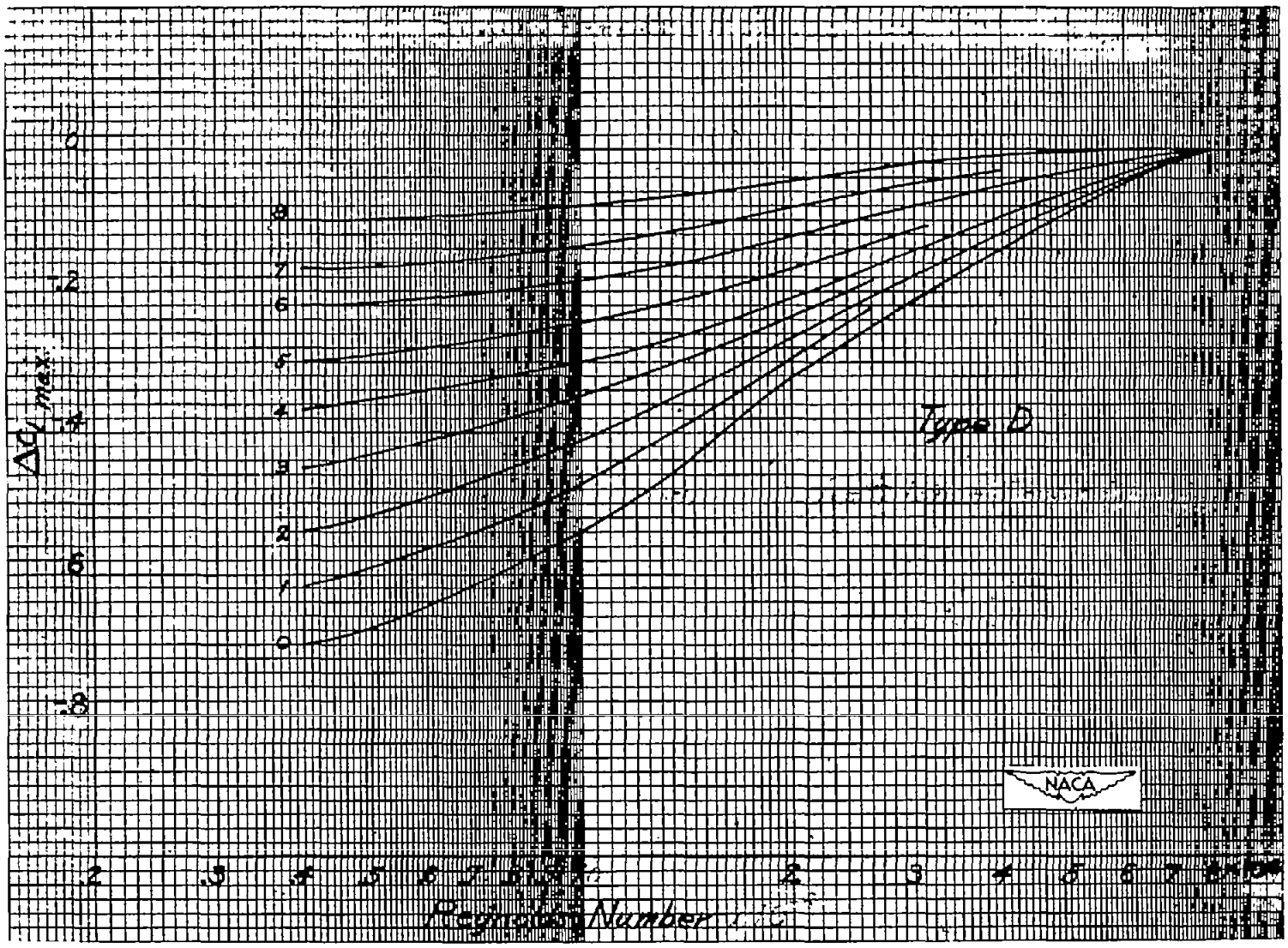

Figure 34.- Scale-effect correction for $c_{l_{max}}$. Data from reference 6.

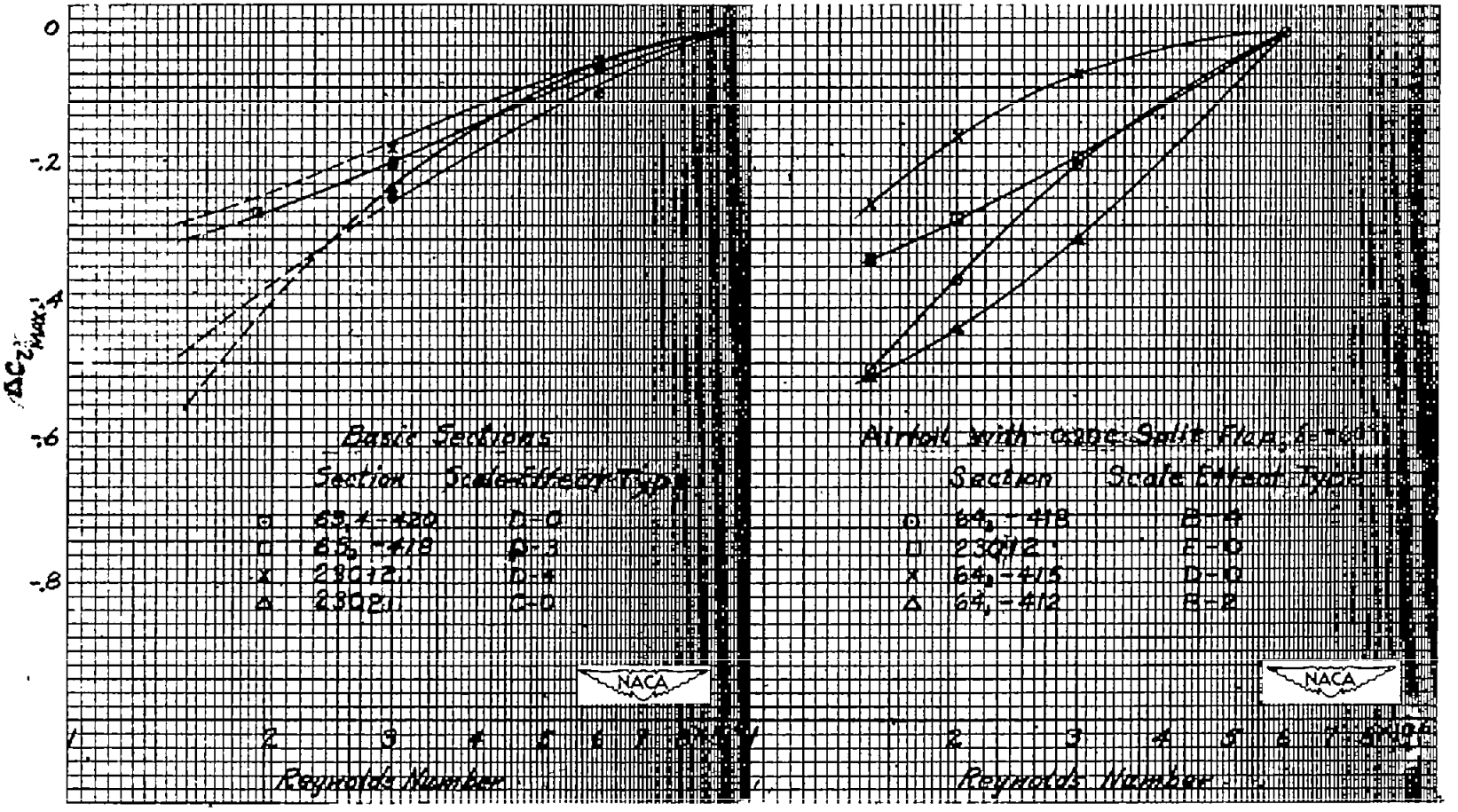

Figure 35.- Scale-effect correction for $c_{l_{max}}$.

Figure 36.- Scale-effect correction for $c_{l_{max}}$.

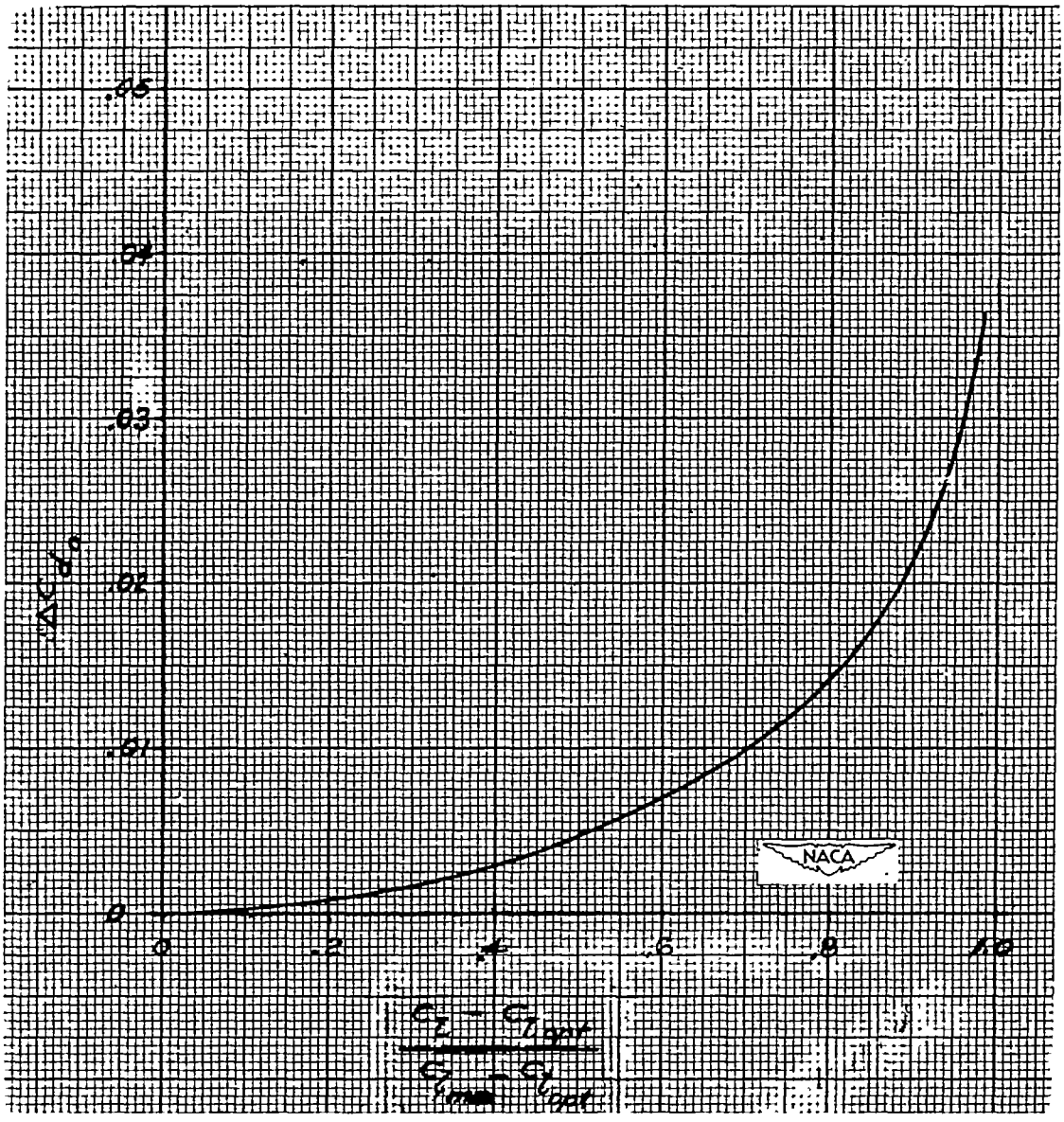

Figure 37.- Generalized variation of Δc_{d_o} with $\frac{c_l - c_{l_{opt}}}{c_{l_{max}} - c_{l_{opt}}}$.

From reference 6.

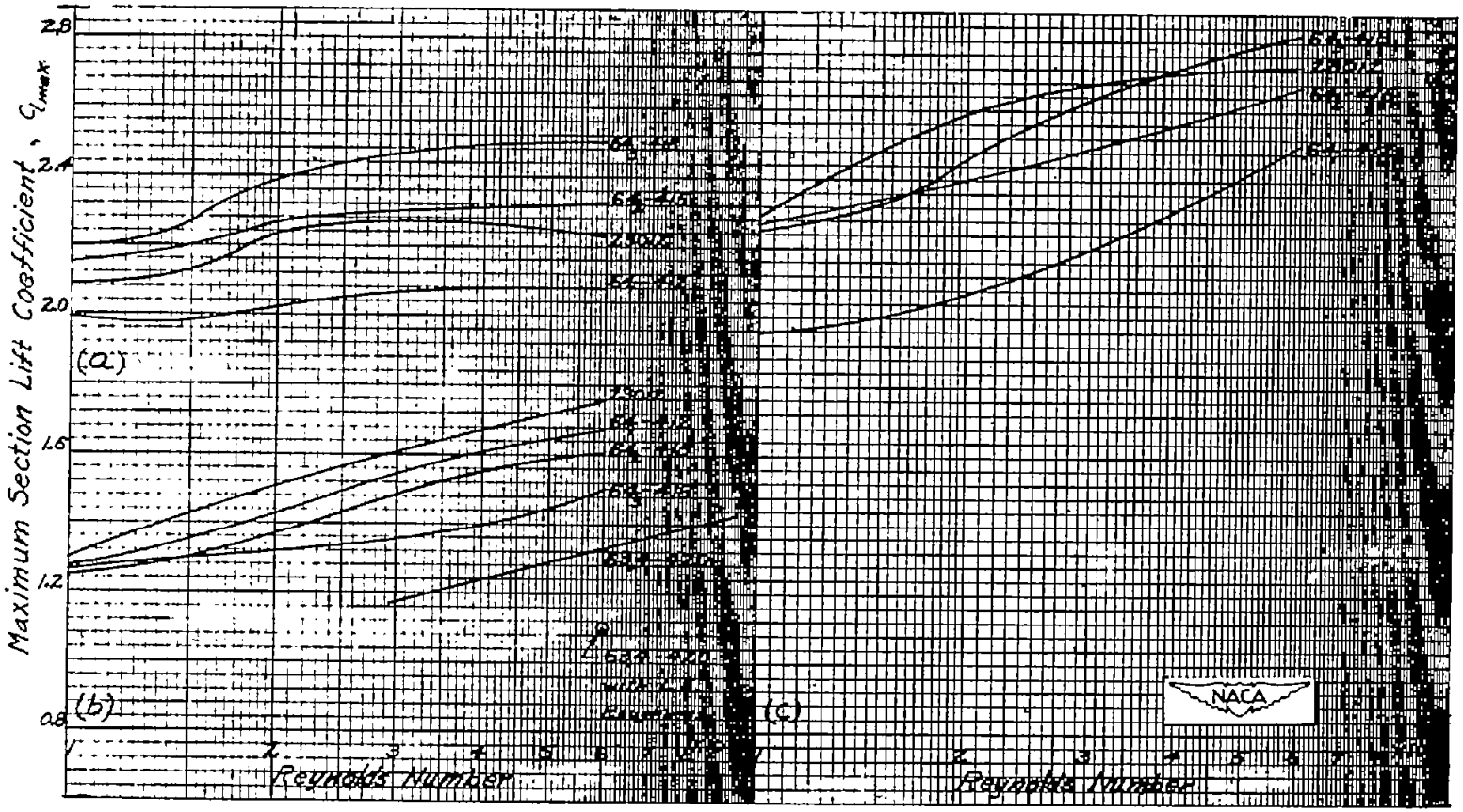

(a) Airfoil with 0.20c split flap and leading-edge roughness; $\delta_f = 60°$; from reference 8.

(b) Smooth airfoil without flap; from references 5 and 8.

(c) Smooth airfoil with 0.20c split flap; $\delta_f = 60°$; from reference 8.

Figure 38.- Effect of Reynolds number, roughness, and flaps on $c_{l_{max}}$ for several NACA airfoils.

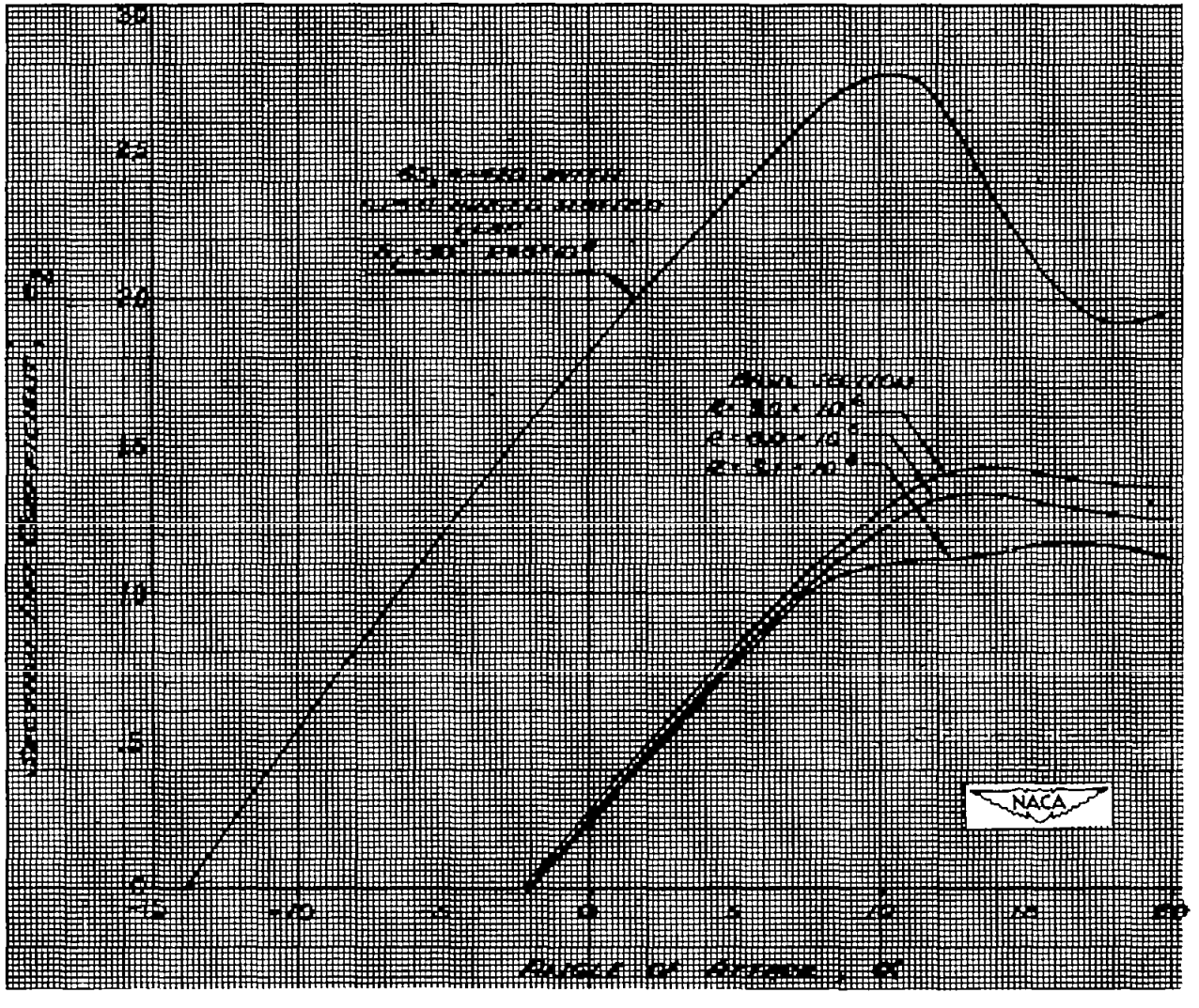

Figure 39.- Section lift coefficient for NACA 63,4-420 airfoil. Data from references 5 and 7.

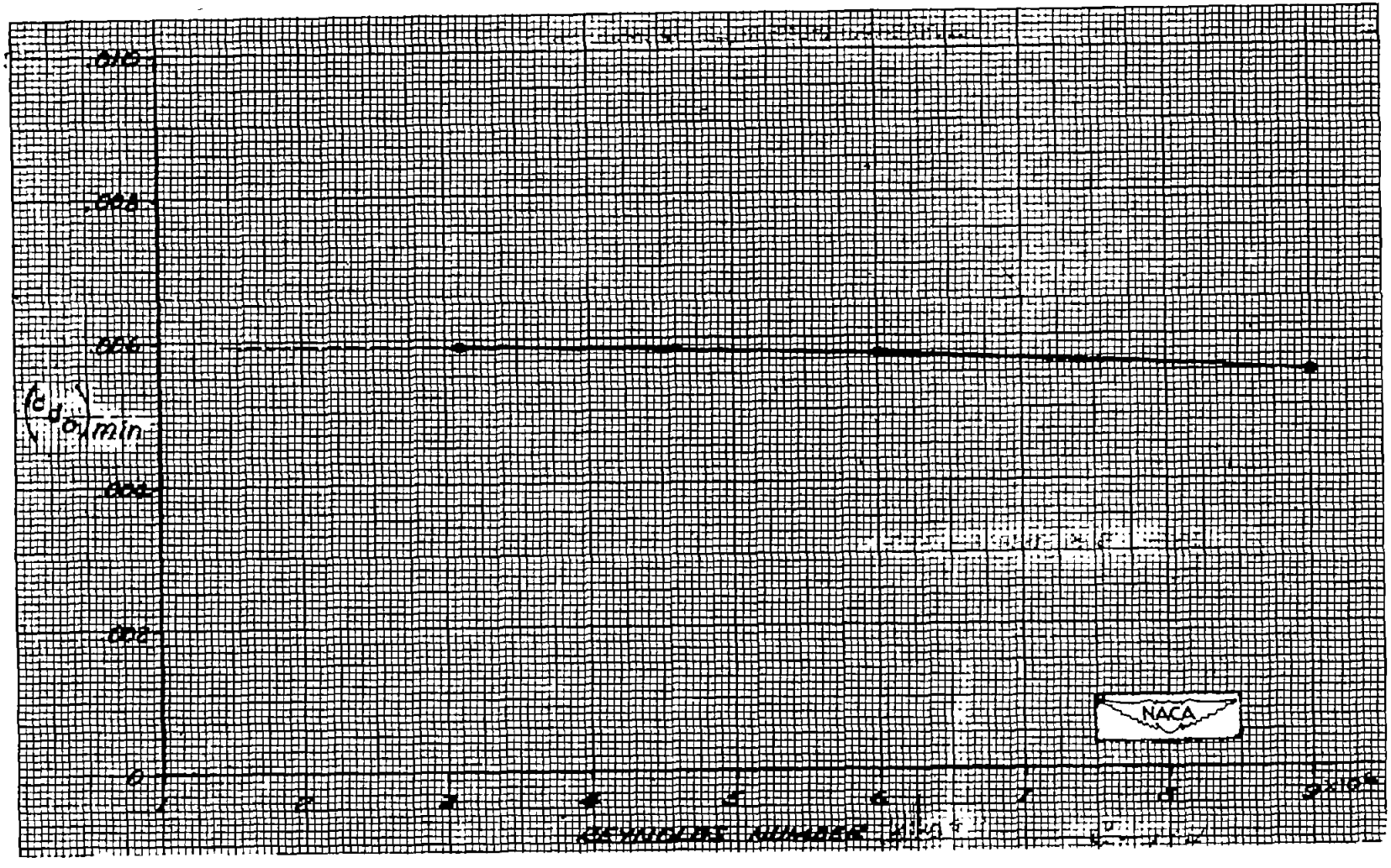

Figure 40.- Variation of $(c_{d_o})_{min}$ with Reynolds number for NACA 63,4-420 airfoil. Data from reference 5.

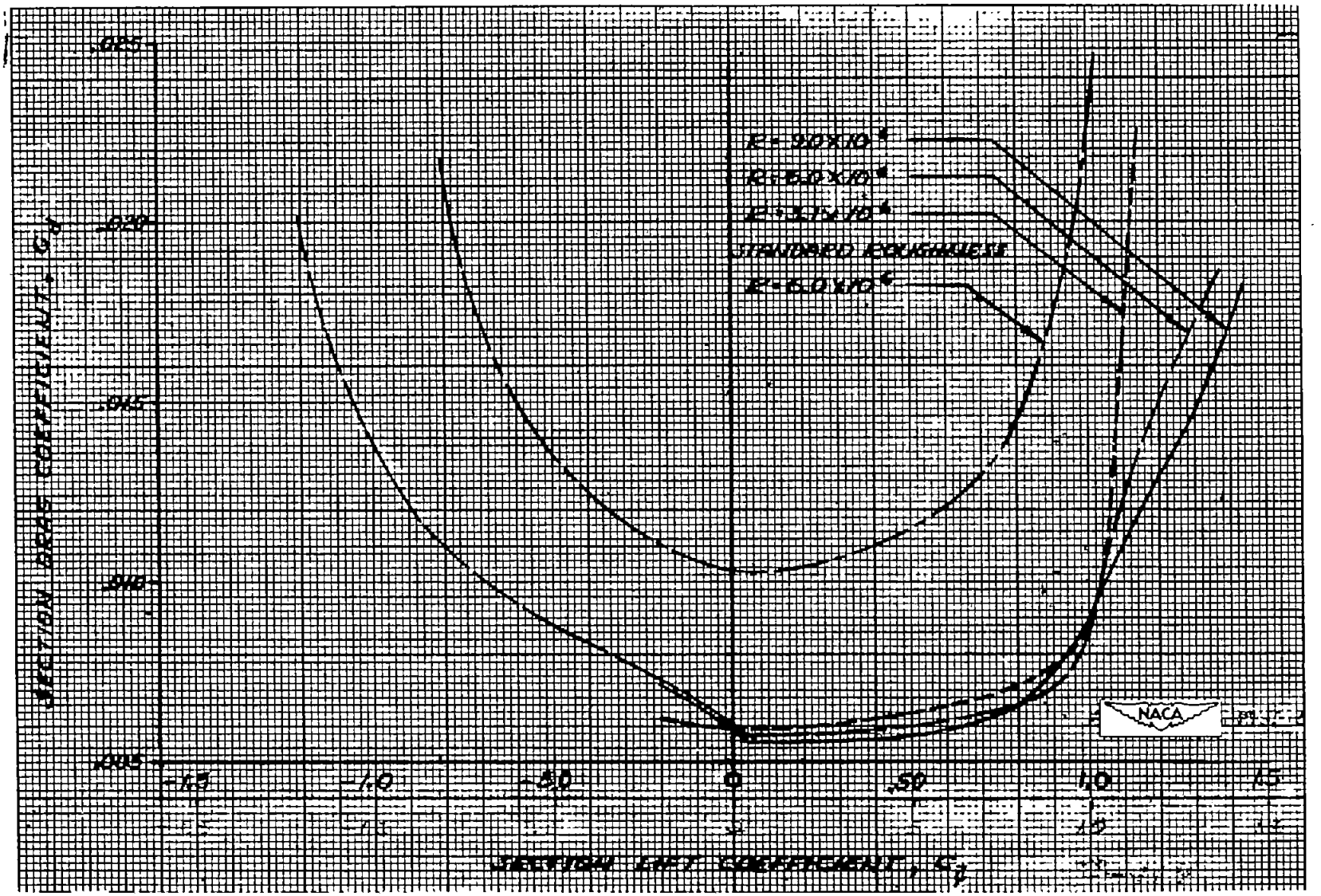

Figure 41.- Section drag coefficient against section lift coefficient.
NACA 63,4-420 airfoil section. Data from reference 5.

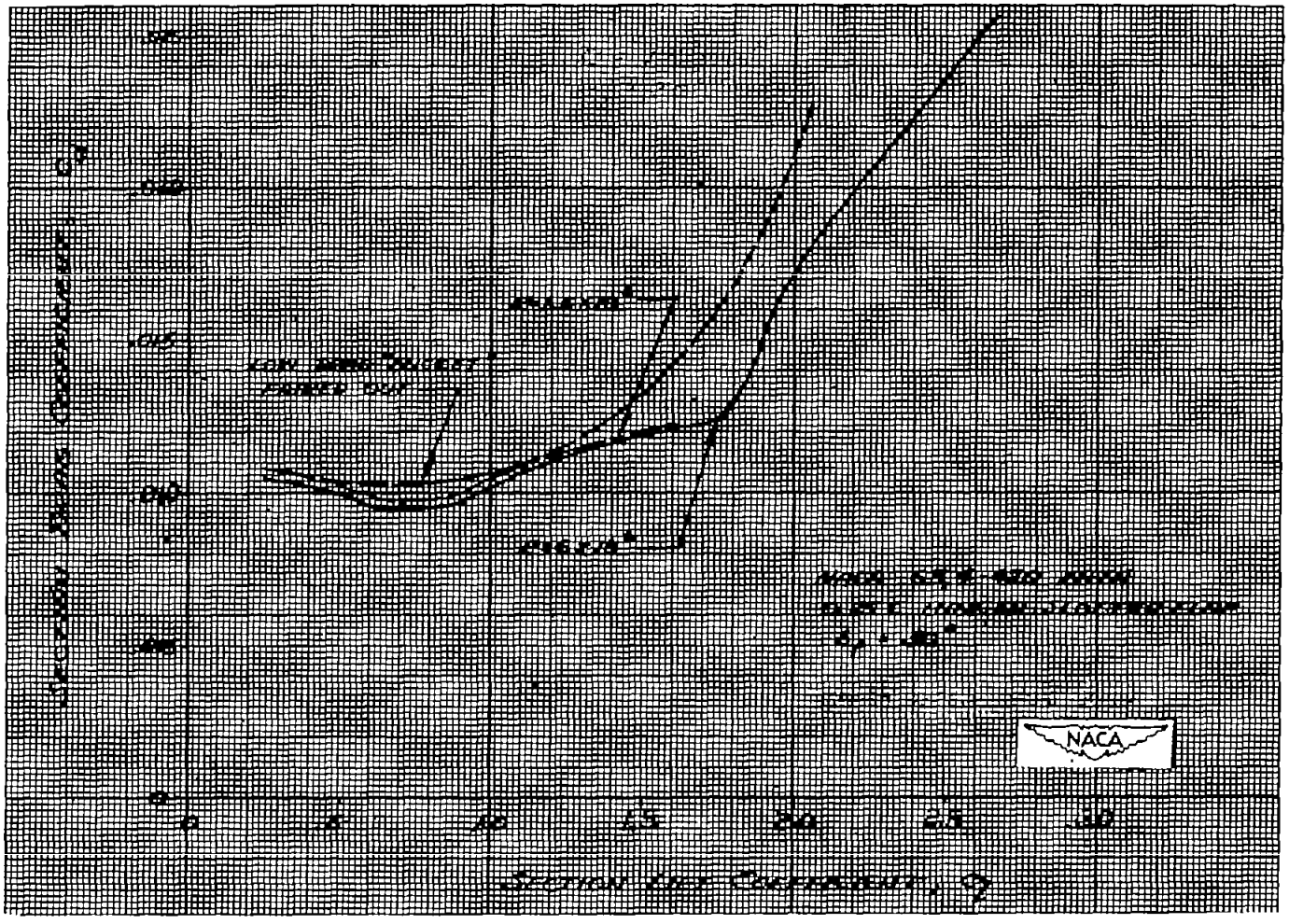

Figure 42.- Determination of c_{d_o} at $0.9c_{l_{max}}$ for NACA 63,4-420 airfoil. $R = 1.5 \times 10^6$; $\delta_f = 30^\circ$; data from reference 7.

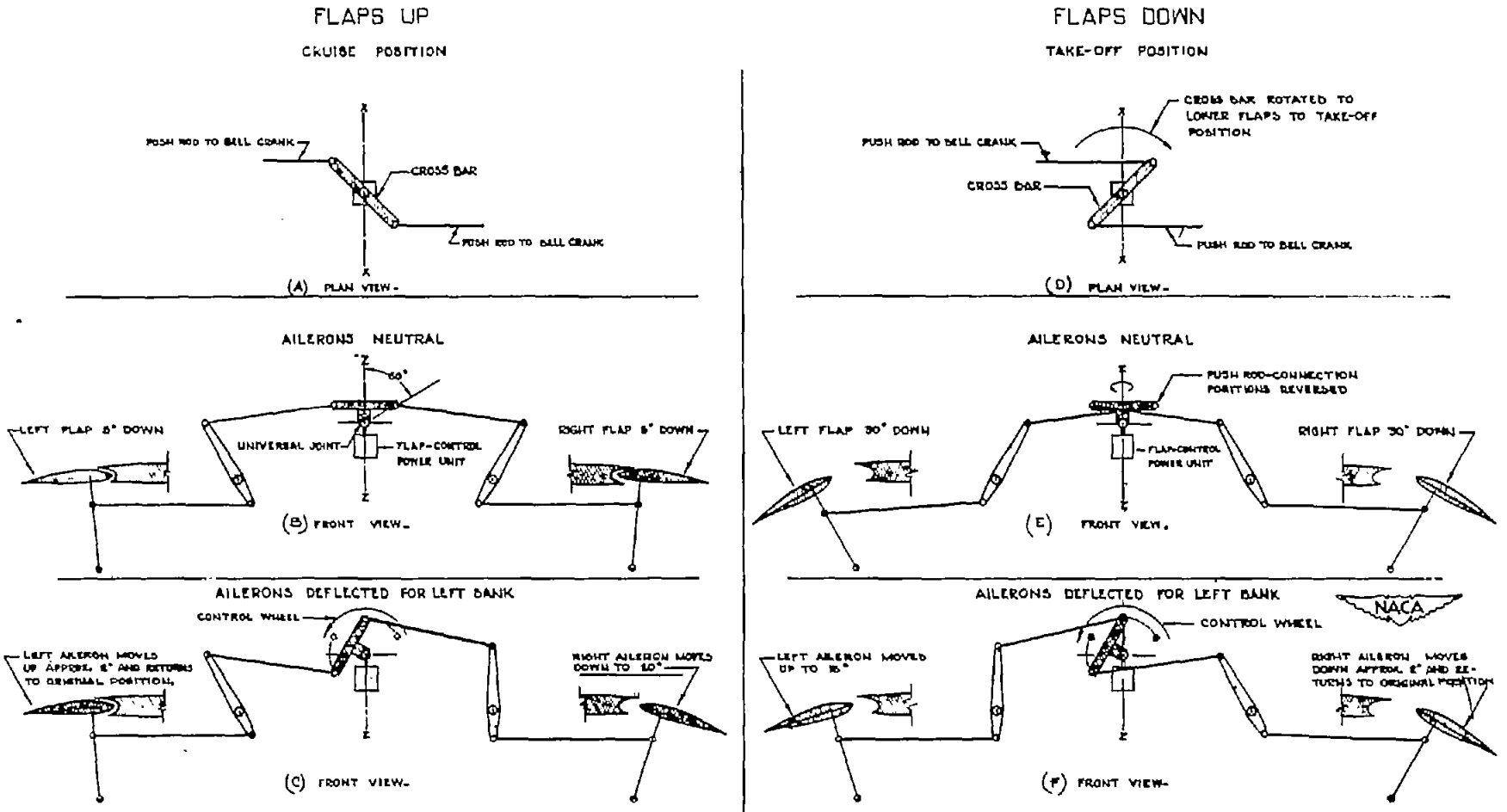

Figure 43.- Flap and aileron control diagram. (Diagrams are schematic; controls, flaps, hinges, etc. are not drawn to scale.)

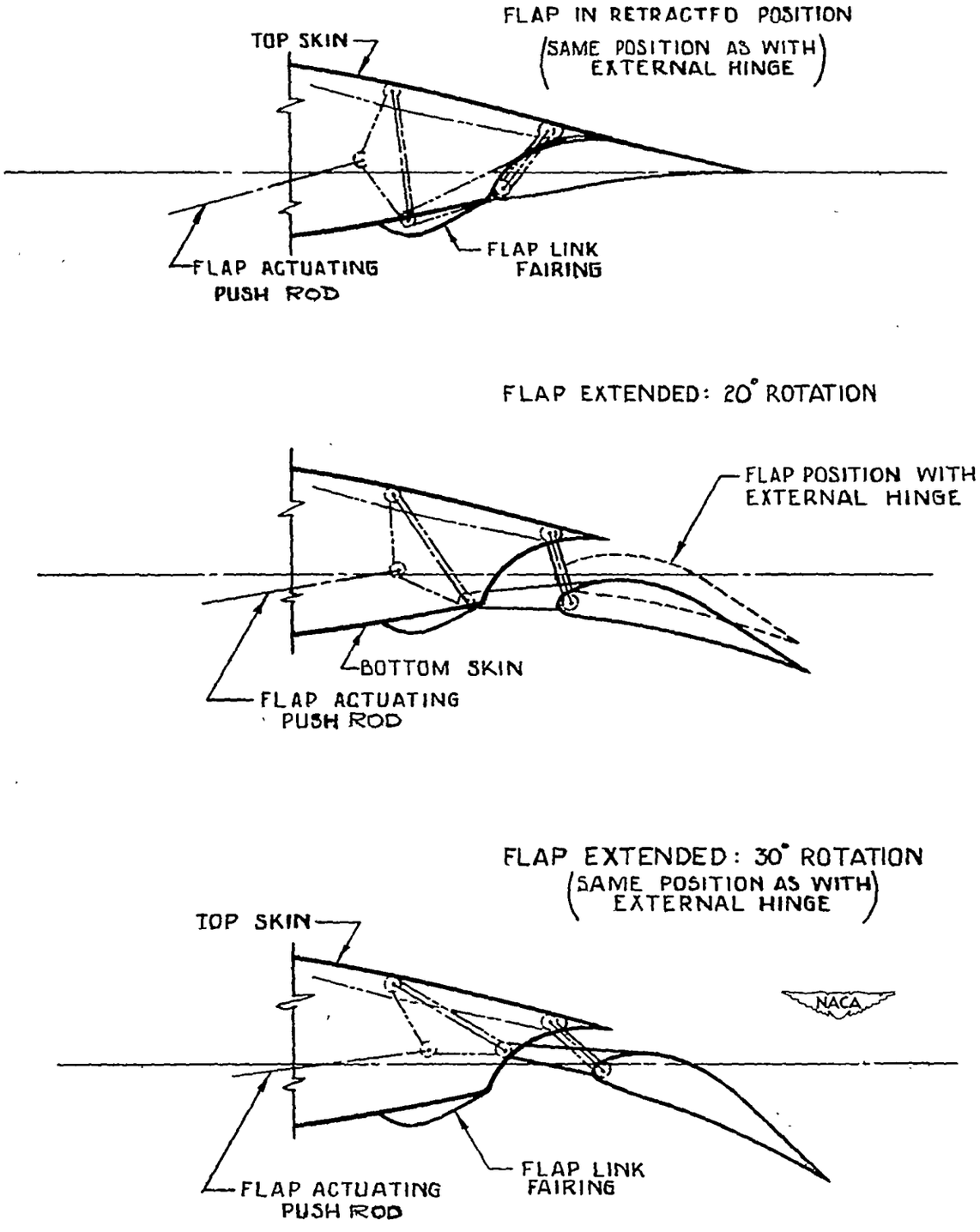

Figure 44.- Typical internal flap linkage.

NACA-Langley - 9-12-51 -1000